Molecular Pharmacology Fast Forward. Published on March 22, 2016 as DOI: 10.1124/mol.115.103200
This article has not been copyedited and formatted. The final version may differ from this version.

Title page

Synthesis and Evaluation of Potent KCNQ2/3-specific Channel Activators

Manoj Kumar, Nicholas Reed, Ruiting Liu, Elias Aizenman, Peter Wipf and Thanos Tzounopoulos

Department of Otolaryngology, University of Pittsburgh School of Medicine, Pittsburgh, Pennsylvania 15261 (M.K., T.T); Department of Chemistry, University of Pittsburgh, Pittsburgh, Pennsylvania 15260 (N.R., R.L., PW); Department of Neurobiology, University of Pittsburgh, Pittsburgh, Pennsylvania 15261 (E.A., T.T.) and Pittsburgh Institute for Neurodegenerative Diseases, University of Pittsburgh School of Medicine (E.A).

Molecular Pharmacology Fast Forward. Published on March 22, 2016 as DOI: 10.1124/mol.115.103200
This article has not been copyedited and formatted. The final version may differ from this version.

Running title page

Novel KCNQ2/3 channel activators

Corresponding authors:

Thanos Tzounopoulos, Department of Otolaryngology and Department of Neurobiology, University of Pittsburgh, Pittsburgh, Pennsylvania 15261

Email: thanos@pitt.edu

Peter Wipf, Department of Chemistry, University of Pittsburgh, Pittsburgh, Pennsylvania 15260

Email: pwipf@pitt.edu

Number of Text pages: 36

Number of Tables: 0

Number of Figures: 9

Number of References: 43

Number of words in Abstract: 133

Number of words in Introduction: 709

Number of words in Discussion: 732

Molecular Pharmacology Fast Forward. Published on March 22, 2016 as DOI: 10.1124/mol.115.103200
This article has not been copyedited and formatted. The final version may differ from this version.

Abbreviations: ADME/tox, Absorption, distribution, metabolism, excretion/ toxicity; Cbz, benzyloxycarbonyl; CHO, chinese hamster ovary; DMSO, dimethyl sulfoxide; DIPEA, di-*iso*propylethylamine; EGTA, ethylene glycol-bis(β-aminoethyl ether)-N,N,N',N'-tetraacetic acid; HEPES, N-(2-hydroxyethyl)-1-piperazineethanesulfonic acid; Kv, voltage-gated potassium channel; PTSA, *para*-toluenesulfonic acid; SAR, structure-activity relationship; S_NAr, nucleophilic aromatic substitution.

Molecular Pharmacology Fast Forward. Published on March 22, 2016 as DOI: 10.1124/mol.115.103200
This article has not been copyedited and formatted. The final version may differ from this version.

Abstract

KCNQ channels are voltage-gated, non-inactivating potassium ion channels, and their down-regulation has been implicated in several hyperexcitability-related disorders, including epilepsy, neuropathic pain and tinnitus. Activators of these channels reduce the excitability of central and peripheral neurons, and, as such, have therapeutic utility. Here, we synthetically modified several moieties of the KCNQ2-5 channel activator retigabine, an FDA approved anti-convulsant. By introducing a CF_3–group at the 4-position of the benzylamine moiety, combined with a fluorine atom at the 3-position of the aniline ring, we generated RL648_81, a new KCNQ2/3-specific activator (EC_{50} 190 nM) that is >15 times more potent and also more selective than retigabine (EC_{50} 3.3 μM). We suggest that RL648_81 is a promising clinical candidate for treating or preventing neurological disorders associated with neuronal hyperexcitability.

Molecular Pharmacology Fast Forward. Published on March 22, 2016 as DOI: 10.1124/mol.115.103200
This article has not been copyedited and formatted. The final version may differ from this version.

Introduction

Epilepsy is the most common neuronal hyperexcitability disorder, affecting 1% of the world population. This neurological condition is generally managed with sodium channel blockers or GABA receptor agonists (Bialer et al., 2010; Bialer and White, 2010). Although there are several drugs in clinical use with distinct mechanism of action, unfortunately approximately 30% of patients do not respond to these agents (Brodie, 2010; Sharma et al., 2015). Thus, there is an urgent need for drug development to broaden the treatment options.

KCNQ (or Kv7) channels play a critical role in maintaining neuronal excitability and have recently emerged as a potential target for the prevention and treatment of epilepsy and other hyperexcitability-related disorders, including neuropathic pain and tinnitus (Brown and Passmore, 2009; Gribkoff, 2008; Grunnet et al., 2014; Miceli et al., 2008; Wickenden and McNaughton-Smith, 2009; Wulff et al., 2009; Li et al., 2013). KCNQ channels are voltage-gated, non-inactivating potassium ion channels (Brown and Adams, 1980). These channels are open at resting membrane potentials and function as a 'brake' on the excitability of central and peripheral neurons (Robbins, 2001). The KCNQ family comprises of five subunits (KCNQ1-5): KCNQ2-5 are confined to the nervous system including brainstem and inner ear whereas KCNQ1 is limited to the heart and peripheral epithelial and smooth muscle cells (Howard et al., 2007). Genetic mutations in either KCNQ2 or KCNQ3 subunits are linked to benign familial neonatal convulsions, whereas noise-induced reduction in KCNQ2/3 channel current leads to development of tinnitus in mice (Biervert et al., 1998; Jentsch, 2000; Li et al., 2013; Li et al., 2015). Moreover, pathological reduction in KCNQ2/3 channel activity is involved in different classes of seizures, neuropathic pain, migraine, anxiety, attention deficient-hyperactivity disorder, schizophrenia, mania and bipolar disease (Grunnet et al., 2014; Hansen et al., 2008;

Molecular Pharmacology Fast Forward. Published on March 22, 2016 as DOI: 10.1124/mol.115.103200
This article has not been copyedited and formatted. The final version may differ from this version.

Munro and Dalby-Brown, 2007). As a result, KCNQ channel activators, which lead to the opening of these channels at more hyperpolarized potentials, have recently been employed to treat or prevent epilepsy (Gribkoff, 2008; Miceli et al., 2008; Xiong et al., 2008).

Several Kv7 channel openers are under active development for the management of hyperexcitability disorders (Dalby-Brown et al., 2013; Davoren et al., 2015; Grunnet et al., 2014; Stott et al., 2014). Retigabine, which activates all KCNQ2-5 channels, is the only FDA approved anti-convulsant KCNQ activator (Gunthorpe et al., 2012; Tatulian et al., 2001). However, recent data showed severe side effects associated with retigabine, including urinary retention, blue skin discoloration and retinal abnormalities (Jankovic and Ilickovic, 2013). As a result, the FDA limited its use to patients who have not responded to alternative treatments. The undesirable side effects are likely due to the poor selectivity of retigabine among KCNQ2-5 channels as well as metabolic degradation products of its aniline ring. For example, retigabine activates KCNQ4 and KCNQ5, which are not involved in the pathology of hyperexcitability-related disorders. KCNQ4 is the primary potassium channel in the smooth muscle of the bladder, where it regulates contractility (Greenwood and Ohya, 2009; Jentsch, 2000). Activation of KCNQ4 leads to membrane hyperpolarization and results in significantly reduced contractility, which may be the cause for urinary retention associated with the use of retigabine. Moreover, a form of dominant deafness arises from loss of function of KCNQ4 (Kharkovets et al., 2000), and therefore opening of these channels may affect hearing. In addition to expression in the CNS, KCNQ4 and KCNQ5 are also found in skeletal muscle (Iannotti et al., 2013; Iannotti et al., 2010; Jentsch, 2000). Accordingly, there is an urgent need for the development of potent and selective KCNQ2/3 channel activators, which, unlike retigabine, do not activate KCNQ4 and KCNQ5 channels.

Molecular Pharmacology Fast Forward. Published on March 22, 2016 as DOI: 10.1124/mol.115.103200
This article has not been copyedited and formatted. The final version may differ from this version.

To achieve this aim, we synthesized and evaluated several novel KCNQ2/3-specific channel activators. To maximize potency, we manipulated the different chemical components or "zones" of retigabine (Figure 1). Particularly, by introducing a CF_3-group in zone 1 at the 4-position of the benzylamine moiety, combined with a fluorine atom in zone 2 at the 3-position of the aniline ring, we generated RL648_81, a new KCNQ2/3-specific activator that is 3 times more potent and also more selective than SF0034, a recently described retigabine analog with increased potency and selectivity for KCNQ2/3 channels (Kalappa et al., 2015). We propose that RL648_81 is a promising clinical candidate for the treatment or prevention of hyperexcitability-related neurological disorders.

Molecular Pharmacology Fast Forward. Published on March 22, 2016 as DOI: 10.1124/mol.115.103200
This article has not been copyedited and formatted. The final version may differ from this version.

Materials and Methods

Constructs and Chemicals. The KCNQ2, KCNQ3, KCNQ4, KCNQ5 and KCNQ2 (W236L) constructs, as well as the PIPKIγ90 plasmid used in this study have been described previously (Soh and Tzingounis, 2010; Kalappa et al., 2015) and were generously provided by Dr. Anastassios Tzingounis (University of Connecticut, Connecticut, USA). Buffers and salts were purchased from Sigma-Aldrich (St. Louis, Missouri, USA). Compounds stock solutions (20 mM) were made in DMSO. All stock solutions were stored at -20 °C. On the day of experiment, fresh working drug concentrations were prepared from stock solutions by dissolving them in physiological buffer solution.

Cell Culture and Transfection. Chinese hamster ovary (CHO) cells were platted on glass coverslips in 35-mm culture dishes and were incubated and maintained at 37 °C in a humidified incubator with 5% CO_2. To get heterologous KCNQ2/3 configuration, CHO cells were transfected with human KCNQ2 and KCNQ3 subunits cDNA in a 1:1 (0.5 μg : 0.5 μg) ratio with 0.5 μg of GFP plasmid using *lipofectamine transfection reagent* (Thermo Fisher Scientific, MA, USA) and used for recording within 24-72 h of post transfection. For homomeric KCNQ4 and KCNQ5 channels, 1 μg of plasmid cDNA was used. To record robust KCNQ5 currents, we cotransfected KCNQ5 with pIRES-dsRed-PIPKIγ90. PIPKIγ90 increases KCNQ channel open probability (Li et al., 2005).

Whole cell patch clamp electrophysiology. We used whole-cell patch clamp electrophysiology used to assess effects of retigabine and synthesized compounds on KCNQ channel currents. We conducted electrophysiology experiments at room temperature (22-25 °C). Patch pipettes of borosilicate glass (BF150-110-10; Sutter Instrument Company, Novato, CA) were pulled to a tip resistance of 4–6 MΩ. Patch pipettes were filled with a solution consisting of (in mM): 132 K-

Molecular Pharmacology Fast Forward. Published on March 22, 2016 as DOI: 10.1124/mol.115.103200
This article has not been copyedited and formatted. The final version may differ from this version.

gluconate, 10 KCl, 4 Mg•ATP, 20 HEPES, and 1 EGTA•KOH, pH 7.2–7.3. Coverslips containing cultured cells were placed in the recording chamber on the stage of an inverted light microscope and superfused continuously with an external solution consisting of (in mM): 144 NaCl, 2.5 KCl, 2.25 $CaCl_2$, 1.2 $MgCl_2$, 10 HEPES, and 22 D-glucose, pH 7.2–7.3. Osmolarity was adjusted to 300–305 mOsm and pH to 7.2–7.3 with NaOH. Cells were clamped at -85 mV and currents were elicited by 1 s depolarization potentials, in 10 mV increments, from -105 to + 15 mV followed by a return step to -70 mV. Currents elicited by each voltage step were measured and used to generate the conductance-voltage (G-V) curves as described in the figure legends. These values are adjusted for the calculated junction potential, which was -15 mV. Series resistance was compensated by 75%. To quantify the potency of the tested compounds, we measured the shift in $V_{1/2}$ at increasing concentrations and used a Hill equation fit to calculate their EC_{50}, which is the concentration of the compound that produces a half-maximal shift in $V_{1/2}$. Data were acquired through an Axopatch 200 amplifier (Molecular Devices, Sunnyvale, CA), low-pass filtered at 2 kHz, sampled at 10 kHz using pClamp 10 data acquisition system.

Data analysis and statistics. We used the Boltzmann function to fit the conductance–voltage curves and determine the maximal conductance (Gmax) and half-maximal activation voltage ($V_{1/2}$) of KCNQ currents, where $G = G\text{max}/[1 + e\text{^}\{-(V - V_{1/2})/k\}]$ and k is the slope factor. To calculate the dependence of the shift in $V_{1/2}$ with the concentration of different KCNQ channel activators, we measured the $V_{1/2}$ of KCNQ2/3 currents in presence of various concentrations of compounds (100 nM-30 μM). We then fitted the agonist dependence of the shift of the $V_{1/2}$ obtained by different concentrations with a Hill equation, where $\Delta V_{1/2} = V_{1/2}$ max * [activator] $^n/([\text{activator}]^n + EC_{50}{}^n$. $\Delta V_{1/2}$ is the change in $V_{1/2}$ caused by the activator, EC_{50} is the concentration of the KCNQ channel activator that causes 50% of the maximal effect in $V_{1/2}$, n is

Molecular Pharmacology Fast Forward. Published on March 22, 2016 as DOI: 10.1124/mol.115.103200
This article has not been copyedited and formatted. The final version may differ from this version.

the Hill coefficient, and [activator] is the concentration of KCNQ activator. All data are presented as mean values ± S.E.M. Statistical significance between control and test conditions was determined using Student's *t*-test (paired or unpaired) and one-way analysis of variance. Tukey-Kramer *post hoc* test for multiple comparisons was performed as needed. Data analysis and statistical tests were performed using GraphPad Prism version 6 and OriginLab 2015.

Molecular Pharmacology Fast Forward. Published on March 22, 2016 as DOI: 10.1124/mol.115.103200
This article has not been copyedited and formatted. The final version may differ from this version.

Results

Retigabine and its derivative SF0034 shift the voltage dependent opening of KCNQ channels towards more hyperpolarized potentials, leading to increased K^+ currents at resting membrane potential (Kalappa et al., 2015; Tatulian et al., 2001). To generate KCNQ2/3 channel activators with increased potency and selectivity, we partitioned retigabine's chemical structure into three distinct zones (Figure 1). During the first round of chemical synthesis we mainly modified zones 1 and 3, whereas in the second iteration of our structure-activity relationship (SAR) analysis, we combined the beneficial modifications found for zones 1 and 3 with previously known beneficial modifications on zone 2, which led to the development of SF0034 (Figure 1, Kalappa et al., 2015). Based on the site of modification, we also categorized 1st generation compounds into three classes. Class I compounds had substitutions at the phenyl ring in zone 1, class II compounds had substitutions at the methylene group in zone 1, and class III compounds featured substitutions in zone 3 (Figure 2). Our guiding principle for this round of SAR studies was to modulate both steric and, in particular, electronic features in zone 1 by introducing fluoride, trifluoromethyl, and, importantly, a novel pentafluorosulfanyl group, which is considered a "super-trifluoromethyl" substituent (Alverez et al., 2015; Mo et al., 2010; Wipf et al., 2009). These modifications led to our class I analogs NR561_29, NR561_40, NR561_45, and NR561_50. As part of our class II analog design, we introduced substituents at the benzylic methylene group, designed to slow down metabolic degradation (trifluoromethyl: NR579_04; deuterium: NR561_87). Moreover, we introduced a preliminary series of heterocycle analogs of the phenyl group in zone 1, i.e. a more electron-rich thiophene (NR579_46) and a more electron-deficient thiazole (NR579_38). Finally, our class III design modified the steric size of the ethylcarbamate in zone 3 by introducing an *iso*-propyl group (NR561_62) and the solubilizing

Molecular Pharmacology Fast Forward. Published on March 22, 2016 as DOI: 10.1124/mol.115.103200
This article has not been copyedited and formatted. The final version may differ from this version.

oxetane derivatives NR579_45 and NR579_36 (Skoda et al., 2014; Sprachman and Wipf, 2012; for synthesis details and spectroscopic information on these compounds, see supplemental data).

Incorporation of highly fluorinated substituents at the phenyl ring of retigabine increases the potency of KCNQ2/3 channel activation

To set the control conditions for assessing the potency and selectivity of the newly synthesized compounds, we first evaluated the ability of two standard activators, retigabine and SF0034, in potentiating KCNQ2/3 channel-mediated K^+-currents under our assay conditions (Fig. 3). We transiently expressed heterologous KCNQ2/3 channels in CHO cells and tested the effect of increasing concentrations (100 nM to 30 µM) of retigabine and SF0034 on KCNQ2/3 currents. We employed whole cell patch clamp electrophysiological techniques (Kalappa et al., 2015). 100 nM SF0034 increased KCNQ2/3 currents at hyperpolarized potentials, whereas 100 nM retigabine failed to show any effect (Fig. $3A_1$, B_1). Consistent with our previous studies (Kalappa et al., 2015), SF0034 was approximately five times more potent than retigabine in shifting the $V_{1/2}$ of KCNQ2/3 currents (Fig. 3A-D; retigabine: EC_{50} 3.3 ± 0.8 µM, n=4-11; SF0034: EC_{50} 0.60 ± 0.06 µM, n=5-21, p <0.01).

Next, we tested the ability of the newly synthesized compounds to shift the $V_{1/2}$ of KCNQ2/3 currents. We used different concentrations of these analogs to evaluate whether the new substituents resulted in gain or loss of potency in activating KCNQ2/3 currents compared to retigabine and SF0034. A concentration of 100 nM of NR561_40 (CF_3-group at the 4-position of the phenyl ring) increased the KCNQ2/3 currents at hyperpolarized potentials (Fig. $4A_1$).

Molecular Pharmacology Fast Forward. Published on March 22, 2016 as DOI: 10.1124/mol.115.103200
This article has not been copyedited and formatted. The final version may differ from this version.

Consistent with this finding, a Boltzmann fit of the G-V relationship revealed a significant shift in the $V_{1/2}$ towards hyperpolarized potentials in the presence of 100 nM or 10 µM NR561_40 without altering G_{max} ($G_{max:nor}$: control: 0.95 ± 0.015; n=9, 100 nM: 0.99 ± 0.043; n=5, 10 µM: 0.97 ± 0.108; n=4) (Fig. $4A_2$, A_3). Similarly, we measured the shift in $V_{1/2}$ in the presence of increasing concentrations of NR561_40 (100 nM - 30 µM) and calculated the EC_{50} values (Fig. $4A_4$). NR561_40 showed a similar potency as SF0034 (Fig. 5A). Because retigabine has only one fluorine atom at the 4-position of the phenyl ring, these results suggested that increasing the steric bulk and electron-withdrawing properties at this position improves the potency at KCNQ2/3 channels. NR561_29, which has an even larger and more electronegative SF_5-group at this position, demonstrated a 4-5 fold higher potency compared to retigabine, but showed a significantly lower maximal $\Delta V_{1/2}$ compared to NR561_40 and SF0034, maximal $\Delta V_{1/2}$ values were calculated from the observed shift in $V_{1/2}$ at 10 µM concentrations of the compound (Fig. 5B). This result suggested that a large steric size in zone 1 might limit the potency/efficacy at KCNQ2/3 channels (Fig. 5). Furthermore, when either the smaller CF_3-group or the larger SF_5-group were introduced at the 3-position of the phenyl ring, the resulting NR561_50 (Fig. 4B) and NR561_45, both showed similar potency but a lower maximal $\Delta V_{1/2}$ compared to NR561_40 and SF0034. From this result we concluded that the exact position of the fluorinated groups at the phenyl ring plays a critical role in determining the potency/efficacy of KCNQ activators at KCNQ2/3 channels.

Likewise, we tested class II and class III compounds for their potency and efficacy at shifting the $V_{1/2}$ of KCNQ2/3 currents. Class II compounds NR579_38, NR579_46 and NR561_87 shifted the $V_{1/2}$ of KCNQ2/3 channels, but did not show any improvement in EC_{50} values relative to retigabine. Interestingly, NR579_04 failed to show any effect on KCNQ2/3 channel currents,

Molecular Pharmacology Fast Forward. Published on March 22, 2016 as DOI: 10.1124/mol.115.103200
This article has not been copyedited and formatted. The final version may differ from this version.

even at concentrations as high as 10 µM, demonstrating the need for a small linker between the phenyl ring and the benzylic amine (Figs. 4C, 5). Among class III compounds, only NR561_62 demonstrated potency that was 2-3 fold better than retigabine; the more hydrophilic substituents were not tolerated (Fig. 4D). Taken together, our SAR results demonstrate that the position and the steric size of fluorinated groups in zone 1 of retigabine are critical determinants of compound potency and efficacy. Addition of CF_3- and SF_5-groups in positions 3 and 4 of the phenyl ring of retigabine generates KCNQ2/3 activators with increased potency over retigabine. Incorporation of a trifluoromethyl substituent specifically at the *para*-position of the benzylamine moiety resulted in the maximal improvement in potency and efficacy at KCNQ2/3 channels, eclipsing that of SF0034. Manipulation of the retigabine structure as probed in class II and III compounds did not provide further improvements in KCNQ2/3 channel potency, with the exception of NR561_62, where the ethyl group was replaced with a more lipophilic *iso*-propyl chain in the carbamate moiety.

KCNQ2/3 selectivity of CF_3- and SF_5-containing analogs

Next, we determined the selectivity profile of class I compounds that showed increased potency for KCNQ2/3 channels, i.e. NR561_40, NR561_50 and NR561_29. To assess the selectivity of these analogs, we quantified their effect on homomeric KCNQ4 and KCNQ5 channels. First, we tested NR561_50 at homomeric KCNQ4 channels. A concentration of 100 nM of NR561_50 failed to alter the $V_{1/2}$ of KCNQ4 channels (Fig. $6A_1$). A Boltzmann fit of the G-V relationship in presence of 100 nM or 1 µM compound did not shift the $V_{1/2}$ of KCNQ4 channels (Fig. $6A_2$, A_3). Similarly, NR561_50 did not shift the $V_{1/2}$ of KCNQ5 channels (Fig. 6B). Although 100 nM NR561_40 and NR561_29 did not change the $V_{1/2}$, at 1 µM concentration, both NR561_40 and

Molecular Pharmacology Fast Forward. Published on March 22, 2016 as DOI: 10.1124/mol.115.103200
This article has not been copyedited and formatted. The final version may differ from this version.

NR561_29 shifted the $V_{1/2}$ of KCNQ4 currents towards more hyperpolarized potentials (Fig. 6C, E). Furthermore, NR561_40 and NR561_29 increased KCNQ5 currents and shifted the $V_{1/2}$ to more hyperpolarized potentials at 100 nM and 1 μM (Fig. 6D, F). Taken together, NR561_50 proved to be selective for KCNQ2/3 channels whereas NR561_40 and NR561_29 were found to be less selective. This profile suggests that incorporation of a trifluoromethyl group at the *meta*-position of the benzylamine generates activators with enhanced KCNQ2/3 selectivity.

Incorporation of a fluorine substituent in zone 2 in analogs with CF_3- and SF_5- functions in zone 1 generates the most potent KCNQ2/3 activator yet described

Because incorporation of a fluorine atom at the 3-position of the aniline ring of retigabine improved the potency and selectivity at KCNQ2/3 channels (Kalappa et al., 2015), we hypothesized that addition of fluorinated groups in zone 2 might also further improve the potency and selectivity of class I compounds. To test our hypothesis, we selected the most potent and efficacious compounds based on the 1st generation SAR (Fig. 5) and introduced a fluorine atom at the 3-position of the aniline. In this fashion, RL648_81 was obtained as the fluorinated analogue of NR561_40, RL648_73 as the fluorinated analogue of NR648_50, RL648_86 as the fluorinated analogue of NR561_62, and RL673_02 as the fluorinated analogue of NR561_45 (Fig. 7; for synthetic and spectroscopic details, see supplemental data).

We first evaluated the effect of different concentrations of RL648_81 at KCNQ2/3-mediated currents (Fig. 8A$_1$). Application of 100 nM RL648_81 robustly shifted the $V_{1/2}$ of KCNQ2/3 channels towards hyperpolarized potentials. Also, increased concentrations of 1 μM or 10 μM compound showed a more robust shift in $V_{1/2}$ compared to the shift caused by 1 μM or 10 μM

Molecular Pharmacology Fast Forward. Published on March 22, 2016 as DOI: 10.1124/mol.115.103200
This article has not been copyedited and formatted. The final version may differ from this version.

SF0034 (Fig. 8A2-A4). Evaluation of the EC_{50} revealed that RL648_81 is 3 times more potent than SF0034 at shifting the voltage dependence of KCNQ2/3 channels to more hyperpolarized potentials (Fig. 8D; EC_{50} 0.19 ± 0.02 µM, n= 5). This shift in $V_{1/2}$ was not associated by changes in G_{max} (Fig. $8A_{1-3}$; $G_{max:nor}$: control: 0.96 ± 0.012; n=9, 100 nM: 1.01 ± 0.108; n=5, 01 µM: 1.01 ± 0.012; n=4, 10 µM: 0.95 ± 0.070; n=4). To assess the selectivity of RL648_81, we tested 100 nM, 1 µM and 10 µM of RL648_81 on homomeric KCNQ4 and KCNQ5 channel currents (Fig. 8B, C). RL648_81 did not shift the $V_{1/2}$ of either KCNQ4 or KCNQ5, suggesting that RL648_81 is a KCNQ2/3-specific activator (Fig. 8B, C).

Next, we evaluated RL648_76, RL648_86 and RL673_02 for their potency and selectivity at KCNQ2/3 channels. RL648_73 and RL648_86 showed 2-fold improved potency compared to SF0034 at KCNQ2/3 channels, whereas RL673_02 did not show a significant difference from SF0034, in agreement with the previously noted attenuation of potency with the sterically demanding SF_5 substituent (Fig. 8D left). These compounds, with the exception of the effect of 10 µM RL673_02 on KCNQ4 channels, also did not show any significant effect on either KCNQ4 or KCNQ5 channel currents (Fig. 8E, F).

The conserved residue, tryptophan (W) in the intracellular end of the S5 helix, W236 for KCNQ2 numbering and W265 for KCNQ3 numbering, is necessary for the enhancing effect of retigabine (Schenzer et al., 2005). To determine whether the gating effect of RL648_81 also requires the same W residue, we examined the influence of RL648_81 in KCNQ2 channels that lack W236. Indeed, although RL648_81 had a strong gating effect on KCNQ2 channels, this efficacy was abolished upon substitution of W236 to L (Fig. 9 A, B). These results suggest that RL648_81, like retigabine and SF0034, requires W236 to exert its enhanced gating properties.

Molecular Pharmacology Fast Forward. Published on March 22, 2016 as DOI: 10.1124/mol.115.103200
This article has not been copyedited and formatted. The final version may differ from this version.

Taken together, our SAR investigations led to the discovery of several highly selective and potent channel agonists, including the most potent KCNQ2/3-specific channel activator reported to date, RL648_81, which demonstrated three times higher potency than SF0034. Moreover, RL648_73 and RL648_86, which are two times more potent than SF0034, represent useful secondary lead compounds. ADME/tox data for SF0034 are not available yet, but in view of the undesired side effects associated with retigabine, we suggest that these more potent, selective and electronically deactivated KCNQ2/3 activators may be attractive candidates for treating or preventing hyperexcitability disorders at lower dosage and with reduced side effects.

Molecular Pharmacology Fast Forward. Published on March 22, 2016 as DOI: 10.1124/mol.115.103200
This article has not been copyedited and formatted. The final version may differ from this version.

Discussion

Epilepsy is a hyperexcitability disorder that affects approximately 65 million people worldwide (Bialer and White, 2010). Despite the availability of more than 20 antiepileptic drugs, 25-40% of epileptics are refractory to the treatment (Brodie, 2010). Moreover, even when currently available drugs are helpful, they are not without adverse effects (Bialer et al., 2010; Thurman et al., 2011). Therefore, there is an urgent need for novel drugs with improved therapeutic index characterized by increased potency and reduced toxicity.

Retigabine, which stabilizes the open state of KCNQ2-5 channels and shifts the voltage-dependence towards more hyperpolarized potentials (Wuttke et al., 2005), is an FDA approved KCNQ channel activator that serves as an add-on for the treatment of resistant partial-onset seizures (Gunthorpe et al., 2012). However, recently identified side effects of retigabine, including retinal abnormalities, skin discoloration and urinary retention, are significantly limiting its clinical use.

Here, we disclose the preparation and biological analysis of RL648_81 and related analogs, and report that this compound is the most potent KCNQ2/3-specific channel activator known to date. Due to its higher, yet selective agonism on KCNQ2/3 channels, RL648_81 is expected to be more effective at a lower dose than retigabine and its analog, SF0034, in preventing seizures. In addition, RL648_81 does not activate either KCNQ4 or KCNQ5. Because of its enhanced specificity over retigabine, RL648_81 is expected to have fewer side effects.

Although the mechanism by which retigabine-mediated toxicity influences skin and retina remains poorly understood, one hypothesis is that UV radiation may cause photodegradation and oxidation of retigabine's aniline ring, which may lead to the formation of colored deposits in skin and eyes. The incorporation of electron-withdrawing highly fluorinated substituents significantly

Molecular Pharmacology Fast Forward. Published on March 22, 2016 as DOI: 10.1124/mol.115.103200
This article has not been copyedited and formatted. The final version may differ from this version.

reduces the highest occupied molecular orbital energy of RL648_81 (-8.33 eV) vs. retigabine (-8.06 eV), and thus should render the former compound less prone to formation of reactive metabolites (Kawai et al., 2007). The trifluoromethylated RL648_81 is also expected to be more resistant to photodegradation and therefore less toxic to the eye and to the skin (Dow et al.; 2006). In particular, the electronic properties of RL648_81 (Fig. S2C) compared to retigabine (Fig. S2A) suggest that its aniline π-system as well as all three attached nitrogen atoms are considerably more electron-deficient. Furthermore, the CF_3-substituent is a stronger deactivator of the benzylamine π-system, and also presents a greater steric barrier to potential cytochrome P450-induced arene hydroxylation. The electrostatic potential map for RL673_02 (Fig. S2B) and RL648_73 (Fig. S2D) is closely related to that of RL648_81, with the SF_5-substituent in RL673_02 providing even greater steric and electronic deactivation of the compound.

The conserved residue W236 is necessary for the enhancing effect of retigabine, SF0034, and RL648_81 on the gating properties of KCNQ2 channels (Schenzer et al., 2005). Whereas it was thought that the critical property of W was its hydrophobicity (Wuttke et al., 2005), recent studies revealed that the ability of W to form H-bonds with the carbonyl/carbamate oxygen atom present in retigabine makes this contact critical (Kim et al., 2015). These studies suggest that the strength of the H-bond between retigabine and W236 determines the potency of retigabine. In part, the improved potency of SF0034 and RL648_81 is probably due to their ability to form stronger H-bonds with W236 than retigabine. However, besides W265, other residues are important for the gating effects of retigabine, such as L272, L314, and Leu-338 (KCNQ3 numbering) and G301/G340 (KCNQ2/KCNQ3 numbering) (Schenzer et al., 2005; Wuttke et al., 2005; Lange et al., 2009). Thus based on our SAR studies, we also suggest that the activity of analogs can be further modulated by hydrophobic interactions at the benzylamine moiety, which

the carbamate-W236 interaction positions into the vicinity of L272, L314, and L338 (Lange et al., 2008), and that the more lipophilic RL648_81 (logP=3.4) is a better fit than retigabine (logP=2.5) for this hydrophobic pocket at the pore-forming S5 inner loop and S6 helix domains, located near the intracellular voltage-operated gate of KCNQ2–5 channels.

In conclusion, our investigation of fluorinated substituents on retigabine, in particular the effect of highly fluorinated polar and lipophilic CF_3- and SF_5-groups in the benzylamine portion of the KCNQ2-5 channel activator, yielded a series of submicromolar affinity activators with exquisite selectivity for KCNQ2/3. We propose that the combination of increased potency and selectivity of RL648_81, as well as its structural features and modified electrostatic properties, may provide a solution to the problems associated with the undesirable side effects associated with retigabine.

Molecular Pharmacology Fast Forward. Published on March 22, 2016 as DOI: 10.1124/mol.115.103200
This article has not been copyedited and formatted. The final version may differ from this version.

Acknowledgements

We thank Dr. Anastassios Tzingounis for providing KCNQ2/3 mutants and Karen Hartnet for help with cell culture and plasmid preparation.

Authorship Contributions

Participated in research design: MK, PW, EA and TT

Conducted experiments: MK, NR, PW and RL

Contributed new reagents or analytic tools: RL, MK, and EA

Performed data analysis: MK, TT, RL, NR and PW

Wrote or contributed to the writing of the manuscript: MK, EA, PW, RL and TT

References

Alverez C, Arkin MR, Bulfer SL, Colombo R, Kovaliov M, LaPorte MG, Lim C, Liang M, Moore WJ, Neitz RJ, Yan Y, Yue Z, Huryn DM and Wipf P (2015) Structure–Activity Study of Bioisosteric Trifluoromethyl and Pentafluorosulfanyl Indole Inhibitors of the AAA ATPase p97. *ACS Medicinal Chemistry Letters* 6(12): 1225-1230.

Bialer M, Johannessen SI, Levy RH, Perucca E, Tomson T and White HS (2010) Progress report on new antiepileptic drugs: a summary of the Tenth Eilat Conference (EILAT X). *Epilepsy research* 92(2-3): 89-124.

Bialer M and White HS (2010) Key factors in the discovery and development of new antiepileptic drugs. *Nature reviews Drug discovery* 9(1): 68-82.

Biervert C, Schroeder BC, Kubisch C, Berkovic SF, Propping P, Jentsch TJ and Steinlein OK (1998) A potassium channel mutation in neonatal human epilepsy. *Science (New York, NY)* 279(5349): 403-406.

Brodie MJ (2010) Antiepileptic drug therapy the story so far. *Seizure* 19(10): 650-655.

Brown DA and Adams PR (1980) Muscarinic suppression of a novel voltage-sensitive K+ current in a vertebrate neurone. *Nature* 283(5748): 673-676.

Brown DA and Passmore GM (2009) Neural KCNQ (Kv7) channels. *British journal of pharmacology* 156(8): 1185-1195.

Dalby-Brown W, Jessen C, Hougaard C, Jensen ML, Jacobsen TA, Nielsen KS, Erichsen HK, Grunnet M, Ahring PK, Christophersen P, Strobaek D and Jorgensen S (2013)

Characterization of a novel high-potency positive modulator of K(v)7 channels. *European journal of pharmacology* 709(1-3): 52-63.

Davoren JE, Claffey MM, Snow SL, Reese MR, Arora G, Butler CR, Boscoe BP, Chenard L, DeNinno SL, Drozda SE, Duplantier AJ, Moine L, Rogers BN, Rong S, Schuyten K, Wright AS, Zhang L, Serpa KA, Weber ML, Stolyar P, Whisman TL, Baker K, Tse K, Clark AJ, Rong H, Mather RJ and Lowe JA, 3rd (2015) Discovery of a novel Kv7 channel opener as a treatment for epilepsy. *Bioorganic & medicinal chemistry letters* 25(21): 4941-4944.

Dow GS, Heady TN, Bhattacharjee AK, Caridha D, Gerena L, Gettayacamin M, Lanteri CA, Obaldia N, Roncal N, Shearer T, Smith PL, Tungtaeng A, Wolf L, Cabezas M, Yourick D, Smith,KS (2006) "Utility of alkylaminoquinolinyl methanols as new antimalarial drugs." *Antimicrob. Agents Chemother 50*, 4132-4143

Greenwood IA and Ohya S (2009) New tricks for old dogs: KCNQ expression and role in smooth muscle. *British journal of pharmacology* 156(8): 1196-1203.

Gribkoff VK (2008) The therapeutic potential of neuronal K V 7 (KCNQ) channel modulators: an update. *Expert opinion on therapeutic targets* 12(5): 565-581.

Grunnet M, Strobaek D, Hougaard C and Christophersen P (2014) Kv7 channels as targets for anti-epileptic and psychiatric drug-development. *European journal of pharmacology* 726: 133-137.

Gunthorpe MJ, Large CH and Sankar R (2012) The mechanism of action of retigabine (ezogabine), a first-in-class K+ channel opener for the treatment of epilepsy. *Epilepsia* 53(3): 412-424.

Hansen HH, Waroux O, Seutin V, Jentsch TJ, Aznar S and Mikkelsen JD (2008) Kv7 channels: interaction with dopaminergic and serotonergic neurotransmission in the CNS. *The Journal of physiology* 586(7): 1823-1832.

Howard RJ, Clark KA, Holton JM and Minor DL, Jr. (2007) Structural insight into KCNQ (Kv7) channel assembly and channelopathy. *Neuron* 53(5): 663-675.

Iannotti FA, Barrese V, Formisano L, Miceli F and Taglialatela M (2013) Specification of skeletal muscle differentiation by repressor element-1 silencing transcription factor (REST)-regulated Kv7.4 potassium channels. *Molecular biology of the cell* 24(3): 274-284.

Iannotti FA, Panza E, Barrese V, Viggiano D, Soldovieri MV and Taglialatela M (2010) Expression, localization, and pharmacological role of Kv7 potassium channels in skeletal muscle proliferation, differentiation, and survival after myotoxic insults. *The Journal of pharmacology and experimental therapeutics* 332(3): 811-820.

Jankovic S and Ilickovic I (2013) The preclinical discovery and development of ezogabine for the treatment of epilepsy. *Expert opinion on drug discovery* 8(11): 1429-1437.

Jentsch TJ (2000) Neuronal KCNQ potassium channels: physiology and role in disease. *Nature reviews Neuroscience* 1(1): 21-30.

Kalappa BI, Soh H, Duignan KM, Furuya T, Edwards S, Tzingounis AV and Tzounopoulos T (2015) Potent KCNQ2/3-specific channel activator suppresses in vivo epileptic activity and prevents the development of tinnitus. *The Journal of neuroscience : the official journal of the Society for Neuroscience* 35(23): 8829-8842.

Kawai, M, Sakurada I, Morita A, Iwamuro Y, Ando K, Omura H, Sakakibara S, Masuda T, Koike H, Honma T, Hattori K, Takashima T, Mizuno K, Mizutani M, Kawamura M (2007) "Structure-activity relationship study of novel NR2B-selective antagonists with arylamides to avoid reactive metabolites formation." *Bioorg. Med. Chem. Lett. 17*, 5537-5542.

Kharkovets T, Hardelin JP, Safieddine S, Schweizer M, El-Amraoui A, Petit C and Jentsch TJ (2000) KCNQ4, a K+ channel mutated in a form of dominant deafness, is expressed in the inner ear and the central auditory pathway. *Proceedings of the National Academy of Sciences of the United States of America* 97(8): 4333-4338.

Kim RY, Yau MC, Galpin JD, Seebohm G, Ahern CA, Pless SA and Kurata HT (2015) Atomic basis for therapeutic activation of neuronal potassium channels. *Nature communications* 6: 8116.

Lange W, Geißendorfer J, Schenzer A, Grotzinger J, Seebohm G,Friedrich T, and Michael Schwake M (2008) Refinement of the Binding Site and Mode of Action of the Anticonvulsant Retigabine on KCNQ K_ Channels. *Molecular pharmacology* 75(2): 272-80.

Li S, Choi V and Tzounopoulos T (2013) Pathogenic plasticity of Kv7.2/3 channel activity is essential for the induction of tinnitus. *Proceedings of the National Academy of Sciences of the United States of America* 110(24): 9980-9985.

Li S, Kalappa BI and Tzounopoulos T (2015) Noise-induced plasticity of KCNQ2/3 and HCN channels underlies vulnerability and resilience to tinnitus. *eLife* 4.

Li, Y., Gamper, N., Hilgemann, D.W. & Shapiro, M.S. (2005) Regulation of Kv7 (KCNQ) K+ channel open probability by phosphatidylinositol 4,5-bisphosphate. *The Journal of neuroscience : the official journal of the Society for Neuroscience*, **25**, 9825-9835.

Miceli F, Soldovieri MV, Martire M and Taglialatela M (2008) Molecular pharmacology and therapeutic potential of neuronal Kv7-modulating drugs. *Current opinion in pharmacology* 8(1): 65-74.

Mo T, Mi X, Milner EE, Dow GS and Wipf P (2010) Synthesis of an 8-pentafluorosulfanyl analog of the antimalarial agent mefloquine. *Tetrahedron Letters* 51(39): 5137-5140.

Munro G and Dalby-Brown W (2007) Kv7 (KCNQ) channel modulators and neuropathic pain. *Journal of medicinal chemistry* 50(11): 2576-2582.

Robbins J (2001) KCNQ potassium channels: physiology, pathophysiology, and pharmacology. *Pharmacology & therapeutics* 90(1): 1-19.

Schenzer A, Friedrich T, Pusch M, Saftig P, Jentsch TJ, Grotzinger J and Schwake M (2005) Molecular determinants of KCNQ (Kv7) K+ channel sensitivity to the anticonvulsant retigabine. *The Journal of neuroscience : the official journal of the Society for Neuroscience* 25(20): 5051-5060.

Sharma AK, Rani E, Waheed A and Rajput SK (2015) Pharmacoresistant Epilepsy: A Current Update on Non-Conventional Pharmacological and Non-Pharmacological Interventions. *Journal of epilepsy research* 5(1): 1-8.

Skoda EM, Sacher JR, Kazancioglu MZ, Saha J and Wipf P (2014) An uncharged oxetanyl sulfoxide as a covalent modifier for improving aqueous solubility. *ACS Med Chem Lett* 5(8): 900-904.

Soh H and Tzingounis AV (2010) The specific slow afterhyperpolarization inhibitor UCL2077 is a subtype-selective blocker of the epilepsy associated KCNQ channels. *Molecular pharmacology* 78(6): 1088-1095.

Sprachman MM and Wipf P (2012) A bifunctional dimethylsulfoxide substitute enhances the aqueous solubility of small organic molecules. *Assay and drug development technologies* 10(3): 269-277.

Stott JB, Jepps TA and Greenwood IA (2014) K(V)7 potassium channels: a new therapeutic target in smooth muscle disorders. *Drug discovery today* 19(4): 413-424.

Tatulian L, Delmas P, Abogadie FC and Brown DA (2001) Activation of expressed KCNQ potassium currents and native neuronal M-type potassium currents by the anti-convulsant drug retigabine. *The Journal of neuroscience : the official journal of the Society for Neuroscience* 21(15): 5535-5545.

Thurman DJ, Beghi E, Begley CE, Berg AT, Buchhalter JR, Ding D, Hesdorffer DC, Hauser WA, Kazis L, Kobau R, Kroner B, Labiner D, Liow K, Logroscino G, Medina MT, Newton CR, Parko K, Paschal A, Preux PM, Sander JW, Selassie A, Theodore W, Tomson T and Wiebe S (2011) Standards for epidemiologic studies and surveillance of epilepsy. *Epilepsia* 52 Suppl 7: 2-26.

Wickenden AD and McNaughton-Smith G (2009) Kv7 channels as targets for the treatment of pain. *Current pharmaceutical design* 15(15): 1773-1798.

Wipf P, Mo T, Geib SJ, Caridha D, Dow GS, Gerena L, Roncal N and Milner EE (2009) Synthesis and biological evaluation of the first pentafluorosulfanyl analogs of mefloquine. *Organic & Biomolecular Chemistry* 7(20): 4163-4165.

Wulff H, Castle NA and Pardo LA (2009) Voltage-gated potassium channels as therapeutic targets. *Nature reviews Drug discovery* 8(12): 982-1001.

Wuttke TV, Seebohm G, Bail S, Maljevic S and Lerche H (2005) The new anticonvulsant retigabine favors voltage-dependent opening of the Kv7.2 (KCNQ2) channel by binding to its activation gate. *Molecular pharmacology* 67(4): 1009-1017.

Xiong Q, Gao Z, Wang W and Li M (2008) Activation of Kv7 (KCNQ) voltage-gated potassium channels by synthetic compounds. *Trends in pharmacological sciences* 29(2): 99-107.

Footnotes

This work was supported by the Department of Defense, the Joint Warfighter Medical Research Program [W81XWH-14-1-0117] to T.T. and P.W..

Molecular Pharmacology Fast Forward. Published on March 22, 2016 as DOI: 10.1124/mol.115.103200
This article has not been copyedited and formatted. The final version may differ from this version.

Figure Legends

Figure 1. Zone SAR model of retigabine analogs.

Figure 2. Structure and classification of 1st generation compounds. Three classes of 1st generation KCNQ channel activators were synthesized based on our zone model. In class I and II, modifications were made in zone 1, in class III zone 3 was varied.

Figure 3. SF0034 is five-times more potent than retigabine in activating KCNQ2/3 channel currents. CHO cells transiently expressing heterologous KCNQ2/3 channels were clamped at -85 mV and KCNQ2/3 currents were elicited by 1 s depolarization step, in 10 mV increments, from -105 to +15 mV followed by return step to -70 mV; the voltage protocol is shown below A1. **A_1, B_1,** Representative current traces of KCNQ2/3 channels recorded at increasing membrane potentials in absence and presence of 100 nM retigabine (A_1) and 100 nM SF0034 (B_1). **A_2, B_2.** Representative curves of normalized G-V relationship of KCNQ2/3 currents at control and at increasing concentration of retigabine (A_2) and SF0034 (B_2). **C**. Summary bar graph representing half activation ($V_{1/2}$) of KCNQ2/3 currents calculated from normalized G-V Boltzmann curves at control and at increasing concentration of retigabine and SF0034. SF0034 at 100 nM significantly shifts the $V_{1/2}$ of KCNQ2/3 currents from control, whereas retigabine failed to show an effect at a 100 nM concentration. **D.** Representative curves showing the half activation shift ($\Delta V_{1/2}$) by retigabine with EC_{50} 3.3± 0.8 μM (n=4-11, black) and SF004 with EC_{50} 0.60 ± 0.06 μM (n=5-21, red) in a concentration dependent manner (100 nM – 30 μM). Curves were fitted with a hill equation and EC_{50} values were calculated. Error bars represent

Molecular Pharmacology Fast Forward. Published on March 22, 2016 as DOI: 10.1124/mol.115.103200
This article has not been copyedited and formatted. The final version may differ from this version.

mean ± SEM. ** p <0.01, *** p <0.001. Detailed values in supplemental data (Values for main figures).

Figure 4. Addition of a trifluoromethyl group at the 3- or 4-position of phenyl ring in zone 1 significantly increased the potency in activating KCNQ2/3 currents. CHO cells transiently expressing heterologous KCNQ2/3 channels were clamped at -85 mV and KCNQ2/3 currents were elicited by 1 s depolarization step, in 10 mV increments, from -105 to +15 mV followed by return step to -70 mV; the voltage protocol is shown below A1. **A-D$_1$.** Representative current traces of KCNQ2/3 channels recorded at increasing membrane potentials in absence and in presence of 100 nM NR561_40 (A_1), 100 nM NR561_50 (B_1), 100 nM NR579_04 (C_3) and 100 nM NR561_62 (D_1). **A-D$_2$.** Representative curves of normalized G-V relationship of KCNQ2/3 currents at control and at increasing concentration of NR561_40 (A_2), NR561_50 (B_2), NR579_04 (C_2) and NR561_62 (D_2). **A-D$_3$.** Summary bar graphs representing half activation ($V_{1/2}$) of KCNQ2/3 currents calculated from normalized G-V Boltzmann curves at control and at increasing concentration of NR561_40 (A_3), NR561_50 (B_3), NR579_04 (C_3) and NR561_62 (D_3). **A-D$_4$.** Representative curves showing half activation shift ($\Delta V_{1/2}$) by NR561_40 (EC_{50} 0.91 ± 0.08 µM, n=4-8; red) (A_4), by NR561_50 (EC_{50} 0.74 ± 0.07 µM, n=4-9; red) (B_4), by NR579_04 (EC_{50} NA, n=4-9; Red) (C_4) and by NR561_62 (EC_{50} 1.48 ± 0.18 µM, n=4-9; Red) (D4). NR561_40 and NR561_50 showed similar potency as of SF0034 in activating KCNQ2/3 channel currents. NR561_62 showed 2-3 times lower potency than SF0034 whereas NR579_04 did not activate KCNQ2/3 currents at all. Curves were fitted with a hill equation and EC50 values were calculated. Error bars represent mean ± SEM. * p <0.05, ** p <0.01. Detailed values in supplemental data (Values for main figures).

Molecular Pharmacology Fast Forward. Published on March 22, 2016 as DOI: 10.1124/mol.115.103200
This article has not been copyedited and formatted. The final version may differ from this version.

Figure 5. Summary bar graphs representing (A) EC_{50} and (B) maximal (max) $\Delta V_{1/2}$ of first generation compounds tested at KCNQ2/3 channels. Like SF0034, first generation class I compounds NR561_40, NR561_50 and NR561_29 showed 4-5 times higher potency than retigabine in activating KCNQ2/3 channel currents. However, NR561_29 showed significant lower max $\Delta V_{1/2}$ compared to retigabine and SF0034. EC_{50} is the concentration of the compound that produces a half-maximal shift in $V_{1/2}$. Max $\Delta V_{1/2}$ is the shift in $V_{1/2}$ caused by 10 μM of the tested compound. Detailed values in supplemental data (Values for main figures).

Figure 6. NR561_50 does not activate KCNQ4 and KCNQ5 channel currents. CHO cells transiently expressing heterologous homomeric KCNQ4 or KCNQ5 channels were clamped at -85 mV and currents were elicited by 1 s depolarization step, in 10 mV increments, from -105 to +15 mV followed by return step to -70 mV; the voltage protocol is shown below A1. **A_1**, **B_1** Representative current traces of KCNQ4 (A_1) and KCNQ5 (B_1) channels recorded at increasing membrane potentials in absence and in presence of 100 nM NR561_50. **A_2**, **B_2.** Representative curves of normalized G-V relationship of KCNQ4 (B_1) and KCNQ5 (B_2) currents at control, 100 nM and 1 μM NR561_50. **A_3**, **B_3**. Summary bar graph representing half activation voltage ($V_{1/2}$) of KCNQ4 (A_3) and KCNQ5 (B_3) channel currents calculated from normalized G-V Boltzmann curves at control, 100 nM and 1 μM NR561_50. **C_1**, **D_1**. Representative current traces of KCNQ4 (C_1) and KCNQ5 (D_1) channels recorded at increasing membrane potentials in absence and in presence of 100 nM NR561_40. **C_2**, **D_2**. Representative curves of normalized G-V relationship of KCNQ4 (C_2) and KCNQ5 (D_2) currents at control, 100 nM and 1 μM NR561_40. **C_3**, **D_3**. Summary bar graph representing half activation voltage ($V_{1/2}$) of KCNQ4 (C_3) and KCNQ5 (D_3)

Molecular Pharmacology Fast Forward. Published on March 22, 2016 as DOI: 10.1124/mol.115.103200
This article has not been copyedited and formatted. The final version may differ from this version.

channel currents calculated from normalized G-V Boltzmann curves at control, 100 nM and 1 μM NR561_40. **E_1, F_1** Representative current traces of KCNQ4 (E_1) and KCNQ5 (F_1) channel recorded at increasing membrane potentials in absence and in presence of 100 nM NR561_40. **E_2., F_2.** Representative curves of normalized G-V relationship of KCNQ4 (E_2) and KCNQ5 (F_2) currents at control, 100 nM and 1 μM NR561_40. **E_3, F_3.** Summary bar graph representing half activation voltage ($V_{1/2}$) of KCNQ4 **(E_3)** and KCNQ5 (**F_3)** channel currents calculated from normalized G-V Boltzmann curves at control, 100 nM and 1 μM NR561_40. Error bars represent mean ± SEM. **p* <0.05, ***p* <0.01. Detailed values in supplemental data (Values for main figures).

Figure 7. Structures of 2nd generation compounds synthesized. Addition of a fluorine atom in zone 2 resulted in RL648_73, RL648_81, RL648_86, and RL673_02.

Figure 8. RL648_81 is three times more potent than SF0034 in activating KCNQ2/3 channel currents and does not potentiate KCNQ4 and KCNQ5 channel currents. CHO cells transiently expressing heterologous KCNQ2/3 channels or homomeric KCNQ4 and KCNQ5 channels were clamped at -85 mV and currents were elicited by 1 s depolarization step, in 10 mV increments, from -105 to +15 mV followed by return step to -70 mV; the voltage protocol is shown in A1 (left). **A_1.** Representative current traces of KCNQ2/3 channels recorded at increasing membrane potentials in absence and presence of 100 nM or 1 μM RL648_81. **A_2.** Representative curves of normalized G-V relationship of KCNQ2/3 currents at control and at increasing concentration of RL648_81. **A_3.** Summary bar graph representing half activation ($V_{1/2}$) of KCNQ2/3 currents calculated from normalized G-V Boltzmann curves at control and at

Molecular Pharmacology Fast Forward. Published on March 22, 2016 as DOI: 10.1124/mol.115.103200
This article has not been copyedited and formatted. The final version may differ from this version.

increasing concentration of RL648_81 **A_4.** Representative curves showing half activation voltage shift ($\Delta V1/2$) by RL648_81 (EC_{50} 0.19 ± 0.02 µM, n=4-11; red) and SF0034 (EC_{50} 0.60 ± 0.06 µM, n=5-21; black) in a concentration dependent manner (100 nM – 30 µM). Curves were fitted with a hill equation and EC_{50} values were calculated. **B_1.** Representative current traces of KCNQ4 currents at increasing membrane potentials in absence and in presence of 100 nM RL648_81. **B_2.** Representative curves of normalized G-V relationship of KCNQ4 currents at control, 100 nM, 1 µM and 10 µM NR648_81. **B_3.** Summary bar graph representing half activation voltage ($V_{1/2}$) of KCNQ4 currents calculated from normalized G-V relationship curves at control, 100 nM, 1 µM and 10 µM RL648_81**. C_1.** Representative current traces of KCNQ5 currents at increasing membrane potentials absence and presence of 100 nM RL648_81. **C_2.** Representative curves of normalized G-V relationship of KCNQ5 currents at control, 100 nM, 1 µM and 10 µM NR648_81. **C_3.** Summary bar graph representing half activation voltage ($V_{1/2}$) of KCNQ5 currents calculated from normalized G-V Boltzmann curves at control, 100 nM, 1 µM and 10 µM RL648_81. **D.** Summary bar graphs representing EC_{50} and maximal $\Delta V_{1/2}$ values of second generation compounds tested at KCNQ2/3 channels in comparison with SF0034. RL648_73 and RL_86 showed 2 times higher potency than SF0034 in activating KCNQ2/3 channels. **E.** Summary bar graph representing half activation ($V_{1/2}$) of KCNQ4 currents calculated from normalized G-V Boltzmann curves in presence of 100 nM, 1 µM and 10 µM of RL648_73, RL648_86 and RL673_02. **F.** Summary bar graph representing half activation voltage ($V_{1/2}$) of KCNQ5 currents calculated from normalized G-V Boltzmann curves in presence of 100 nM, 1 µM and 10 µM of RL648_73, RL648_86 and RL673_02. Error bars represent mean ± SEM. **p* <0.05, ****p* <0.001. Detailed values in supplemental data (Values for main figures).

Molecular Pharmacology Fast Forward. Published on March 22, 2016 as DOI: 10.1124/mol.115.103200
This article has not been copyedited and formatted. The final version may differ from this version.

Figure 9 Conserved residue tryptophan at S5 of KCNQ2-5 subunit is critical for potentiation effect of RL648_81 at KCNQ2 currents. CHO cells transiently expressing homomeric KCNQ2WT and KCNQ2(W236L) channels were clamped at -85 mV and currents were elicited by 1 s depolarization step, in 10 mV increments, from -105 to +15 mV followed by return step to -70 mV; the voltage protocol is shown below A1. **A_1, B_1**, Representative current traces of KCNQ2WT (A_1) and KCNQ2(W236L) (B_1) channels recorded at increasing membrane potentials in absence and presence of 10 μM RL648_81. **A_2, B_2**. Representative curves of normalized G-V (conductance-voltage) relationship of KCNQ2WT (A_2) and KCNQ2(W236L) (B_2) currents at control and at increasing concentration of RL648_81. **C_1, C_2**. Summary bar graph representing half activation ($V_{1/2}$) of KCNQ2WT (C_1) and KCNQ2(W236L) (C_2) calculated from normalized G-V Boltzmann curves at control and at increasing concentration of RL648_81. Mutation of W236L at KCNQ2 subunit abolished the potentiation effect of RL648_81 at KCNQ2 currents. Error bars represent mean ± SEM. **p* <0.05, ***p* <0.01. Detailed values in supplemental data (Values for main figures).

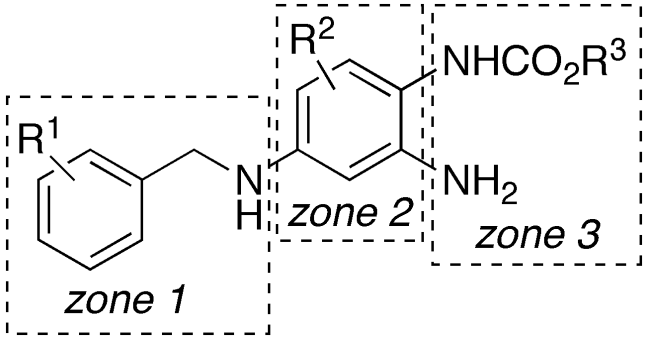

Figure 1.

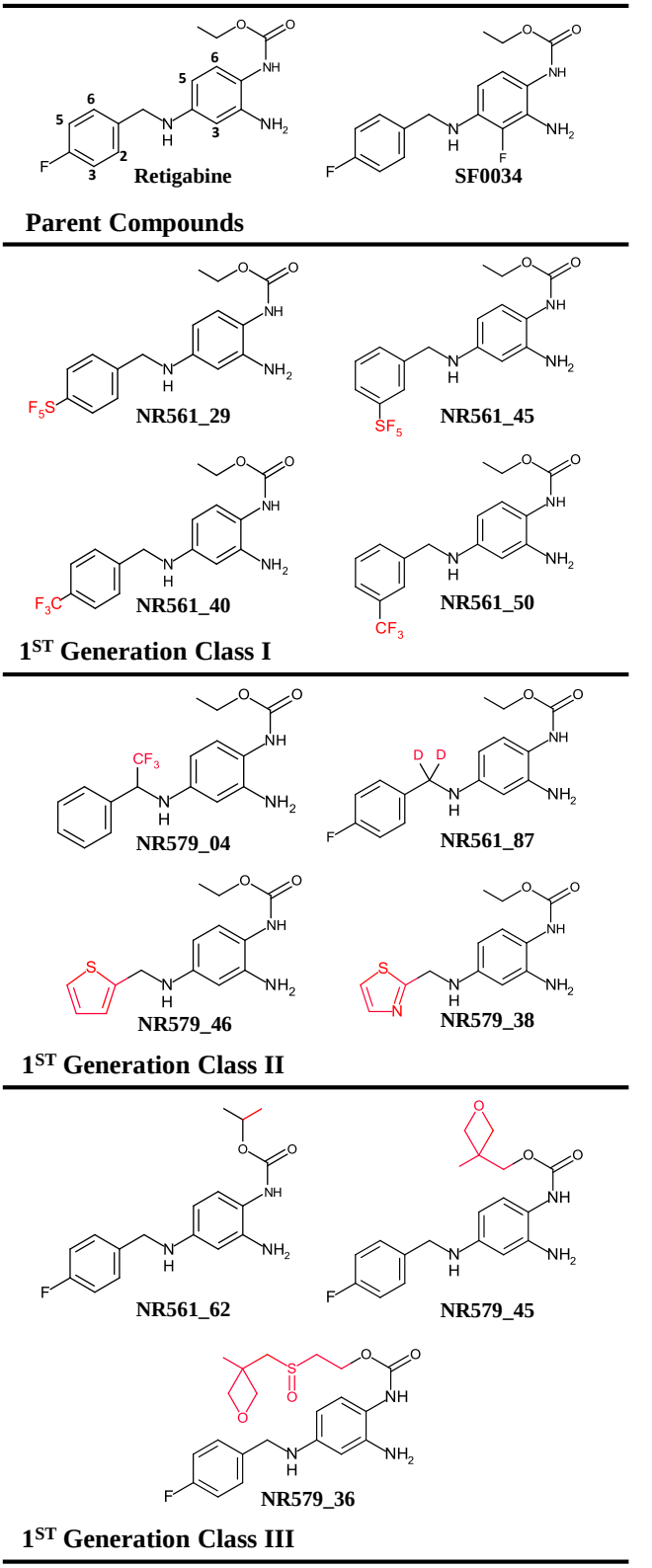
Retigabine
SF0034
Parent Compounds
NR561_29
NR561_45
NR561_40
NR561_50
1ST Generation Class I
NR579_04
NR561_87
NR579_46
NR579_38
1ST Generation Class II
NR561_62
NR579_45
NR579_36
1ST Generation Class III

Figure 2.

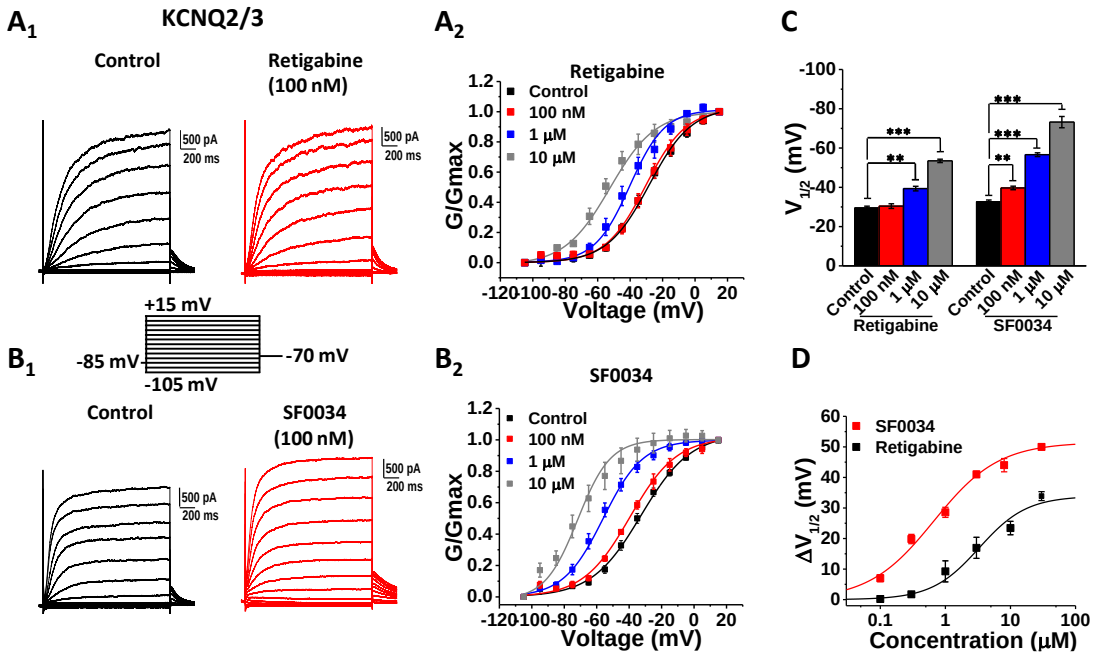
A1
KCNQ2/3
Control
Retigabine
(100 nM)
500 pA
200 ms
+15 mV
-85 mV
-70 mV
-105 mV
B1
Control
SF0034
(100 nM)
A2
Retigabine
Control
100 nM
1 μM
10 μM
G/Gmax
Voltage (mV)
B2
SF0034
C
V1/2 (mV)
Control
100 nM
1 μM
10 μM
Retigabine
SF0034
D
SF0034
Retigabine
ΔV1/2 (mV)
Concentration (μM)

Figure 3.

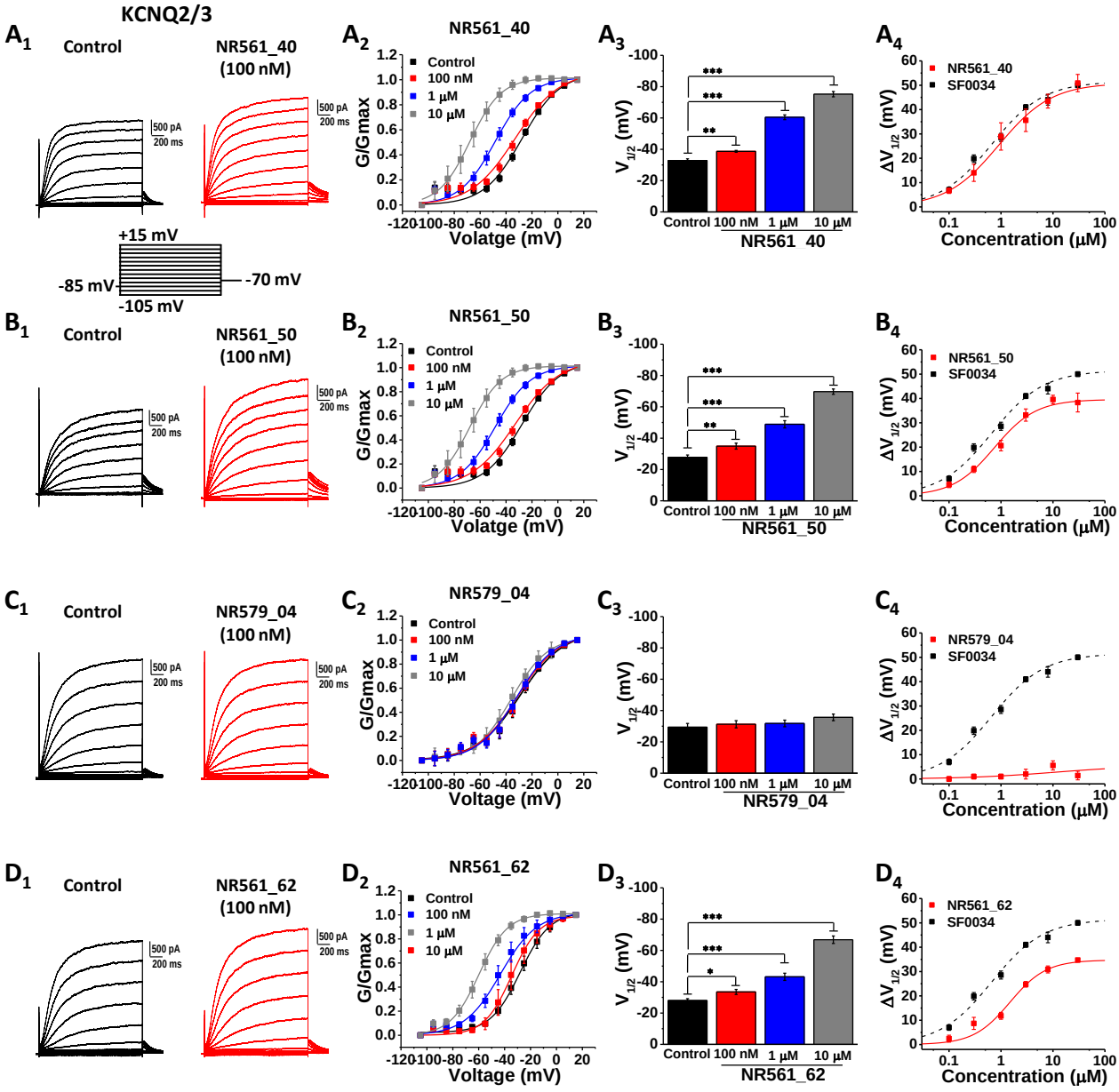
KCNQ2/3
A1
Control
NR561_40
(100 nM)
500 pA
200 ms
+15 mV
-85 mV
-70 mV
-105 mV
A2
NR561_40
Control
100 nM
1 μM
10 μM
G/Gmax
Volatge (mV)
A3
V1/2 (mV)
Control 100 nM 1 μM 10 μM
NR561_40
A4
NR561_40
SF0034
ΔV1/2 (mV)
Concentration (μM)
B1
Control
NR561_50
(100 nM)
B2
NR561_50
B3
NR561_50
B4
NR561_50
SF0034
C1
Control
NR579_04
(100 nM)
C2
NR579_04
Voltage (mV)
C3
NR579_04
C4
NR579_04
SF0034
D1
Control
NR561_62
(100 nM)
D2
NR561_62
D3
NR561_62
D4
NR561_62
SF0034

Figure 4.

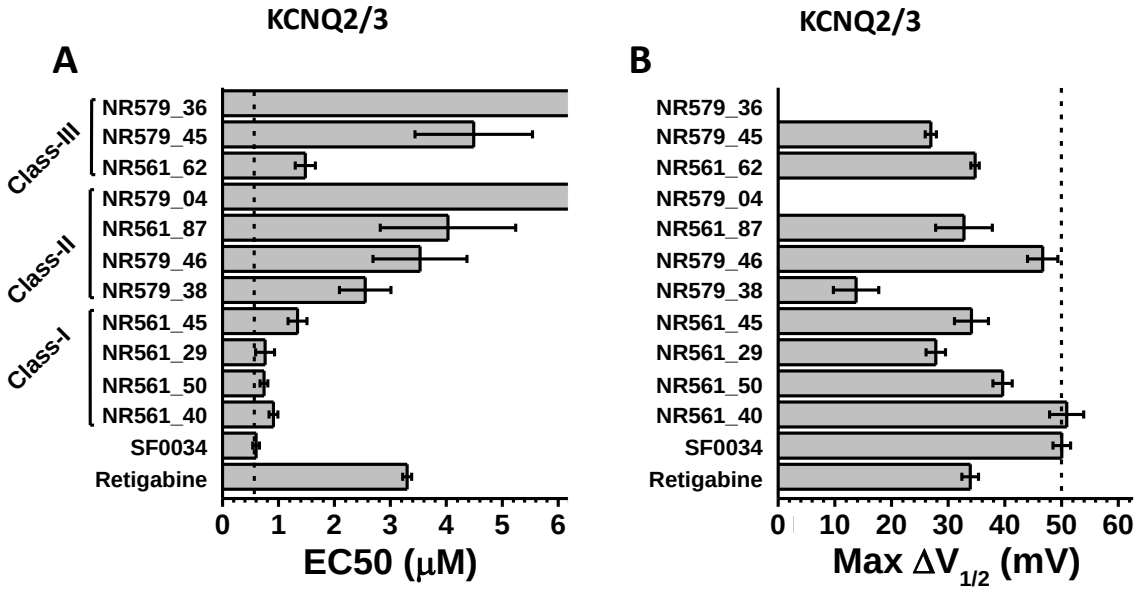
KCNQ2/3
A
Class-III
Class-II
Class-I
NR579_36
NR579_45
NR561_62
NR579_04
NR561_87
NR579_46
NR579_38
NR561_45
NR561_29
NR561_50
NR561_40
SF0034
Retigabine
0 1 2 3 4 5 6
EC50 (μM)
KCNQ2/3
B
NR579_36
NR579_45
NR561_62
NR579_04
NR561_87
NR579_46
NR579_38
NR561_45
NR561_29
NR561_50
NR561_40
SF0034
Retigabine
0 10 20 30 40 50 60
Max ΔV1/2 (mV)

Figure 5.

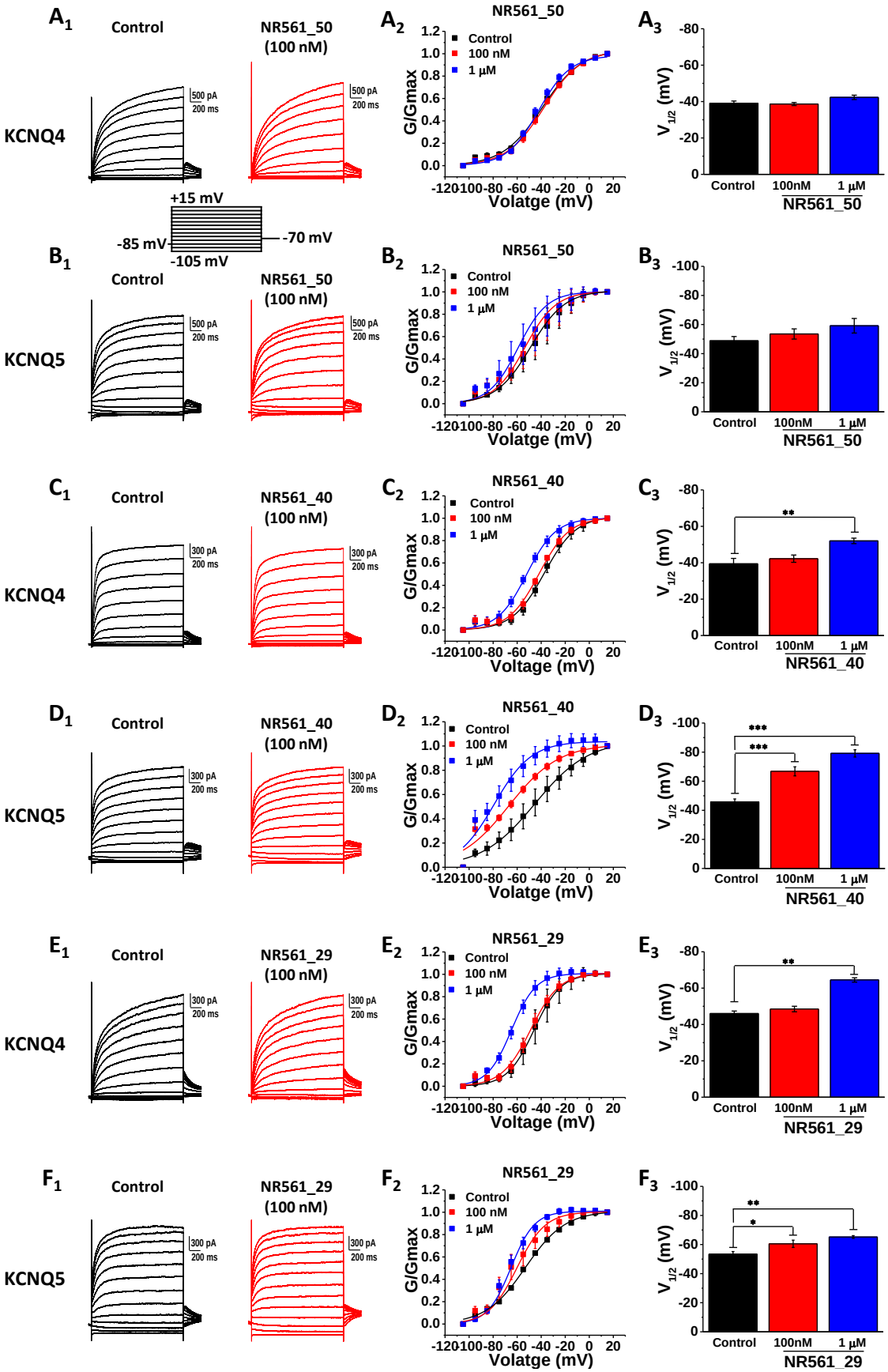
A1
Control
NR561_50
(100 nM)
KCNQ4
500 pA
200 ms
+15 mV
-85 mV
-70 mV
-105 mV
A2
NR561_50
Control
100 nM
1 μM
G/Gmax
Volatge (mV)
A3
V1/2 (mV)
Control
100nM
1 μM
NR561_50
B1
Control
NR561_50
(100 nM)
KCNQ5
B2
NR561_50
B3
C1
Control
NR561_40
(100 nM)
KCNQ4
300 pA
200 ms
C2
NR561_40
Voltage (mV)
C3
**
D1
Control
NR561_40
(100 nM)
KCNQ5
D2
NR561_40
D3
***
***
E1
Control
NR561_29
(100 nM)
KCNQ4
E2
NR561_29
E3
**
F1
Control
NR561_29
(100 nM)
KCNQ5
F2
NR561_29
F3
**
*

Figure 6.

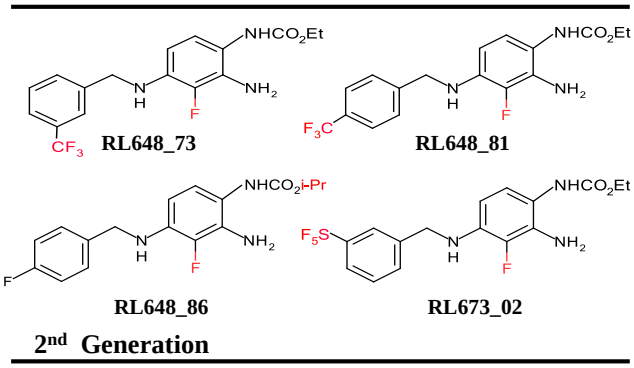

Figure 7.

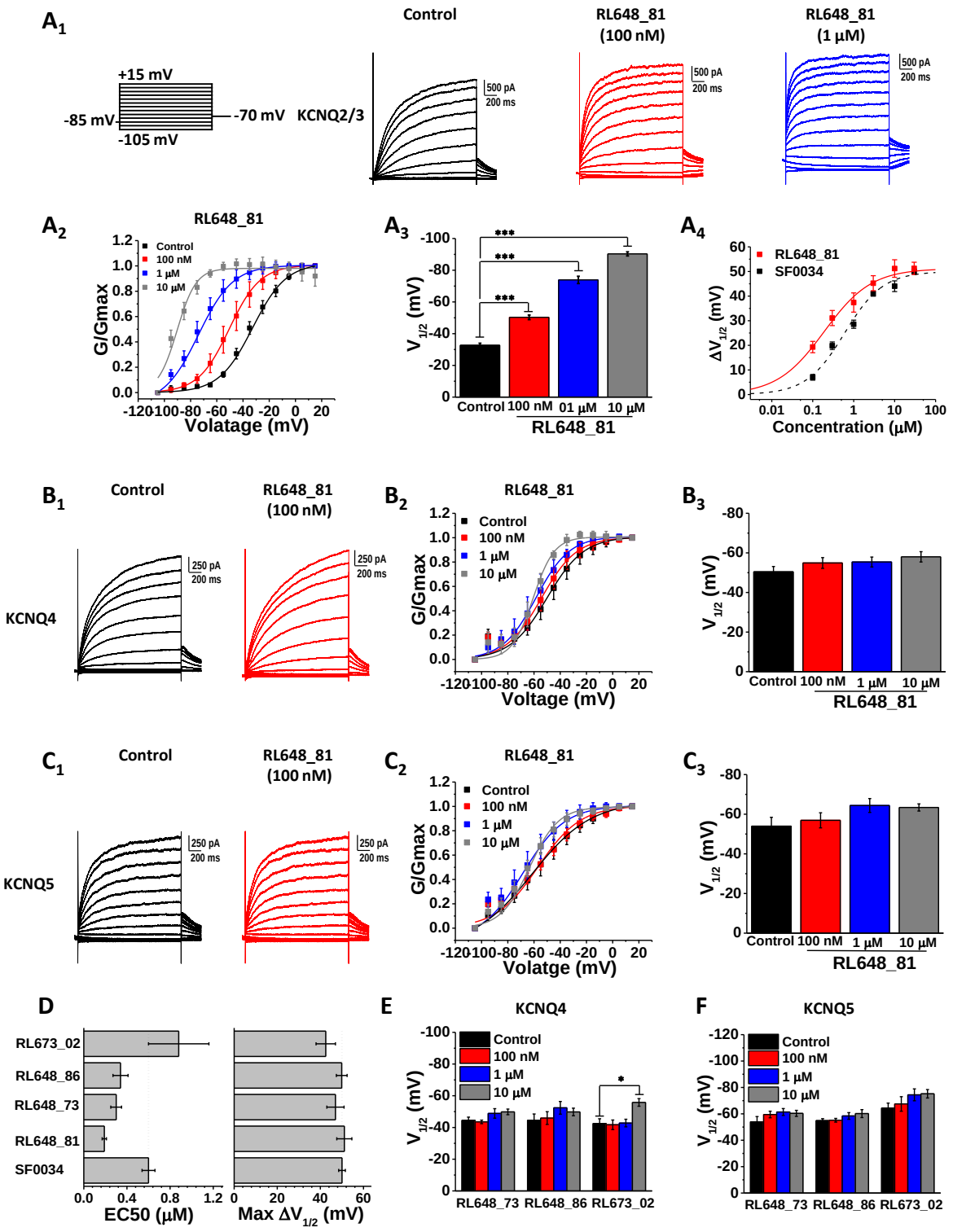
A1
Control
RL648_81 (100 nM)
RL648_81 (1 μM)
+15 mV
-85 mV
-70 mV
-105 mV
KCNQ2/3
500 pA
200 ms
A2
RL648_81
Control
100 nM
1 μM
10 μM
G/Gmax
Volatage (mV)
A3
V1/2 (mV)
Control
100 nM
01 μM
10 μM
RL648_81
A4
RL648_81
SF0034
ΔV1/2 (mV)
Concentration (μM)
B1
Control
RL648_81 (100 nM)
KCNQ4
250 pA
200 ms
B2
RL648_81
Voltage (mV)
B3
C1
Control
RL648_81 (100 nM)
KCNQ5
C2
RL648_81
Volatge (mV)
C3
D
RL673_02
RL648_86
RL648_73
RL648_81
SF0034
EC50 (μM)
Max ΔV1/2 (mV)
E
KCNQ4
RL648_73
RL648_86
RL673_02
F
KCNQ5

Figure 8.

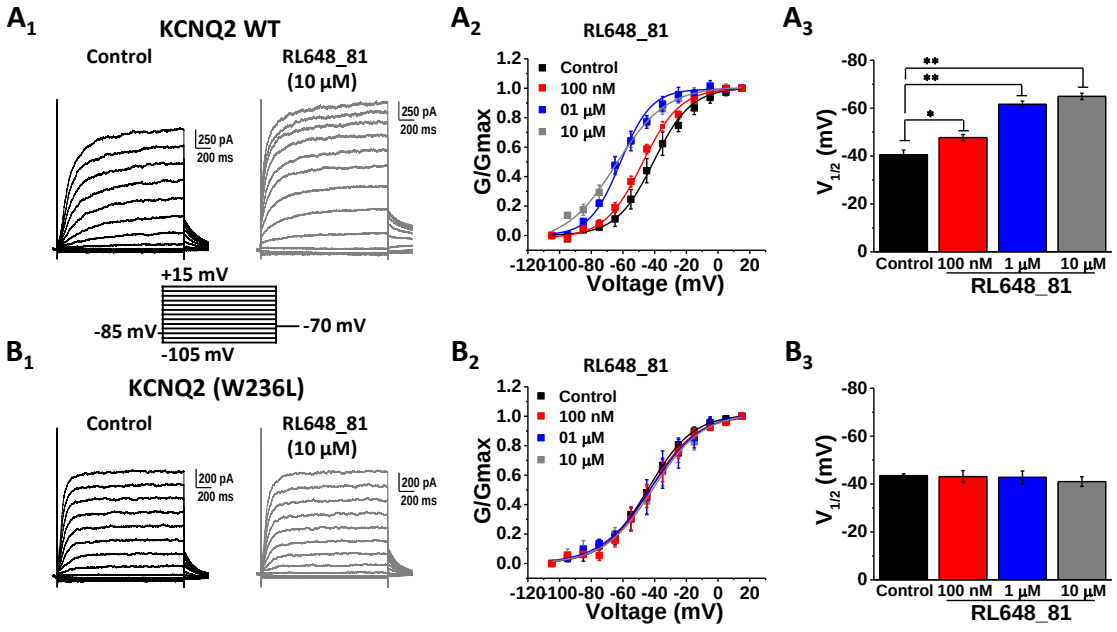
A1
KCNQ2 WT
Control
RL648_81
(10 µM)
250 pA
200 ms
250 pA
200 ms
+15 mV
-85 mV
-70 mV
-105 mV
A2
RL648_81
Control
100 nM
01 µM
10 µM
G/Gmax
Voltage (mV)
A3
V1/2 (mV)
Control
100 nM
1 µM
10 µM
RL648_81
B1
KCNQ2 (W236L)
Control
RL648_81
(10 µM)
200 pA
200 ms
200 pA
200 ms
B2
RL648_81
Control
100 nM
01 µM
10 µM
G/Gmax
Voltage (mV)
B3
V1/2 (mV)
Control
100 nM
1 µM
10 µM
RL648_81

Figure 9.

Molecular Pharmacology

Supplemental Data

Synthesis and Evaluation of Potent KCNQ2/3-specific Channel Activators

Manoj Kumar[1], Nicholas Reed[2], Ruiting Liu[2], Elias Aizenman[3,4], Peter Wipf[2] and Thanos Tzounopoulos[1,3]

1: Department of Otolaryngology, University of Pittsburgh School of Medicine, Pittsburgh, Pennsylvania 15261

2: Department of Chemistry, University of Pittsburgh, Pittsburgh, Pennsylvania 15260

3: Department of Neurobiology, University of Pittsburgh, Pittsburgh, Pennsylvania 15261

4: Pittsburgh Institute for Neurodegenerative Diseases, University of Pittsburgh School of Medicine

Synthetic Route A:

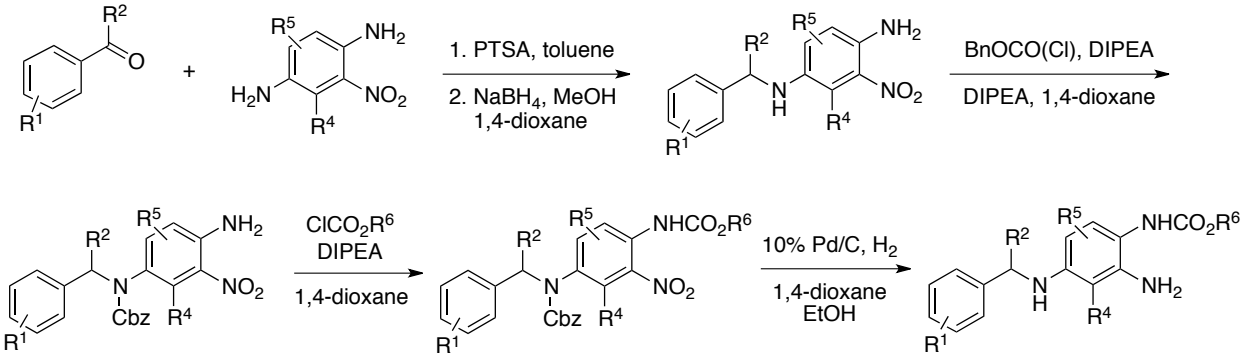

Synthetic Route B:

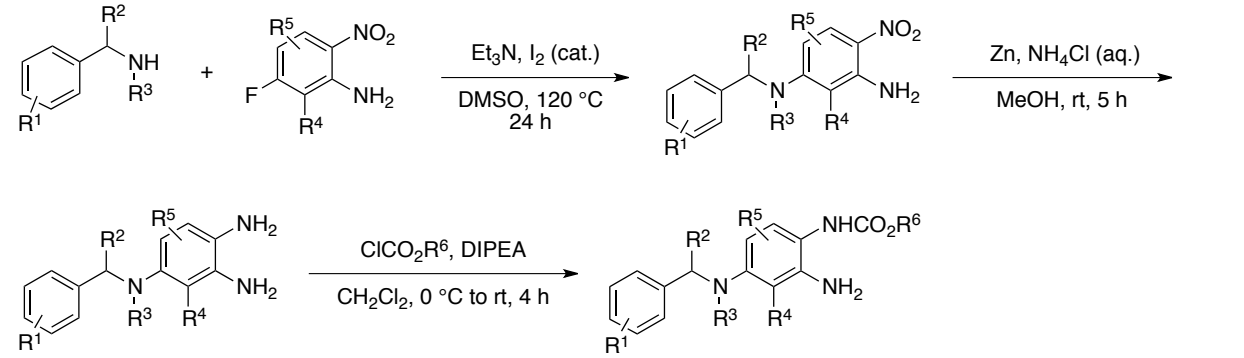

Figure S1.

Figure S1. General synthetic scheme for the analog synthesis.

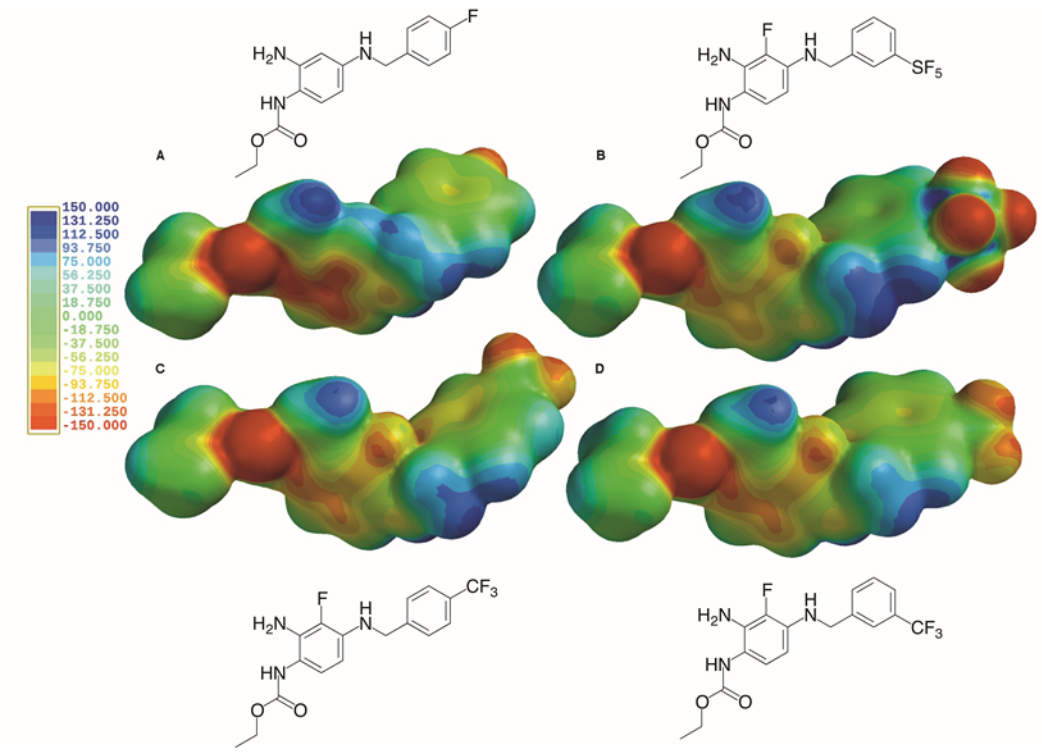

Figure S2.

Figure S2. Combined steric and electronic features of retigabine and new KCNQ2/3-specific channel activators, illustrating the effects of fluorinations on the aromatic rings and their substituents. A: retigabine; **B:** RL673_02; **C:** RL648_81; **D:** RL648_73. The color coding on the electron-density surface reflects the electrostatic potential experienced by a positive probe charge (red=attractive to blue=repulsive). Electron-density surfaces encoded with electrostatic potential maps were calculated in Spartan 10 (Wave Function, Inc., Irvine, CA) with PM6 parametrization. Compared to retigabine (Fig. S2A), RL648_81 (Fig. S2C) has an electron-depleted aniline aromatic system, which also influences the electron density in the attached three nitrogen atoms, decreasing their negative partial charges. The CF_3-substituent in RL648_81 is a stronger deactivator of the benzylamine π-system, but, in particular, increases steric bulk at this

terminus of the molecule and would be expected to pose a steeper steric barrier to cytochrome P450-induced arene hydroxylation and compound metabolism. The electrostatic potential maps for RL673_02 (Fig. S2B) and RL648_73 (Fig. S2D) are also shown for comparison. Both are closely related to that of RL648_81 at the carbamate termini, but show steric and electronic differences in the benzylamine region. The SF_5-substituent in RL673_02 provides the largest steric barrier and electronic deactivation in this series.

Compound	**KCNQ2/3**		**KCNQ4 Max $\Delta V_{1/2}$ (mV)**	**KCNQ5 Max $\Delta V_{1/2}$ (mV)**
	EC50 (μM)	**$\Delta V_{1/2}$ (mV)**		
Retigabine	3.3 ± .08	33.9 ± 1.5	Not Tested (NT)	NT
SF0034	0.06 ± 0.6	50.1 ± 1.6	NT	NT
NR561_40	0.91 ± .08	50.9 ± 3.1	12.7 ± .75	29.7 ± 3.5
NR561_50	0.74 ± .07	39.6 ± 1.7	2.7 ± .85	5.6 ± 1.6
NR561_29	0.76 ± .17	27.8 ± 1.7	19.4 ± 1.7	9.5 ± 1.7
NR561_45	1.34 ± .17	34.1 ± 2.9	NT	NT
NR579_38	2.55 ± .46	13.7 ± 3.9	NT	NT
NR579_46	3.53 ± .54	46.7 ± 2.6	NT	NT
NR561_87	4.03 ± 1.2	32.8 ± 4.9	NT	NT
NR579_04	Not Shifted (NS)	(NS)	NT	NT
NR561_62	1.48 ± .18	34.7 ± .74	NT	NT
NR579_45	4.49 ± 1.0	26.9 ± 1.1	NT	NT
NR579_36	NS	NS	NT	NT
RL673_02	0.88 ± .28	42.5 ± 4.5	9.7 ± .25	7.4 ± 1.3
RL648_86	0.34 ± .07	49.9 ± 2.5	2.6 ± .65	3.6 ± 1.4
RL648_73	0.30 ± .05	47.0 ± 4.1	4.3 ± .71	5.4 ± 1.5
RL648_81	0.19 ± .02	51.1 ± 3.5	5.1 ± 1.3	6.7 ± 1.5

Table S1

Table S1. Summary values of EC_{50} and maximal (Max) $\Delta V_{1/2}$ for all compounds tested. EC_{50} is the concentration of the compound that produces a half-maximal shift in $V_{1/2}$. Maximal (max) $\Delta V_{1/2}$ is the shift in $V_{1/2}$ at 10 μM concentrations of the compound. NS: $V_{1/2}$ was not shifted by this compound. NT: (Max) $\Delta V_{1/2}$ was not tested for this compound.

Synthesis: The synthesis of these compounds followed the general routes A and B shown in Figure S1. Briefly, in route A we performed a reductive amination to link the benzylic amine portion with the aniline moiety. After selective introduction of the benzyloxycarbonyl (Cbz) protective group, the *ortho*-nitroaniline was acylated and the Cbz group was removed concomitantly with the reduction of the nitro group to generate the desired analogs. In synthetic route B, we added suitably substituted benzylic amines to *para*-nitrofluorobenzenes under S_NAr conditions, followed by reduction of the nitro group with zinc and ammonium chloride, and selective N-acylation of the resulting *para*-aminoaniline.

General Experimental Details. All reactions were performed under an N_2 atmosphere and all glassware was dried in an oven at 130 ^oC for at least 2 h prior to use and allowed to cool under an atmosphere of dry N_2 or Ar. Reactions carried out below 0 ^oC employed a dry ice/acetone or a low-temperature automated cooler and an acetone bath. THF and Et_2O were distilled over sodium/benzophenone ketyl radical anion; CH_2Cl_2 and toluene were distilled over CaH_2, and 1,4-dioxane, and MeOH, and MeCN were dried over 3 Å molecular sieves unless otherwise noted. Et_3N and other volatile amines were distilled from CaH_2 and stored over KOH. Concentration under reduced pressure refers to the use of a rotary evaporator connected to a PIAB Lab Vac

H40 line to remove solvent, and drying under high vacuum refers to the use of a Fischer Scientific Maxima C *Plus* vacuum pump (0.5-4 mmHg) to remove traces of solvent. All chromatography was performed on normal phase SiO_2 (Silicycle, 40-63 μm particle size) using literature conditions [Still, W. C.; Kahn, M.; Mitra, A. Rapid chromatographic technique for preparative separations with moderate resolution. *J. Org. Chem.* **1978**, *43*, 2923-2925] unless stated otherwise. Reactions were monitored by thin-layer chromatography (Merck pre-coated silica gel 60 F_{254} plates, 250 μm layer thickness) and visualization was accomplished with a 254 nm UV light, by staining with a $KMnO_4$ solution (prepared by dissolving 1.5 g of $KMnO_4$ and 1.5 g of K_2CO_3 in 100 mL of a 0.1% NaOH solution), or by staining with *p*-anisaldehyde solution (2.5 mL of *p*-anisaldehyde, 2 mL of AcOH, and 3.5 mL of conc. H_2SO_4 in 100 mL of 95% EtOH). Melting points were obtained using a Laboratory Devices Mel-Temp II with open capillaries and are uncorrected. ^{1}H and ^{13}C NMR spectra were obtained on Bruker Avance 300, 400, 500, 600, or 700 MHz instruments as indicated in $CDCl_3$ solution unless otherwise noted. Chemical shifts were reported in parts per million with the residual solvent peak used as an internal standard. ^{1}H NMR spectra were obtained and are tabulated as follows: chemical shift, multiplicity (s = singlet, d = doublet, t = triplet, q = quartet, quint = quintet, dd = double of doublets, dt = doublet of triplets, m = multiplet, br = broad, app = apparent), number of protons, and coupling constant(s). ^{13}C NMR were recorded at 75, 100, 125, or 175 MHz as specified using a proton-decoupled pulse sequence and tabulated by observed peak. Infrared spectra were measured on ATR-IR instruments. High resolution mass spectra were obtained on a Thermo Fisher Exactive Orbitrap LC-MS using heated electrospray ionization (HESI).

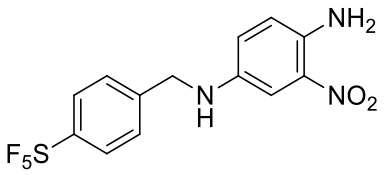

(4-Amino-3-nitro)phenyl-[(4-(pentafluorothio)phenyl)methyl]amine. To a solution of 2-nitro-*p*-phenylenediamine (0.751 g, 4.66 mmol) and PTSA (0.045 g, 0.24 mmol) in toluene (25 mL) was added 4-(pentafluorothio)-benzaldehyde (1.115 g, 4.707 mmol). The resulting solution was heated to reflux with a Dean-Stark trap for 21 h, the mixture was filtered through a Buchner funnel packed with a thin pad of SiO_2, and the filtrate was stirred and allowed to cool to rt. The solvent was removed under reduced pressure to give the crude imine (1.10 g) as a bright orange-red solid that was suspended in a mixture of 1,4-dioxane (5.2 mL) and MeOH (1.3 mL), and $NaBH_4$ (0.120 g, 3.14 mmol) was added in 3 portions at 15 min intervals. The solution was allowed to stir at rt for 3 h, quenched with H_2O (25 mL) and the resulting solid was collected by filtration. The crude product was washed with H_2O (500 mL) and dried under high vacuum to give (4-amino-3-nitro)phenyl-[(4-(pentafluorothio)phenyl)methyl]amine (1.09 g, 2.95 mmol, 63%) as a dark purple powder: Mp 129-130 ^oC (H_2O); IR (ATR) 3522.9, 3397.9, 1576.9, 1531.8, 1327.7, 1216.3 cm^{-1}; ^1H NMR ($CDCl_3$, 400 MHz) δ 7.73 (d, 2 H, J = 8.4 Hz), 7.61 (d, 2 H, J = 8.4 Hz), 7.27 (d, 1 H, 2.8 Hz), 6.84 (dd, 1 H, J = 9.2, 2.8 Hz), 6.71 (d, 1 H, J = 8.8 Hz), 5.74 (br s, 2 H), 4.37 (s, 2 H), 3.92 (br s, 1 H); ^{13}C NMR ($CDCl_3$, 100 MHz) δ 153.2 (app. t, J = 17.5 Hz), 143.0, 138.9, 138.5, 132.6, 127.7, 126.5 (quint., J = 4.6 Hz), 125.3, 120.4, 106.2, 48.1; HRMS (HESI) *m/z* calcd for $C_{13}H_{13}N_3O_2F_5S$ $[M+H]^+$ 370.0643, found 370.0645.

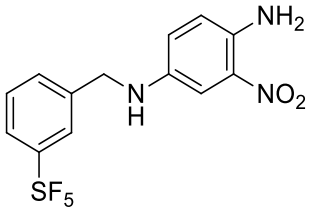

(4-Amino-3-nitro)phenyl-[(3-(pentafluorothio)phenyl)methyl]amine. A solution of 2-nitro-*p*-phenylenediamine (0.756 g, 4.69 mmol) and PTSA (0.054 g, 0.28 mmol) in toluene (25 mL) was treated with 3-(pentafluorothio)benzaldehyde (1.10 g, 4.56 mmol) via syringe and the resulting solution was heated to reflux with a Dean-Stark trap for 5 h. The mixture was filtered through a Buchner funnel packed with a thin pad of SiO_2 and the filtrate was stirred and allowed to cool to rt. The solvent was removed under reduced pressure to give the crude imine (1.571 g) as a bright orange-red solid that was suspended in a mixture of 1,4-dioxane (5.2 mL) and MeOH (1.3 mL), and $NaBH_4$ (0.126 g, 3.30 mmol) was added in 3 portions at 15 min intervals. The solution was allowed to stir at rt for 3 h, quenched with H_2O (25 mL), and extracted from brine with CH_2Cl_2 (3 x 200 mL). The solvent was removed under reduced pressure and the resulting residue dried under high vacuum at 60 ^oC for 12 h to give (4-amino-3-nitro)phenyl-[(3-(pentafluorothio)phenyl)methyl]amine (1.36 g, 3.69 mmol, 79%) as a dark red-purple powder: Mp 128-129 ^oC (CH_2Cl_2); IR (ATR) 3477.6, 3422.5, 3360.7, 3110.0, 1574.8, 1515.2, 1206.6; ^1H NMR ($CDCl_3$, 400 MHz) δ 7.77 (s, 1 H), 7.68 (d, 1 H, J = 8.4 Hz), 7.53 (d, 1 H, 7.6 Hz), 7.47-7.43 (m, 1 H), 7.30 (d, 1 H, J = 2.8 Hz), 6.86 (dd, 1 H, J = 8.8, 2.8 Hz), 6.72 (d, 1 H, J = 8.8 Hz), 5.75 (br s, 2 H), 4.37 (s, 2 H), 3.89 (br s, 1 H); ^{13}C NMR ($CDCl_3$, 100 MHz) 154.4 (quint., J = 18.0 Hz), 140.3, 139.0, 138.5, 132.6, 130.7, 129.3, 125.4, 125.3-125.1 (overlapping quint.), 120.4, 106.4, 48.6; HRMS (HESI) *m/z* calcd for $C_{13}H_{13}N_3O_2F_5S$ $[M+H]^+$ 370.0643, found 370.0641.

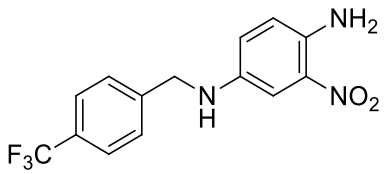

(4-Amino-3-nitro)phenyl{[4-(trifluoromethyl)phenyl]methyl}amine. A solution of 2-nitro-*p*-phenylenediamine (0.754 g, 4.68 mmol) and PTSA (0.054 g, 0.28 mmol) in toluene (25 mL) was treated via syringe with 4-(trifluoromethyl)benzaldehyde (0.640 mL, 4.69 mmol). The mixture was heated at reflux with a Dean-Stark trap for 5 h, filtered through a Buchner funnel packed with a thin pad of SiO_2, and the filtrate was stirred and allowed to cool to rt. The solvent was removed under reduced pressure to give the crude imine (1.23 g) as a bright orange-red solid that was suspended in a mixture of 1,4-dioxane (5.2 mL) and MeOH (1.3 mL), and $NaBH_4$ (0.120 g, 3.14 mmol) was added in 3 portions at 15 min intervals. The resulting solution was allowed to stir at rt for 3 h, quenched with H_2O (25 mL) and extracted from brine with CH_2Cl_2 (3 x 200 mL). The solvent was removed under reduced pressure and the residue dried under high vacuum at 60 ^oC to give (4-amino-3-nitro)phenyl{[4-(trifluoromethyl)phenyl]methyl}amine (1.141 g, 3.666 mmol, 78%) as a dark purple oil: IR (CH_2Cl_2) 3483.6, 3370.0, 1573.9, 1521.1, 1325.0 cm^{-1}; ^1H NMR ($CDCl_3$, 400 MHz) δ 7.60 (d, 2 H, J = 8.0 Hz), 7.48 (d, 2 H, J = 8.0 Hz), 7.28 (d, 1 H, J = 2.8 Hz), 6.85 (dd, 1 H, J = 8.8, 2.8 Hz), 6.71 (d, 1 H, J = 8.8 Hz), 5.47 (br s, 2 H), 4.37 (s, 2 H), 3.92 (br s, 1 H); ^{13}C NMR ($CDCl_3$ 100 MHz) δ 143.1, 139.1, 138.4, 132.6, 129.9 (q, J = 32.1 Hz), 127.8, 125.8 (q, J = 3.6 Hz), 125.3, 124.2 (q, J = 270.0 Hz), 120.3, 106.1, 48.5; HRMS (HESI) *m/z* calcd for $C_{14}H_{13}N_3O_2F_3$ $[M+H]^+$ 312.0954, found 312.0955.

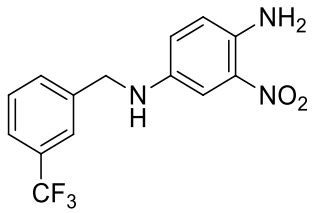

(4-Amino-3-nitro)phenyl{[3-(trifluoromethyl)phenyl]methyl}amine. A solution of 2-nitro-*p*-phenylenediamine (0.753 g, 4.67 mmol) and PTSA (0.050 g, 0.26 mmol) in toluene (25 mL) was treated via syringe with 3-(trifluoromethyl)benzaldehyde (0.620 mL, 4.64 mmol). The resulting

solution was heated to reflux with a Dean-Stark trap for 5 h, filtered through a Buchner funnel packed with a thin pad of SiO_2, and allowed to cool to rt. The solvent was removed under reduced pressure to give the crude imine (1.203 g) as bright orange solid, that was suspended in a mixture of 1,4-dioxane (3.7 mL) and MeOH (0.90 mL) and $NaBH_4$ (0.117 g, 0.655 mmol) was added in 3 portions at 15 minute intervals. The resulting solution was allowed to stir at rt for 3 h, quenched with H_2O (25 mL), and extracted with CH_2Cl_2 (3 x 100 mL). The combined organic extracts were washed with brine, dried (Na_2SO_4), filtered, and the solvent evaporated under reduced pressure to give crude product (1.141 g). Purification by chromatography on SiO_2 (70% CH_2Cl_2 in hexanes) gave (4-amino-3-nitro)phenyl{[3-(trifluoromethyl)phenyl]methyl}amine (1.10 g, 3.35 mmol, 72%) as a dark purple powder: Mp 95-96 ^oC (CH_2Cl_2); IR (ATR) 3456.00, 3396.7, 3330.7, 1515.1, 1323.5 cm^{-1}; ^1H NMR ($CDCl_3$, 400 MHz) δ 7.64 (s, 1 H), 7.55 (m, 2 H), 7.47 (m, 1 H), 7.29 (d, 1 H, J = 2.8 Hz), 6.86 (dd, 1 H, J = 8.8, 2.8 Hz), 6.71 (d, 1 H, J = 8.8 Hz), 5.74 (br s, 2 H), 4.36 (s, 2 H), 3.89 (br s, 1 H); ^{13}C NMR ($CDCl_3$, 100 MHz) δ 140.0, 139.16, 138.5, 132.6, 131.2 (q, J = 32 Hz), 131.0, 129.3, 125.4, 124.5 (q, J = 3.7 Hz), 124.4 (q, J = 3.8 Hz), 124.2 (q, J = 271 Hz), 120.3, 106.2, 48.6; HRMS (ESI) *m/z* calcd for $C_{14}H_{13}N_2O_3F_3$ $[M+H]^+$ 312.0954, found 312.0947.

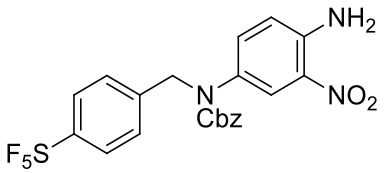

***N*-(4-Amino-3-nitro)phenyl-(phenylmethoxy)-*N*-{[4-(pentafluorothio)phenyl]methyl}carboxamide**. A solution of (4-amino-3-nitro)phenyl-[(4-(pentafluorothio)phenyl)methyl]amine (0.207 g, 0.544 mmol) and DIPEA (0.110 mL, 0.665 mmol) in 1,4-dioxane (2.8 mL) at rt was treated dropwise via syringe with benzyl chloroformate

(0.100 mL, 0.682 mmol). The resulting solution was allowed to stir for 18 h and was then quenched with H_2O:CH_2Cl_2 (1:1, 6.5 mL). The phases were separated and the aqueous phase was extracted with CH_2Cl_2 (3 x 5 mL). The combined organic layers were washed with brine, dried (Na_2SO_4), filtered, and the solvent evaporated to give crude *N*-(4-amino-3-nitro)phenyl-(phenylmethoxy)-*N*-{[4-(pentafluorothio)phenyl]methyl}carboxamide (0.280 g) as an orange foam that was used without further purification.

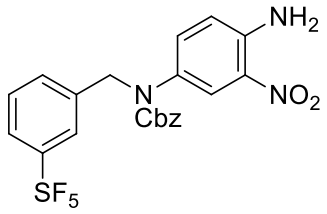

***N*-(4-Amino-3-nitro)phenyl(phenylmethoxy)-*N*-{[3-(pentafluorothio)phenyl]methyl}carboxamide**. A solution of (4-amino-3-nitro)phenyl-[(3-(pentafluorothio)phenyl)methyl]amine (0.202 g, 0.531 mmol) and DIPEA (0.090 mL, 0.54 mmol) in 1,4-dioxane (2.8 mL) at rt was treated dropwise via syringe with benzyl chloroformate (0.080 mL, 0.55 mmol). The reaction mixture was stirred for 3 h and then quenched with 6.50 mL of H_2O:CH_2Cl_2 (1:1). The phases were separated and the aqueous phase was extracted with CH_2Cl_2 (3 x 5 mL). The combined organic layers were washed with brine, dried (Na_2SO_4), filtered, and the solvent was evaporated to give crude *N*-(4-amino-3-nitrophenyl)(phenylmethoxy)-*N*-{[3-(pentafluorothio)phenyl]methyl}carboxamide (0.309 g) as an orange oil which was used without further purification.

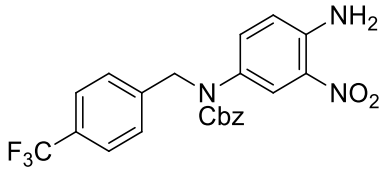

***N*-(4-Amino-3-nitro)phenyl(phenylmethoxy)-*N*-{[4-(trifluoromethyl)phenyl]methyl}carboxamide**. A solution of (4-amino-3-nitro)phenyl{[4-(trifluoromethyl)phenyl]methyl}amine (0.199 g, 0.639 mmol) and DIPEA (0.110 mL, 0.666 mmol) in 1,4-dioxane (3.2 mL) at rt was treated dropwise via syringe with benzyl chloroformate (0.100 mL, 0.682 mmol). The resulting solution was allowed to stir for 4 h and was then quenched with H_2O:CH_2Cl_2 (1:1, 6.5 mL). The phases were separated and the aqueous phase was extracted with CH_2Cl_2 (3 x 5 mL). The combined organic layers were washed with brine, dried (Na_2SO_4), filtered, and the solvent was evaporated to give crude *N*-(4-amino-3-nitro)phenyl(phenylmethoxy)-*N*-{[4-(trifluoromethyl)phenyl]methyl}carboxamide (0.328 g) as a dark orange oil which was used without further purification.

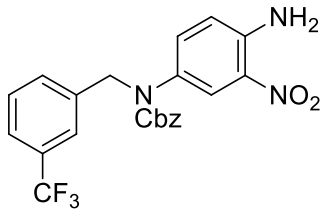

***N*-(4-Amino-3-nitro)phenyl(phenylmethoxy)-*N*-{[3-(trifluoromethyl)phenyl]methyl}carboxamide**. A solution of (4-amino-3-nitro)phenyl{[3-(trifluoromethyl)phenyl]methyl}amine (0.205 g, 0.659 mmol) and DIPEA (0.115 mL, 0.696 mmol) in 1,4-dioxane (3.5 mL) at rt was treated dropwise via syringe with benzyl chloroformate (0.100 mL, 0.682 mmol). The resulting solution was allowed to stir for 4 h at rt and was then quenched with H_2O:CH_2Cl_2 (1:1, 10 mL). The layers were separated, and the aqueous phase was extracted with CH_2Cl_2 (2 x 15 mL). The combined organic phases were washed with H_2O and brine, dried (Na_2SO_4), filtered, and the solvent was evaporated to give crude *N*-(4-amino-3-nitro)phenyl(phenylmethoxy)-*N*-{[3-(trifluoromethyl)phenyl]methyl}carboxamide (0.331 g) as an orange oil which was used without further purification.

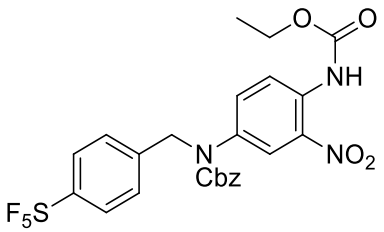

Benzyl (4-((ethoxycarbonyl)amino)-3-nitrophenyl)[4-(pentafluorothio)benzyl]carbamate. A solution of crude *N*-(4-amino-3-nitro)phenyl-(phenylmethoxy)-*N*-{[4-(pentafluorothio)phenyl]methyl}carboxamide (0.050 g, 0.099 mmol) and DIPEA (0.050 mL, 0.30 mmol) in 1,4-dioxane (1.0 mL) at rt was treated dropwise via syringe with ethyl chloroformate (0.030 mL, 0.31 mmol). The resulting solution was allowed to stir at 70 ^{o}C for 24 h and was then quenched with H_2O:CH_2Cl_2 (1:1, 5 mL). The layers were separated and the aqueous layer was extracted with CH_2Cl_2 (3 x 20 mL). The combined organic layers were washed with H_2O and brine, dried ($MgSO_4$), filtered, and the solvent was evaporated under reduced pressure to give crude product (0.050 g) as an orange oil. The oil was purified by chromatography on SiO_2 (30% EtOAc in hexanes) to give benzyl (4-((ethoxycarbonyl)amino)-3-nitrophenyl)[4-(pentafluorothio)benzyl]carbamate (0.036 g, 0.063 mmol, 63%, 82% based on recovered starting material) as an orange oil: IR (CH_2Cl_2) 3365.8, 2094.7, 1738.1, 1706.7, 1515.2 cm^{-1}; ^{1}H NMR ($CDCl_3$, 400 MHz) δ 9.77 (s, 1 H), 8.54 (d, 1 H, *J* = 9.2 Hz), 8.04 (br s, 1 H), 7.68 (d, 2 H, *J* = 8.8 Hz), 7.33-7.27 (m, 5 H), 7.24-7.22 (m, 2 H), 5.19 (s, 2 H), 4.92 (s, 2 H), 4.26 (q, 2 H, *J* = 7.2 Hz), 1.34 (t, 3 H, *J* = 7.2 Hz); ^{13}C NMR ($CDCl_3$, 100 MHz) δ 155.2, 153.4 (quint., *J* = 18.0 Hz),153.2, 153.2, 141.0, 135.8, 135.7, 134.2, 128.8, 128.8, 128.2, 127.9, 126.6 (app. t, *J* = 4.6 Hz), 123.6, 121.4, 68.5, 62.3, 53.4, 14.5; HRMS (HESI) *m/z* calcd for $C_{24}H_{23}N_3O_6F_5S$ $[M+H]^+$ 576.1222, found 576.1221.

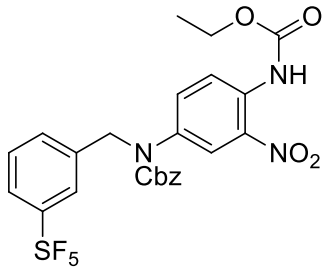

Benzyl (4-((ethoxycarbonyl)amino)-3-nitrophenyl)[3-(pentafluorothio)benzyl]carbamate. A solution of crude *N*-(4-amino-3-nitrophenyl)(phenylmethoxy)-*N*-{[3-(pentafluorothio)phenyl]methyl}carboxamide (0.326 g), DIPEA (0.280 mL, 1.69 mmol), and DMAP (0.003 g, 0.02 mmol) in 1,4-dioxane (4 mL) at rt was treated dropwise via syringe with ethyl chloroformate (0.155 mL, 1.58 mmol). The resulting solution was allowed to stir at 70 ^{o}C for 2 d and was then quenched by the addition of H_2O:CH_2Cl_2 (1:1, 10 mL). The layers were separated and the aqueous layer extracted with CH_2Cl_2 (3 x 20 mL). The combined organic layers were washed with H_2O, 1 M aq. HCl, and brine, dried ($MgSO_4$), filtered, and the solvent was evaporated under reduced pressure to give crude product (0.340 g) as an orange oil. The crude residue was purified by chromatography on SiO_2 (20% EtOAc in hexanes) to give benzyl (4-((ethoxycarbonyl)amino)-3-nitrophenyl)[3-(pentafluorothio)benzyl]carbamate (0.052 g) as a yellow oil which was used without further purification.

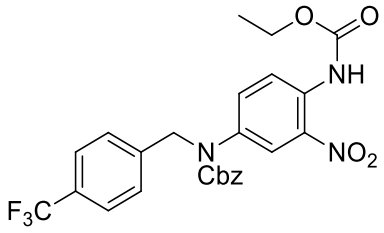

Benzyl (4-((ethoxycarbonyl)amino)-3-nitrophenyl)[4-(trifluoromethyl)benzyl]carbamate. A solution of crude *N*-(4-amino-3-nitro)phenyl(phenylmethoxy)-*N*-{[4-(trifluoromethyl)phenyl]methyl}carboxamide (0.310 g) and DIPEA (0.670 mL, 4.05 mmol) in

1,4-dioxane (5.2 mL) at rt was treated dropwise via syringe with ethyl chloroformate (0.395 mL, 4.03 mmol). The resulting solution was allowed to stir at 70 ^{o}C for 3 d and was then quenched by the addition of H_2O:CH_2Cl_2 (1:1, 10 mL). The phases were separated and the aqueous phase was extracted with CH_2Cl_2 (3 x 20 mL). The combined organic layers were washed with H_2O and brine, dried (Na_2SO_4), filtered, and the solvent was evaporated under reduced pressure to give crude product **(**0.350 g) as an orange solid. The crude solid was purified by chromatography on SiO_2 (20% EtOAc in hexanes) to give benzyl (4-((ethoxycarbonyl)amino)-3-nitrophenyl)[4-(trifluoromethyl)benzyl]carbamate (0.194 g, 0.375 mmol, 59% over 2 steps) as an orange oil: IR (CH_2Cl_2) 3365.8, 2983.2, 1738.2, 1706.4, 1514.4, 1323.3 cm^{-1}; ^{1}H NMR (DMSO-d_6, 400 MHz, 353 K) δ 9.50 (br s, 1 H), 7.96 (d, 1 H, *J* = 2.4 Hz), 7.77 (d, 1 H, *J* = 8.8 Hz), 7.64 (d, 1 H, *J* = 8.4 Hz), 7.60 (dd, 1 H, *J* = 8.8, 2.4 Hz), 7.48 (d, 1 H, *J* = 8.0 Hz), 7.33-7.26 (m, 7 H), 5.19 (s, 2 H), 5.05 (s, 2 H), 4.15 (q, 2 H, *J* = 7.2 Hz), 1.24 (t, 3 H, *J* = 7.2 Hz); ^{13}C NMR (DMSO-d_6, 100 MHz, 353 K) δ 154.2, 152.9, 141.8, 140.0, 136.8, 135.8, 131.8, 130.3, 128.0, 127.9, 127.7, 127.5, 127.1, 124.9 (q, *J* = 3.7 Hz), 123.8 (q, *J* = 270.3 Hz), 123.8, 122.5, 67.0, 60.8, 52.3, 13.8; HRMS (HESI) *m/z* calcd for $C_{25}H_{21}N_3O_6F_3$ (M-H) 516.1377, found 516.1372.

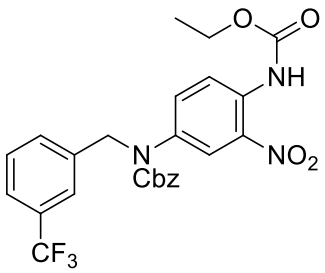

Benzyl (4-((ethoxycarbonyl)amino)-3-nitrophenyl)[3-(trifluoromethyl)benzyl]carbamate. A solution of crude *N*-(4-amino-3-nitro)phenyl(phenylmethoxy)-*N*-{[3-(trifluoromethyl)phenyl]methyl}carboxamide (0.330 g) and DIPEA (0.545 mL, 3.30 mmol) in 1,4-dioxane (5 mL) at rt was treated dropwise via syringe with ethyl chloroformate (0.160 mL,

1.63 mmol). The resulting solution was allowed to stir at 70 °C for 2 d and was then quenched by the addition of 1:1 H_2O:CH_2Cl_2 (10 mL), the layers were separated and the aqueous phase was extracted with CH_2Cl_2 (2 x 20 mL). The combined organic layers were washed with H_2O (2 x 20 mL) and brine (2 x 10 mL), dried ($MgSO_4$), filtered, and the solvent was evaporated under reduced pressure to give crude product (0.310 g) as an orange oil. The crude oil was purified by chromatography on SiO_2 (20% EtOAc in hexanes) to give benzyl (4-((ethoxycarbonyl)amino)-3-nitrophenyl)[3-(trifluoromethyl)benzyl]carbamate (0.113 g) as a yellow oil which was carried on without further purification.

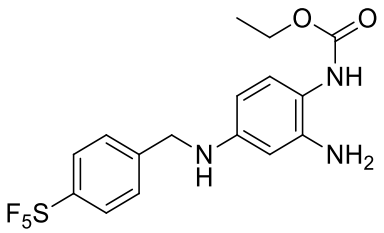

***N*-[2-Amino-4-({[4-(pentafluorothio)phenyl]methyl}amino)phenyl]ethoxycarboxamide (NR561_29)**. A solution of benzyl (4-((ethoxycarbonyl)amino)-3-nitrophenyl)[4-(pentafluorothio)benzyl]carbamate (0.047 g, 0.082 mmol) and 10% Pd/C (0.010 g, 0.009 mmol, 10 mol%) in a mixture of 1,4-dioxane (0.46 mL) and EtOH (0.24 mL) was allowed to stir for 21 h at rt under an H_2 atmosphere (balloon). The reaction mixture was diluted with Et_2O (5 mL) and filtered through a pad of Celite. The organic phase was concentrated under reduced pressure to give crude product (0.037 g) as an orange oil. The crude oil was purified by chromatography on SiO_2 (50% EtOAc in hexanes) to give NR561_29 (0.018 g, 0.044 mmol, 54%) as a light brown solid: Mp 146-147 °C (CH_2Cl_2); IR (ATR) 3377.6, 2925.7, 1697.8, 1620.9, 1525.7 cm^{-1}; ^1H NMR ($CDCl_3$, 400 MHz) δ 7.70 (d, 2 H, *J* = 8.4 Hz), 7.43 (d, 2 H, *J* = 8.4 Hz), 6.92 (d, 1 H, *J* = 8.4 Hz), 6.02 (dd, 1 H, *J* = 8.4, 2.4 Hz), 5.95 (d, 1 H, *J* = 2.4 Hz), 4.35 (s, 2 H), 4.18 (q, 2 H, *J* =

7.2 Hz), 3.90 (br s, 2 H), 1.28 (t, 3 H, *J* = 7.2 Hz); ^{13}C NMR ($CDCl_3$, 100 MHz) δ 155.6, 152.9 (quint., *J* = 13.5 Hz), 147.4, 143.9, 142.2, 128.1, 127.3, 126.4 (quint., *J* = 4.0 Hz), 114.5, 104.5, 100.8, 61.5, 47.6, 14.7; HRMS (HESI) *m/z* calcd for $C_{16}H_{19}N_3O_2F_5S$ 412.1113, found 412.1111.

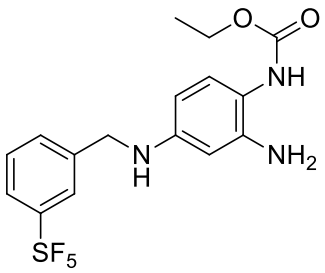

***N*-[2-Amino-4-({[3-(pentafluorothio)phenyl]methyl}amino)phenyl]ethoxycarboxamide (NR561_45)**. A mixture of benzyl (4-((ethoxycarbonyl)amino)-3-nitrophenyl)[3-(pentafluorothio)benzyl]carbamate (0.050 g, 0.087 mmol) and 10% Pd/C (0.010 g, 0.010 mmol) in 1,4-dioxane (0.46 mL) and EtOH (0.24 mL) was allowed to stir under an H_2 atmosphere (balloon) for 18 h. The reaction mixture was diluted with Et_2O (5 mL) and filtered through a pad of Celite. The solvent was removed under reduced pressure to give crude product (0.049 g) as an orange oil. The crude residue was purified by chromatography on SiO_2 (50% EtOAc in hexanes) to give NR561_45 (0.027 g, 0.066 mmol, 76%) as a light brown oil that solidified on standing: Mp 52-53 ^{o}C (CH_2Cl_2); IR (ATR) 3355.4, 2931.1, 1699.4, 1623.1, 1525.2, 1229.4 cm^{-1}; ^{1}H NMR ($CDCl_3$, 400 MHz) δ 7.73 (s, 1 H), 7.65 (d, 1 H, *J* = 8.0 Hz), 7.50 (d, 1 H, *J* = 7.6 Hz), 7.42 (app. t, 1 H, *J* = 7.8 Hz), 6.92 (d, 1 H, *J* = 8.4 Hz), 6.04 (dd, 1 H, *J* = 8.0, 2.0 Hz), 5.98 (d, 1 H, *J* = 2.0 Hz), 4.34 (s, 2 H), 4.18 (q, 2 H, *J* = 7.1 Hz), 3.85 (br s, 2 H), 1.28 (t, 3 H, *J* = 7.2 Hz); ^{13}C NMR ($CDCl_3$, 175 MHz) δ 155.6, 154.4 (quint., *J* = 16.8 Hz), 147.4, 143.1, 141.1, 130.4, 129.1, 128.0, 124.9 (quint., *J* = 4.2 Hz), 124.8 (quint., *J* = 4.4 Hz), 114.5, 104.5, 100.9, 61.5, 48.1, 14.7; HRMS (HESI) *m/z* calcd for $C_{16}H_{19}N_3O_2F_5S$ $[M+H]^+$ 412.1113, found 412.1101.

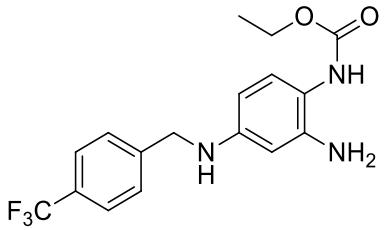

***N*-[2-Amino-4-({[4-(trifluoromethyl)phenyl]methyl}amino)phenyl]ethoxycarboxamide (NR561_40)**. A mixture of benzyl (4-((ethoxycarbonyl)amino)-3-nitrophenyl)[4-(trifluoromethyl)benzyl]carbamate (0.090 g, 0.174 mmol) and 10% Pd/C (0.018 g, 0.017 mmol) in a mixture of 1,4-dioxane (1 mL) and EtOH (0.50 mL) was allowed to stir at rt for 18 h under an H_2 atmosphere (balloon). The reaction mixture was diluted with Et_2O (5 mL) and filtered through a pad of Celite. The organic phase was concentrated under reduced pressure to give crude product (0.051 g) as a light brown solid. The crude solid was purified by chromatography on SiO_2 (50% EtOAc in hexanes) to give NR561_40 (0.044 g, 0.12 mmol, 72%) as a grey solid: Mp 171-172 ^{o}C (CH_2Cl_2); IR (ATR) 3279.6, 2980.6, 1677.2, 1527.0 cm^{-1}; ^{1}H NMR ($CDCl_3$, 400 MHz) δ 7.59 (d, 2 H, *J* = 8.4 Hz), 7.46 (d, 2 H, *J* = 8.0 Hz), 6.92 (d, 1 H, *J* = 8.4 Hz), 6.05 (dd, 1 H, *J* = 8.4, 2.4 Hz), 5.98 (d, 1 H, *J* = 2.4 Hz), 4.37 (s, 2 H), 4.19 (q, 2 H, *J* = 7.2 Hz), 4.06 (br s, 1 H), 3.74 (br s, 2 H), 1.28 (t, 3 H, *J* = 7.0 Hz); ^{13}C NMR ($CDCl_3$, 100 MHz δ 155.7, 147.6, 143.9, 143.2, 129.6 (q, *J* = 32.0 Hz), 128.1, 127.5, 125.7 (q, *J* = 3.7 Hz), 124.3 (q, *J* = 270.2 Hz), 114.3, 104.5, 100.6, 61.5, 48.0, 14.8; HRMS (HESI) *m/z* calcd for $C_{17}H_{19}N_3O_2F_3$ $[M+H]^+$ 354.1424, found 354.1425.

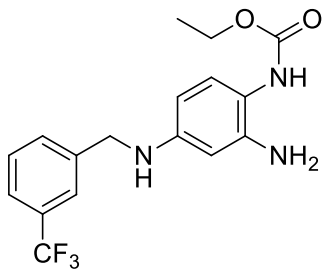

***N*-[2-Amino-4-({[3-(trifluoromethyl)phenyl]methyl}amino)phenyl]ethoxycarboxamide (NR561_50)**. A mixture of crude benzyl (4-((ethoxycarbonyl)amino)-3-nitrophenyl)[3-(trifluoromethyl)benzyl]carbamate (0.100 g, 0.193 mmol) and 10% Pd/C (0.020 g, 0.018 mmol, 10 mol%) in 1,4-dioxane (1 mL) and EtOH (0.50 mL) was allowed to stir at rt for 18 h under an H_2 atmosphere (balloon). The reaction mixture was diluted with Et_2O, filtered through a pad of Celite, and the solvent removed under reduced pressure to give crude product (0.067 g) as a dark brown oil, which was purified by chromatography on SiO_2 (50% EtOAc in hexanes) to give NR561_50 (0.056 g, 0.16 mmol, 24% over 3 steps) as an off-white solid: Mp 103-104 ^oC (CH_2Cl_2); IR (ATR) 3335.1, 2987.6, 1723.5, 1679.8, 1535.3 cm^{-1}; ^1H NMR ($CDCl_3$, 400 MHz) δ 7.61 (s, 1 H), 7.53 (app. t, 2 H, *J* = 7.0 Hz), 7.46-7.42 (m, 1 H), 6.92 (d, 1 H, *J* = 8.0 Hz), 6.05 (dd, 1 H, *J* = 8.4, 2.4 Hz), 5.98 (d, 1 H, *J* = 2.4 Hz), 4.34 (s, 2 H), 4.19 (q, 2 H, *J* = 7.2 Hz), 3.76 (br s, 2 H), 1.28 (t, 3 H, *J* = 7.2 Hz); ^{13}C NMR ($CDCl_3$, 100 MHz) δ 155.6, 147.6, 143.2, 140.8, 131.1 (q, *J* = 32.0 Hz), 130.7, 129.2, 128.0, 124.3 (q, *J* = 270.9 Hz), 124.2-124.1 (overlapping q.), 114.3, 104.5, 100.8, 61.5, 48.1, 14.7; HRMS (HESI) *m/z* calcd for $C_{17}H_{19}N_3O_2F_3$ $[M+H]^+$ 354.1424, found 354.1421.

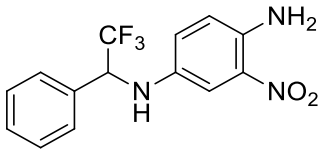

(4-Amino-3-nitrophenyl)(2,2,2-trifluoro-1-phenylethyl)amine. A solution of 2-nitro-*p*-phenylenediamine (0.504 g, 3.13 mmol) and PTSA (0.034 g, 0.17 mmol) in toluene (15 mL) at rt was treated with 2,2,2-trifluoroacetophenone (0.544 g, 3.09 mmol). The reaction mixture was stirred at reflux for 24 h with a Dean-Stark trap, and filtered through a pad of SiO_2. The solvent was evaporated under reduced pressure to give the crude imine (0.170 g), which was suspended

in 1,4-dioxane (4 mL) and MeOH (1 mL), and $NaBH_4$ (0.125 g, 3.27 mmol) was added in 3 portions at 15-min intervals. The resulting solution was allowed to stir at rt for 3 h, quenched with H_2O (25 mL) and extracted with CH_2Cl_2 (3 x 20 mL). The organic phase was dried (Na_2SO_4), filtered, and the solvent was evaporated under reduced pressure. Further drying under high vacuum gave (4-amino-3-nitrophenyl)(2,2,2-trifluoro-1-phenylethyl)amine (0.120 g, 0.386 mmol, 12%) as a dark red solid: Mp 126-127 ^oC (CH_2Cl_2); IR (ATR) 3436.0, 3388.0, 333.4, 1581.3, 1514.4, 1326.1, 1237.6; ^1H NMR ($CDCl_3$, 400 MHz) δ 7.44-7.38 (m, 5 H), 7.33 (d, 1 H, J = 2.8 Hz), 6.89 (dd, 1 H, J = 9.2, 2.8 Hz), 6.69 (d, 1 H, J = 8.8 Hz), 5.75 (br s, 2 H), 4.84 (m, 1 H), 4.13 (d, 1 H, J = 7.6 Hz); ^{13}C NMR ($CDCl_3$, 100 MHz) δ 139.2, 136.6, 133.6, 132.3, 129.51, 129.2, 128.0, 126.0, 125.1 (q, J = 280.3 Hz), 120.3, 108.6, 61.4 (q, J = 30.0 Hz); HRMS (HESI) *m/z* calcd for $C_{14}H_{13}N_3O_2F_3$ $[M+H]^+$ 312.0954, found 312.0953.

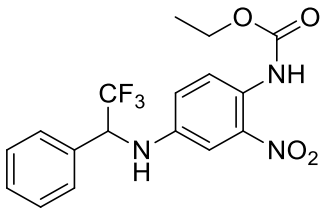

Ethyl (2-nitro-4-((2,2,2-trifluoro-1-phenylethyl)amino)phenyl)carbamate. A solution of (4-amino-3-nitrophenyl)(2,2,2-trifluoro-1-phenylethyl)amine (0.060 g, 0.19 mmol) and DIPEA (0.065 mL, 0.39 mmol) in 1,4-dioxane (1.3 mL) at rt was treated dropwise via syringe with ethyl chloroformate (0.020 mL, 0.20 mmol). The resulting solution was allowed to stir at 50 ^oC for 18 h and was then quenched by the addition of 1:1 H_2O:CH_2Cl_2 (10 mL). The layers were separated and the aqueous phase was extracted with CH_2Cl_2 (3 x 10 mL). The combined organic phases were washed with H_2O (2 x 10 mL) and brine (2 x 10 mL), dried (Na_2SO_4), filtered, and the solvent was evaporated under reduced pressure to give crude product (0.100 g) as an orange-red oil that was purified by chromatography on SiO_2 (40-60% CH_2Cl_2 in hexanes) to give ethyl (2-

nitro-4-((2,2,2-trifluoro-1-phenylethyl)amino)phenyl)carbamate (0.054 g, 0.14 mmol, 73%) as a red oil: IR (CH_2Cl_2) 3373.0, 2983.9, 1719.0, 1523.1, 1324.1 cm^{-1}; ^1H NMR ($CDCl_3$, 500 MHz) δ 9.39 (s, 1 H), 8.30 (d, 1 H, *J* = 9.0 Hz), 7.46-7.40 (m, 6 H), 6.98 (dd, 1 H, *J* = 9.5, 2.2 Hz), 4.91 (m, 1 H), 4.56 (br d, 1 H, *J* = 7.0 Hz), 4.22 (q, 2 H, *J* = 7.0 Hz), 1.31 (t, 3 H, *J* = 7.0 Hz); ^{13}C NMR ($CDCl_3$, 125 MHz) δ 153.6, 140.7, 137.0, 133.1, 129.6, 129.3, 128.0, 127.7, 124.9 (q, *J* = 280.5 Hz), 122.7, 122.6, 121.5, 108.8, 61.9, 60.6 (q, *J* = 30.4 Hz), 14.5; HRMS (HESI) *m/z* calcd for $C_{17}H_{17}N_3O_4F_3$ $[M+H]^+$ 384.1166, found 384.1163.

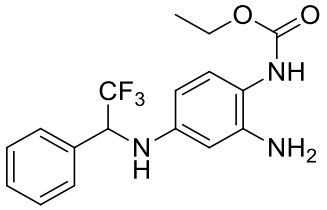

***N*-{2-Amino-4-[(2,2,2-trifluoro-1-phenylethyl)amino]phenyl}ethoxycarboxamide**.

(**NR579_04**) A suspension of ethyl (2-nitro-4-((2,2,2-trifluoro-1-phenylethyl)amino)phenyl)carbamate (0.050 g, 0.13 mmol) and 10% Pd/C (0.014 g, 0.013 mmol) was allowed to stir under an H_2 atmosphere (balloon) for 18 h. The reaction mixture was diluted with Et_2O, filtered through Celite, and the solvent evaporated under reduced pressure to give crude product (0.066 g) as a gray oil that was purified by chromatography on SiO_2 (0-10% EtOAc in CH_2Cl_2) to give NR579_04 (0.041 g, 0.12 mmol, 89%) as a clear, colorless oil that solidified upon standing: Mp 51-52 ^oC (CH_2Cl_2); IR (ATR) 3346.1, 2984.8, 1696.0, 1524.2 cm^{-1}; ^1H NMR ($CDCl_3$, 400 MHz) δ 7.42-7.37 (m, 5 H), 6.90 (d, 1 H, *J* = 8.0 Hz), 6.05 (app. d, 1 H, *J* = 8.4 Hz), 6.01 (app. s, 1 H), 4.84 (m, 1 H), 4.28 (d, 1 H, *J* = 7.2 Hz), 4.17 (q, 2 H, *J* = 7.1 Hz), 3.72 (br s, 2 H), 1.27 (t, 3 H, *J* = 6.6 Hz); ^{13}C NMR ($CDCl_3$, 100 MHz) δ 155.5, 145.3, 143.0, 134.2, 129.2, 129.0, 128.0, 125.1 (q, *J* = 280.2 Hz), 115.5, 105.2, 102.1, 61.5, 60.7 (q, *J* = 29.8 Hz), 14.7; HRMS (HESI) *m/z* calcd for $C_{17}H_{19}N_3O_2F_3$ $[M+H]^+$ 354.1424, found 354.1422.

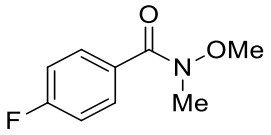

4-Fluoro-*N*-methoxy-*N*-methylbenzamide. A solution of methoxymethylamine hydrochloride (0.634 g, 6.37 mmol) and Et_3N (0.860 mL, 6.12 mmol) in CH_2Cl_2 (3.75 mL) at 0 ^oC was treated dropwise via syringe with 4-fluorobenzoyl chloride (0.370 mL, 3.07 mmol) over 30 min. The reaction mixture was allowed to stir at rt for 2 h, poured into H_2O and extracted with CH_2Cl_2 (3 x 20 mL). The combined organic extracts were washed with brine, dried ($MgSO_4$), and the solvent was removed under reduced pressure. Further drying under high vacuum gave crude 4-fluoro-*N*-methoxy-*N*-methylbenzamide (0.672 g, 2.63 mmol, quant.) which was used without further purification: ^1H NMR ($CDCl_3$, 400 MHz) δ 7.74 (m, 2 H), 7.08 (m, 2 H), 3.53 (s, 3 H), 3.36 (s, 3 H); HRMS (HESI) *m/z* calcd for $C_9H_{11}NO_2F$ $[M+H]^+$ 184.0768, found 184.0768.

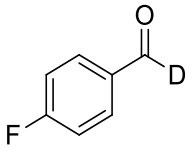

4-Fluoro[*formyl*-^{2}H]benzaldehyde. To a solution of 4-fluoro-*N*-methoxy-*N*-methylbenzamide (0.062 g, 0.338 mmol) in THF (1.9 mL) at -78 ^oC was added $LiAlD_4$ (0.018 g, 0.42 mmol) portionwise. The reaction mixture was stirred for 2 h at -78 ^oC, quenched with H_2O at the same temperature, treated with Et_2O, and the precipitate was removed by filtration through a pad of Celite. The filtrate was washed with H_2O and brine, dried (Na_2SO_4), and concentrated under reduced pressure. Further drying under high vacuum for 1 h gave crude 4-fluoro[*formyl*-^{2}H]benzaldehyde (0.032 g, 0.26 mmol) as a pale yellow oil that was used without further purification.

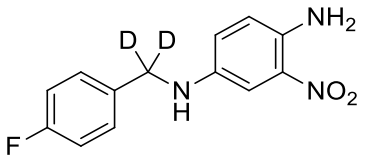

(4-Amino-3-nitrophenyl)[$^2H_2$(4-fluorophenyl)methyl]amine. A solution of 2-nitro-*p*-phenylenediamine (0.602 g, 3.73 mmol), PTSA (0.040 g, 0.21 mmol) and crude 4-fluoro[*formyl*-^{2}H]benzaldehyde (0.273 g) was heated to reflux with a Dean-Stark trap for 18 h. The solution was filtered through a thin pad of SiO_2 and the solvent was evaporated under reduced pressure to give a crude imine (0.328 g) which was suspended in 1,4-dioxane (4 mL) and MeOH (1 mL). After addition of $NaBD_4$ (0.111 g, 2.60 mmol) in 3 portions at 15-min intervals, the reaction mixture was stirred at rt for 3 h, quenched with H_2O (25 mL), and filtered to give (4-amino-3-nitrophenyl)[$^2H_2$(4-fluorophenyl)methyl]amine (0.241 g, 0.915 mmol, 42% over 2 steps) as a dark purple powder: Mp 113-114 ^oC (H_2O); IR (ATR) 3517.2, 3497.0, 3371.2, 1577.4, 1502.5, 1329.5 cm^{-1}; ^1H NMR ($CDCl_3$, 400 MHz) δ 7.34-7.27 (m, 3 H), 7.28 (d, 1 H, J = 2.4 Hz), 7.03 (t, 2 H, J = 8.6 Hz), 6.84 (dd, 1 H, J = 8.8, 2.4 Hz), 5.75 (br s, 2 H), 3.80 (br s, 1 H); ^{13}C NMR ($CDCl_3$, 100 MHz) δ 162.3 (d, J = 244.0 Hz), 139.4, 138.3, 134.5 (d, J = 3.0 Hz), 132.5, 129.3 (d, J = 8.0 Hz), 125.5, 120.2, 115.7 (d, J = 21.3 Hz), 105.9, 47.7 (t, J = 20.6 Hz); HRMS (HESI) *m/z* calcd for $C_{13}H_{11}D_2N_3O_2F$ $[M+H]^+$ 264.1112, found 264.1110.

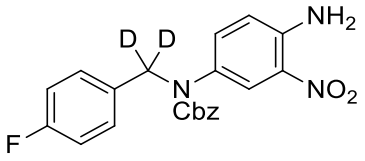

***N*-(4-Amino-3-nitrophenyl)-*N*-[$^2H_2$(4-fluorophenyl)methyl](phenylmethoxy)carboxamide**. A solution of (4-amino-3-nitrophenyl)[$^2H_2$(4-fluorophenyl)methyl]amine (0.100 g, 0.380 mmol)

and DIPEA (0.095 mL, 0.58 mmol) in 1,4-dioxane (1.9 mL) at rt was treated dropwise via syringe with benzyl chloroformate (0.060 mL, 0.41 mmol). The resulting solution was allowed to stir at rt for 18 h and was then quenched by the addition of H_2O/CH_2Cl_2 (1:1, 10 mL). The aqueous layer was extracted with CH_2Cl_2 (3 x 10 mL). The combined organic layers were washed with H_2O (2 x 10 mL) and brine (2 x 10 mL), dried (Na_2SO_4), filtered, and the solvent was evaporated under reduced pressure to give crude *N*-(4-amino-3-nitrophenyl)-*N*-[$^2H_2$(4-fluorophenyl)methyl](phenylmethoxy)carboxamide (0.220 g) as an orange-yellow oil that was used without further purification.

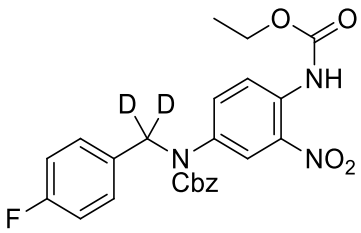

Benzyl (4-((ethoxycarbonyl)amino)-3-nitrophenyl)[$^2H_2$(4-fluorobenzyl)]carbamate. A solution of crude *N*-(4-amino-3-nitrophenyl)-*N*-[$^2H_2$(4-fluorophenyl)methyl](phenylmethoxy)carboxamide (0.220 g) and DIPEA (0.190 mL, 1.15 mmol) in 1,4-dioxane (3.5 mL) at rt was treated dropwise via syringe with ethyl chloroformate (0.090 mL, 0.92 mmol). The reaction mixture was stirred at 70 ^oC for 2 d and quenched by addition of H_2O/CH_2Cl_2 (1:1, 20 mL). The layers were separated and the aqueous phase was extracted with CH_2Cl_2 (2 x 10 mL). The combined organic phases were washed with 1 M aq. HCl (2 x 10 mL) and brine (2 x 10 mL), dried ($MgSO_4$), filtered, and the filtrate was concentrated under reduced pressure. Further drying under high vacuum gave crude product (0.320 g) as an orange-yellow solid that was purified by chromatography on SiO_2 (20% EtOAc in hexanes) to give benzyl (4-((ethoxycarbonyl)amino)-3-nitrophenyl)[$^2H_2$(4-

fluorobenzyl)]carbamate (0.100 g, 0.213 mmol, 56%) as a yellow oil: IR (CH_2Cl_2) 3364.5, 2981.5, 1738.4, 1702.4, 1509.8, 1331.4; ^{1}H NMR ($CDCl_3$, 400 MHz) δ 9.77 (s, 1 H), 8.51 (d, 1 H, *J* = 8.8 Hz), 7.99 (br s, 1 H), 7.36-7.30 (m, 4 H), 7.27-7.25 (m, 2 H), 7.17-7.13 (m, 2 H), 6.96 (tt, 2 H, *J* = 8.6, 2.3 Hz), 5.19 (s, 2 H), 4.26 (q, 2 H, *J* = 7.0 Hz), 1.34 (t, 3 H, *J* = 7.0 Hz); ^{13}C NMR ($CDCl_3$, 100 MHz) δ 162.4 (d, *J* = 245.0 Hz), 155.2, 153.1, 136.0, 135.7, 134.7, 134.0, 132.6 (d, *J* = 3.2 Hz), 129.7, 128.7, 128.4, 128.1, 123.9, 121.1, 115.7 (d, *J* = 21.3 Hz), 68.1, 62.2, 52.8 (br), 14.5; HRMS (HESI) *m/z* calcd for $C_{24}H_{19}D_2N_3O_6F$ [M-H] 468.1534, found 468.1545.

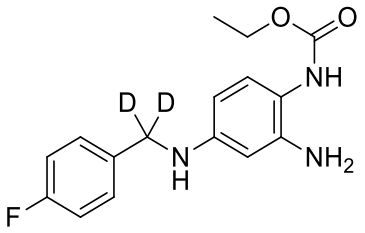

***N*-[2-Amino-4-({[^{2}H$_2$(4-fluorophenyl)]methyl}amino)phenyl]ethoxycarboxamide (NR561_87)**. A suspension of benzyl (4-((ethoxycarbonyl)amino)-3-nitrophenyl)[^{2}H$_2$(4-fluorobenzyl)]carbamate (0.095 g, 0.196 mmol) and 10% Pd/C (0.022 g, 0.020 mmol) in 1,4-dioxane (1.1 mL) and EtOH (0.60 mL) was allowed to stir at rt under an H_2 atmosphere (balloon) for 18 h. The solution was diluted with Et_2O (5 mL), filtered through a pad of Celite, and the solvent was evaporated under reduced pressure to give crude product (0.078 g) as a light brown oil that was purified by chromatography on SiO_2 (55% EtOAc in hexanes) to give NR561_87 (0.045 g, 0.147 mmol, 75%) as a light brown solid: Mp 142-143 ^{o}C (CH_2Cl_2); IR (ATR) 3394.7, 3342.6, 2987.4, 1675.6, 1506.2 cm^{-1}; ^{1}H NMR ($CDCl_3$, 400 MHz) δ 7.32-7.28 (m, 2 H), 7.01 (app. t, 2 H, *J* = 8.6 Hz), 6.91 (d, 1 H, *J* = 8.4 Hz), 6.04 (dd, 1 H, *J* = 8.4, 2.4 Hz), 5.98 (d, 1 H, *J* = 2.4 Hz), 4.18 (q, 2 H, *J* = 7.0 Hz), 3.78 (br s, 2 H), 1.28 (t, 3 H, *J* = 7.0 Hz); ^{13}C NMR ($CDCl_3$, 100 MHz) δ 162.1 (d, *J* = 243.0 Hz), 155.7, 147.8, 143.1, 135.1 (d, *J* = 3.0 Hz), 129.0 (d, *J* = 8.0

Hz), 128.0, 115.5 (d, J = 21.2 Hz), 114.1, 104.4, 100.8, 61.5, 47.1 (t, J = 20.6 Hz), 14.7; HRMS (HESI) *m/z* calcd for $C_{16}H_{17}D_2N_3O_2F$ $[M+H]^+$ 306.1581, found 306.1584.

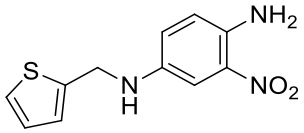

(4-Amino-3-nitrophenyl)(2-thienylmethyl)amine (1-37). A mixture of thiophene-2-carboxaldehyde (0.125 mL, 1.34 mmol), 2-nitro-*p*-phenylenediamine (0.210 g, 1.30 mmol), PTSA (0.035 g, 0.18 mmol), and 4 Å mol. sieves (1.063 g) in CH_2Cl_2 (3.1 mL) and MeOH (3.1 mL) was allowed to stir at rt for 5 h. The reaction mixture was filtered through Celite and the solvent removed under reduced pressure to give a dark brown solid that was dissolved in CH_2Cl_2 (20 mL), filtered through a thin pad of SiO_2 (CH_2Cl_2), and concentrated under reduced pressure to give crude imine (0.250 g) as a bright orange solid. The solid was suspended in 1,4-dioxane (1.5 mL) and MeOH (0.50 mL) and treated with $NaBH_4$ (0.070 g, 1.83 mmol) in 3 portions at 15 min intervals. The solution was allowed to stir at rt for 20 h and quenched by the addition of H_2O/CH_2Cl_2 (1:1, 30 mL). The aqueous layer was extracted with CH_2Cl_2 (3 x 10 mL). The combined organic layers were washed with H_2O (2 x 10 mL) and brine (2 x 10 mL), dried (Na_2SO_4), filtered, and concentrated under reduced pressure. Further drying of the residue under high vacuum at 50 ^oC gave (4-amino-3-nitrophenyl)(2-thienylmethyl)amine (0.230 g, 0.923 mmol, 71%) as a dark red solid: Mp 103-105 ^oC (CH_2Cl_2); IR (ATR) 3506.5, 3380.5, 3116.0, 1576.6, 1518.9, 1332.9 cm^{-1}; ^1H NMR ($CDCl_3$, 400 MHz) δ 7.37 (d, 1 H, J = 2.8 Hz), 7.23 (dd, 1 H, J = 4.8, 1.2 Hz), 7.03-7.02 (m, 1 H), 6.97 (dd, 1 H, J = 5.2, 3.6 Hz), 6.88 (dd, 1 H, J = 8.8, 2.8 Hz), 6.71 (d, 1 H, J = 8.8 Hz), 5.74 (br s, 2 H), 4.48 (s, 2 H), 3.83 (br s, 2 H); ^{13}C NMR ($CDCl_3$, 100 MHz) δ 142.2, 139.0, 138.5, 132.6, 127.1, 125.6, 125.6, 125.0, 120.2, 106.6, 44.2; HRMS (HESI) *m/z* calcd for $C_{11}H_{12}N_3O_2S$ $[M+H]^+$ 250.0645, found 250.0644.

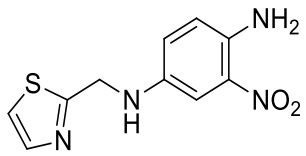

(4-Amino-3-nitrophenyl)(1,3-thiazol-2-ylmethyl)amine. A suspension of 2-thiazolecarboxaldehyde (0.115 mL, 1.27 mmol), 2-nitro-*p*-phenylenediamine (0.209 g, 1.30 mmol), PTSA (0.025 g, 0.13 mmol) and 4 Å molecular sieves (1.15 g) in CH_2Cl_2 (3.1 mL) and MeOH (3.1 mL) was stirred for 18 h at rt and filtered through Celite. The solvent was removed under reduced pressure to give a dark brown residue that was suspended in CH_2Cl_2 (20 mL), filtered through a thin pad of SiO_2 (CH_2Cl_2), concentrated under reduced pressure to give crude imine (0.205 g) as a bright orange solid. The solid was suspended in 1,4-dioxane (2 mL) and MeOH (0.75 mL) and $NaBH_4$ (0.035 g, 0.92 mmol) were added. The reaction mixture was stirred at rt for 8 h and quenched by the addition of H_2O/CH_2Cl_2 (1:1, 15 mL). The aqueous layer was extracted with CH_2Cl_2 (3 x 10 mL). The combined organic layers were washed with H_2O (2 x 10 mL) and brine (2 x 10 mL), dried (Na_2SO_4), filtered, and concentrated under reduced pressure. Further drying under high vacuum at 50 ^oC overnight gave (4-amino-3-nitrophenyl)(1,3-thiazol-2-ylmethyl)amine (0.194 g, 0.775 mmol, 61%) as a dark red solid: Mp 161-162 ^oC (CH_2Cl_2); IR (ATR) 3469.8, 3380.2, 3349.8, 1584.1, 1518.8, 1384.3, 1330.6 cm^{-1}; ^1H NMR (DMSO-d_6, 500 MHz) δ 7.74 (d, 1 H, *J* = 3.0 Hz), 7.58 (d, 1 H, *J* = 3.0 Hz), 7.04 (br s, 2 H), 7.02 (d, 1 H, *J* = 3.0 Hz), 6.99 (d, 1 H, *J* = 2.5 Hz), 6.90 (d, 1 H, *J* = 9.0 Hz), 6.39 (t, 1 H, *J* = 6.0 Hz), 4.54 (d, 2 H, *J* = 6.0 Hz); ^{13}C NMR (DMSO-d_6, 125 MHz) δ 171.8, 142.4, 140.1, 138.2, 129.9, 126.5, 120.4, 119.9, 103.0, 45.6; HRMS (HESI) *m/z* calcd for $C_{10}H_{11}N_4O_2S$ $[M+H]^+$ 251.0597, found 251.0595.

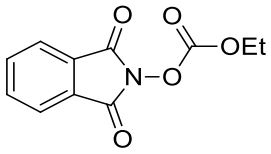

Ethyl (1,3-dioxobenzo[*c*]azolidin-2-yloxy)formate. A suspension of diphthalimidyl carbonate (0.382 g, 1.08 mmol) and EtOH (0.065 mL, 1.1 mmol) in THF (2.5 mL) was treated with Et_3N (0.150 mL, 1.07 mmol). Upon addition of base, the suspension turned yellow, progressing to orange over 30 min. The reaction mixture was stirred for 5 h and the solvent was evaporated. The residue was dissolved in EtOAc (25 mL) and washed with sat. aq. $NaHCO_3$ (5 x 10 mL) until the organic layer became clear. The combined aqueous washings were extracted with EtOAc (2 x 20 mL). The combined organic layers were dried ($MgSO_4$), filtered, and the solvent was evaporated under reduced pressure. Further drying under high vacuum gave ethyl (1,3-dioxobenzo[*c*]azolidin-2-yloxy)formate (0.230 g, 0.978 mmol, 90%) as a light yellow solid: ^{1}H NMR ($CDCl_3$, 300 MHz) δ 7.90-7.84 (m, 2 H), 7.81-7.76 (m, 2 H), 4.40 (q, 2 H, *J* = 7.2 Hz), 1.40 (t, 3 H, *J* = 7.2 Hz); ^{13}C NMR ($CDCl_3$, 75 MHz) δ 161.6, 152.4, 135.0, 128.8, 124.1, 67.7, 14.1.

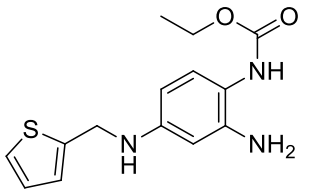

***N*-{2-Amino-4-[(2-thienylmethyl)amino]phenyl}ethoxycarboxamide (NR579_46)**. A suspension of (4-amino-3-nitrophenyl)(2-thienylmethyl)amine (0.104 g, 0.334 mmol, 80% purity) and 10% Pd/C (0.035 g, 0.032 mmol) in 1,4-dioxane (1.7 mL) and EtOH (0.70 mL) was allowed to stir at rt for 16 h under an H_2 atmosphere. The reaction mixture was diluted with Et_2O, filtered through a pad of Celite, and concentrated under reduced pressure. Further drying

under high vacuum gave the crude triamine (0.093 g) as a dark yellow oil. A solution of this oil (0.093 g) and Et_3N (0.080 mL, 0.57 mmol) in CH_2Cl_2 (1.2 mL) at rt was treated dropwise via syringe over 15 min with a solution of ethyl (1,3-dioxobenzo[*c*]azolidin-2-yloxy)formate (0.050 g, 0.21 mmol) in CH_2Cl_2 (1.2 mL). The reaction mixture was allowed to stir at rt for 18 h and concentrated under reduced pressure. The crude residue was dissolved in EtOAc (20 mL) and washed with sat. aq. $NaHCO_3$ (5 x 10 mL). The aqueous washes were extracted with EtOAc (2 x 20 mL) and the combined organic phases were dried ($MgSO_4$), filtered, and concentrated under reduced pressure to give crude product (0.200 g) as a brown-green oil, which was purified by chromatography on SiO_2 (5-10% EtOAc in CH_2Cl_2) to give NR579_46 (0.037 g, 0.13 mmol, 60%) as a gray oil that solidified upon standing: Mp 95-96 ^oC (CH_2Cl_2); IR (ATR) 3403.4, 3287.9, 1677.0, 1518.6 cm^{-1}; ^1H NMR ($CDCl_3$, 500 MHz) δ 7.20 (dd, 1 H, *J* = 5.0, 1.5 Hz), 6.99 (app. d, 1 H, *J* = 2.5 Hz), 6.96 (dd, 1 H, *J* = 5.0, 3.5 Hz), 6.93 (d, 1 H, *J* = 8.5 Hz), 6.09 (dd, 1 H, *J* = 8.3, 2.5 Hz), 6.04 (d, 1 H, *J* = 2.5 Hz), 4.44 (s, 2 H), 4.19 (q, 2 H, *J* = 7.0 Hz), 3.82 (br s, 3 H), 1.28 (t, 3 H, *J* = 6.5 Hz); ^{13}C NMR ($CDCl_3$, 125 MHz) δ 155.6, 147.4, 143.1, 127.8, 127.0, 125.1, 124.7, 114.5, 104.7, 101.2, 61.5, 43.7, 14.7; HRMS (HESI) *m/z* calcd for $C_{14}H_{18}N_3O_2S$ $[M+H]^+$ 292.1120, found 292.1109.

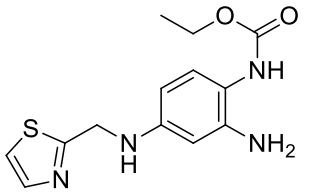

***N*-{2-Amino-4-[(1,3-thiazol-2-ylmethyl)amino]phenyl}ethoxycarboxamide (NR579_38)**. A suspension of (4-amino-3-nitrophenyl)(1,3-thiazol-2-ylmethyl)amine (0.072 g, 0.29 mmol) and Pd/C (0.028 g, 0.026 mmol) was stirred under an H_2 atmosphere (balloon) for 18 h, diluted with Et_2O (10 mL) and filtered through a pad of Celite. The solvent was removed under reduced

pressure to give the crude triamine (0.076 g) as a dark red oil which was used without further purification. A solution of this oil (0.076 g) and Et_3N (0.075 mL, 0.53 mmol) in CH_2Cl_2 (1 mL) at rt was treated dropwise via syringe over 10 min with a solution of ethyl (1,3-dioxobenzo[*c*]azolidin-2-yloxy)formate (0.061 g, 0.26 mmol) in CH_2Cl_2 (1.10 mL). The reaction mixture was stirred for 18 h, concentrated under reduced pressure, resuspended in EtOAc (20 mL), and washed with sat aq. $NaHCO_3$ (4 x 20 mL) until the washes were clear. The aqueous layers were extracted with EtOAc (2 x 20 mL) and the combined organic fractions were washed with H_2O (2 x 20 mL) and brine (2 x 20 mL), dried ($MgSO_4$), filtered, and the solvent evaporated under reduced pressure to give crude product (0.060 g) as a brown-red oil that was purified by chromatography on SiO_2 (70% EtOAc in hexanes) to give NR579_38 (0.045 g, 0.15 mmol, 59% over 2 steps) as a blue-green oil that solidified upon standing: Mp 46-47 ^oC (CH_2Cl_2); IR (CH_2Cl_2) 3352.87, 2981.3, 1696.9, 1621.1, 1523.2 cm^{-1}; ^1H NMR ($CDCl_3$, 400 MHz) δ 7.72 (d, 1 H, *J* = 3.2 Hz), 7.24 (d, 1 H, *J* = 3.2 Hz), 6.91 (d, 1 H, *J* = 8.4 Hz), 6.16 (br s, 1 H), 6.08 (dd, 1 H, *J* = 8.4, 2.4 Hz), 6.02 (d, 1 H, *J* = 2.4 Hz), 4.59 (s, 2 H), 4.17 (q, 2 H, *J* = 7.2 Hz), 3.81 (br s, 2 H), 1.27 (t, 3 H, *J* = 6.8 Hz); ^{13}C NMR ($CDCl_3$, 400 MHz) δ 171.6, 155.7, 146.8, 143.1, 142.7, 127.9, 119.2, 114.8, 104.7, 101.2, 61.5, 46.5, 14.7; HRMS (HESI) *m/z* calcd for $C_{13}H_{17}N_4O_2S$ $[M+H]^+$ 293.1067, found 293.1063.

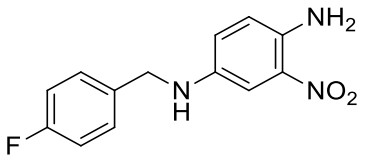

(4-Amino-3-nitrophenyl)[(4-fluorophenyl)methyl]amine. A mixture of 2-nitro-*p*-phenylenediamine (0.998 g, 6.19 mmol) and 3 Å molecular sieves (3 g) in xylenes (30 mL) was heated to 90 ^oC and treated with 4-fluorobenzaldehyde (0.690 mL, 6.27 mmol). The reaction

mixture was allowed to stir for 20 h, filtered through a short pad of SiO_2, and allowed to cool for 6 h. A solid precipitate was filtered off and dried in vacuo to give crude imine (0.719 g), that was dissolved in 1,4-dioxane (4 mL) and MeOH (1 mL) and treated with $NaBH_4$ (0.157 g, 4.11 mmol) in 3 batches at 15 min intervals. The solution was stirred for 10 h, and quenched with H_2O (25 mL). The solid precipitated was filtered and dried to give colorless (4-amino-3-nitrophenyl)[(4-fluorophenyl)methyl]amine (0.573 g, 2.19 mmol, 35%): Mp 113-114 ^oC; IR (ATR) 3518.0, 3497.9, 3395.8, 3372.6, 1578.7, 1503.2, 1406.7, 1330.0 cm^{-1}; ^1H NMR ($CDCl_3$, 400 MHz) δ 7.33 (app. dd, 2 H, *J* = 5.4, 2.2 Hz), 7.30 (d, 1 H, *J* = 2.8 Hz), 7.04 (app. t, 2 H, *J* = 8.6 Hz), 6.84 (dd, 1 H, *J* = 8.8, 2.8 Hz), 6.70 (d, 1 H, *J* = 8.8 Hz), 5.73 (br s, 2 H), 4.26 (d, 2 H, *J* = 4.0 Hz); ^{13}C NMR ($CDCl_3$, 100 MHz) δ 162.3 (d, *J* = 245.0 Hz), 139.4, 138.3, 134.6 (d, *J* = 2.9 Hz), 132.6, 129.4 (d, *J* = 8.0 Hz), 125.4, 120.2, 115.7 (d, *J* = 22.0 Hz), 106.1, 48.4; HRMS (HESI) *m/z* calcd for $C_{13}H_{13}N_3O_2F$ $[M+H]^+$ 262.0986, found 262.0981.

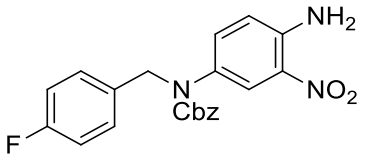

***N*-(4-Amino-3-nitrophenyl)-N-[(4fluorophenyl)methyl](phenylmethoxy)carboxamide**. A solution of (4-amino-3-nitrophenyl)[(4-fluorophenyl)methyl]amine (0.207 g, 0.792 mmol) and DIPEA (0.140 mL, 0.848 mmol) in 1,4-dioxane (4 mL) at rt was treated dropwise via syringe with benzyl chloroformate (0.120 mL, 0.819 mmol). The reaction mixture was allowed to stir at rt for 5 h and was then quenched with H_2O/CH_2Cl_2 (1:1, 6.5 mL). The aqueous layer was extracted with CH_2Cl_2 (3 x 5 mL). The combined organic layers were washed with brine, dried (Na_2SO_4), filtered, and concentrated under reduced pressure to give crude *N*-(4-amino-3-

nitrophenyl)-N-[(4fluorophenyl)methyl](phenylmethoxy)carboxamide (0.420 g) as an orange oil that was used without further purification.

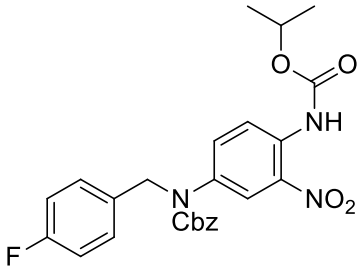

***O*-Benzyl *N*-(4-fluorobenzyl)-*N*-(4-((isopropoxycarbonyl)amino)-3-nitrophenyl)carbamate**. A solution of crude *N*-(4-amino-3-nitrophenyl)-N-[(4fluorophenyl)methyl](phenylmethoxy)-carboxamide (0.415 g) and DIPEA (0.390 mL, 2.36 mmol) in 1,4-dioxane (6.00 mL) at rt was treated dropwise via syringe with a solution of isopropyl chloroformate in toluene (1.95 mL, 1.95 mmol, 1.0 M). The reaction mixture was stirred at 70 ^{o}C for 2 d and quenched by the addition of H_2O/CH_2Cl_2 (1:1, 10 mL). The aqueous layer was extracted with CH_2Cl_2 (3 x 10 mL) and the combined organic layers were washed with water and brine, dried ($MgSO_4$), filtered, and concentrated under reduced pressure to give crude product (0.410 g) as a dark orange oil that was purified by chromatography on SiO_2 (10% EtOAc in hexanes) to give *O*-benzyl *N*-(4-fluorobenzyl)-*N*-(4-((isopropoxycarbonyl)amino)-3-nitrophenyl)carbamate (0.097 g) as a yellow oil along with recovered starting material (0.140 g). The starting material was recycled through the reaction procedure again to give *O*-benzyl *N*-(4-fluorobenzyl)-*N*-(4-((isopropoxycarbonyl)amino)-3-nitrophenyl)carbamate (0.050 g, 0.147 g total, 0.305 mmol, 39% over two steps) as a yellow oil: IR (CH_2Cl_2) 3367.4, 2982.2, 1735.0, 1705.4, 1510.6, 1338.3 cm^{-1}; ^{1}H NMR ($CDCl_3$, 400 MHz) δ 9.72 (s, 1 H), 8.52 (d, 1 H, *J* = 8.8 Hz), 7.98 (br s, 1 H), 7.36-7.25 (m, 5 H), 7.15 (app. t, 2 H, *J* = 6.8 Hz), 6.96 (t, 2 H, *J* = 8.8 Hz), 5.19 (s, 2 H), 5.08-4.96 (m, 2 H), 4.84 (s, 2 H), 1.32 (d, 6 H, *J* = 6.4 Hz); ^{13}C NMR ($CDCl_3$, 100 MHz) δ 162.4 (d, *J* =

245.0 Hz), 155.3, 152.8, 136.0, 135.7, 134.7, 134.2, 132.8 (d, *J* = 3.2 Hz), 129.8, 128.7, 128.4, 128.1, 124.0, 121.1, 115.8 (d, *J* = 21.3 Hz); HRMS (HESI) *m/z* calcd for $C_{25}H_{24}N_3O_6F$ $[M-H]^-$ 480.1565, found 480.1575.

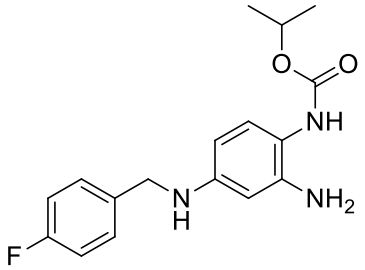

***N*-(2-Amino-4-{[(4-fluorophenyl)methyl]amino}phenyl)(1-methylethoxy)carboxamide (NR561_62)**. A suspension of *O*-benzyl *N*-(4-fluorobenzyl)-*N*-(4-((isopropoxycarbonyl)amino)-3-nitrophenyl)carbamate (0.049 g, 0.10 mmol) and 10% Pd/C (0.013 g, 0.012 mmol, 10 mol%) in 1,4-dioxane (0.60 mL) and EtOH (0.30 mL) was allowed to stir at rt for 18 h under an H_2 atmosphere (balloon). The reaction mixture was diluted with Et_2O (5 mL), filtered through Celite, and the solvent was evaporated under reduced pressure to give crude product (0.033 g) as a brown oil that was purified by chromatography on SiO_2 (50% EtOAc in hexanes) to give NR561_62 (0.024 g, 0.076 mmol, 74%) as an off-white solid: Mp 171-172 ^oC (CH_2Cl_2); IR (ATR) 3396.4, 3342.9, 3289.3, 2981.7, 1674.8; ^1H NMR ($CDCl_3$, 400 MHz) δ 7.31 (app. dd, 2 H, *J* = 8.4, 5.6 Hz), 7.01 (app. t, 2 H, *J* = 10.2 Hz), 6.92 (d, 1 H, *J* = 8.0 Hz), 6.06 (dd, 1 H, *J* = 8.4, 2.4 Hz), 6.00 (d, 1 H, *J* = 2.4 Hz), 4.97 (m, 1 H), 4.25 (s, 2 H), 3.81 (br s, 2 H), 1.27 (d, 6 H, *J* = 6.4 Hz); 13C NMR ($CDCl_3$, 100 MHz) δ 162.2 (d, *J* = 244.0 Hz), 155.3, 147.7, 143.1, 135.3 (d, *J* = 2.9 Hz), 129.1 (d, *J* = 7.9 Hz), 127.8, 115.6 (d, *J* = 21.2 Hz), 114.4, 104.5, 100.8, 68.9, 47.8, 22.3; HRMS (HESI) *m/z* calcd for $C_{17}H_{21}N_3O_2F$ $[M-H]^-$ 318.1612, found 318.1611.

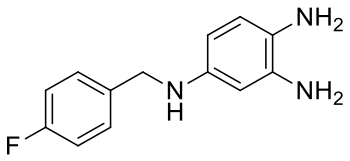

(3,4-Diaminophenyl)[(4-fluorophenyl)methyl]amine. A suspension of (4-amino-3-nitrophenyl)[(4-fluorophenyl)methyl]amine (0.101 g, 0.321 mmol) and 10% Pd/C (0.035 g, 0.032 mmol) in 1,4-dioxane (1.6 mL) and EtOH (0.80 mL) was allowed to stir at rt under an H_2 atmosphere (balloon) for 18 h. The reaction mixture was diluted with Et_2O (10 mL), filtered through a pad of celite, and concentrated under reduced pressure. Further drying under high vacuum gave crude (3,4-diaminophenyl)[(4-fluorophenyl)methyl]amine (0.077 g) as a brown oil which was used without further purification.

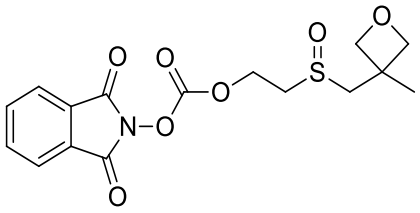

2-{[(3-Methyloxetan-3-yl)methyl]sulfinyl}ethyl(1,3-dioxobenzo[c]azolidin-2-yloxy)formate. A suspension of diphthalimidyl carbonate (0.380 g, 1.08 mmol) and MMS-350 sulfoxide alcohol (Sprachman et al., **2012**, *10*, 269-277) (0.195 g, 1.09 mmol) in THF (5 mL) was treated with Et_3N (0.145 mL, 1.03 mmol). Upon addition of base, the suspension turned yellow, eventually progressing to a clear orange solution after 20 min. The reaction mixture was stirred for 2 h, concentrated under reduced pressure, dissolved in EtOAc (25 mL) and washed with saturated aqueous $NaHCO_3$ (5 x 3 mL) until the organic layer became clear. The combined aqueous washings were extracted with EtOAc (2 x 10 mL). The combined organic layers were dried ($MgSO_4$) and concentrated under reduced pressure to give 1-2-{[(3-methyloxetan-3-

yl)methyl]sulfinyl}ethyl(1,3-dioxobenzo[c]azolidin-2-yloxy)formate (0.265 g, 0.721 mmol, 66%) as a foaming solid which was used without further purification.

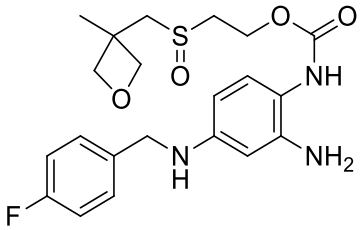

2-(((3-Methyloxetan-3-yl)methyl)sulfinyl)ethyl (2-amino-4-((4-fluorobenzyl)amino)phenyl)carbamate (NR579_36). A solution of crude (3,4-diaminophenyl)[(4-fluorophenyl)methyl]amine (0.062 g, 0.27 mmol) and Et_3N (0.070 mL, 0.50 mmol) in CH_2Cl_2 (1.00 mL) was treated dropwise via syringe over 10 min with a solution of crude 1-2-{[(3-methyloxetan-3-yl)methyl]sulfinyl}ethyl(1,3-dioxobenzo[c]azolidin-2-yloxy)formate (0.095 g, 0.26 mmol) in CH_2Cl_2 (1.00 mL). The reaction mixture was stirred for 18 h at rt, concentrated under reduced pressure, dissolved in EtOAc (20 mL), and washed with sat. aq. $NaHCO_3$ (3 x 10 mL). The combined aqueous layers were extracted with EtOAc (2 x 20 mL) and the combined organic layers were dried ($MgSO_4$), filtered and concentrated under reduced pressure to give crude product (0.090 g) as a dark green oil that was purified by chromatography on SiO_2 (3-5% MeOH in CH_2Cl_2) to give NR579_36 (0.041 g, 0.094 mmol, 39% over two steps) as a light brown oil: IR (CH_2Cl_2) 3362.9, 2257.0, 1712.8, 1619.2, 1525.3, 1508.3 cm^{-1}; ^1H NMR (DMSO-d_6, 500 MHz, 323 K) δ 7.99 (br s, 1 H), 7.38-7.35 (m, 2 H), 7.09 (t, 2 H, J = 8.8 Hz), 6.73 (d, 1 H, J = 8.5 Hz), 5.99 (d, 1 H, J = 2.0 Hz), 5.88 (dd, 1 H, J = 8.5, 2.5 Hz), 5.56 (s, 1 H), 4.64 (d, 1 H, J = 5.5 Hz), 4.55 (d, 1 H, J = 5.5 Hz), 4.45-4.31 (m, 5 H), 4.24 (d, 1 H, J = 6.0 Hz), 4.19 (d, 2 H, J = 4.5 Hz), 3.19-3.13 (m, 2 H), 3.03-3.00 (m, 2 H), 1.49 (s, 3 H); ^{13}C NMR (DMSO-d_6, 125 MHz, 323 K) δ 160.7 (d, J = 240.0 Hz), 154.2, 147.1, 143.2,

136.4, 128.5 (d, J = 7.5 Hz), 126.9, 114.3 (d, J = 21.3 Hz), 112.7, 101.7, 98.9, 90.0, 80.6, 59.8, 56.7, 51.7, 45.9, 37.6, 23.0; HRMS (HESI) *m/z* calcd for $C_{21}H_{27}N_3O_4FS$ $[M+H]^+$ 436.1701, found 436.1698.

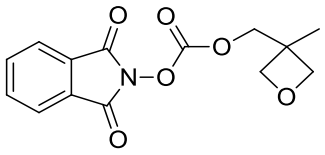

(3-Methyloxetan-3-yl)methyl(1,3-dioxobenzo[*c*]azolidin-2-yloxy)formate. A suspension of diphthalimidyl carbonate (0.381 g, 1.08 mmol) and 3-methyl-3-oxetanemethanol (0.110 mL, 1.08 mmol) in THF (5 mL) was treated with Et_3N (0.160 mL, 1.14 mmol). Upon addition of base, the suspension turned yellow, progressing to orange over 2 h. The reaction mixture was stirred for 14 h, concentrated under reduced pressure, dissolved in EtOAc (25 mL) and washed with sat. aq. $NaHCO_3$ (5 x 10 mL) until the organic layer became clear. The combined aqueous washings were extracted with EtOAc (2 x 20 mL). The combined organic layers were dried ($MgSO_4$), filtered, and concentrated under reduced pressure. Further drying under high vacuum gave (3-methyloxetan-3-yl)methyl(1,3-dioxobenzo[*c*]azolidin-2-yloxy)formate (0.255 g, 0.876 mmol, 81%) as a clear, light yellow oil: IR (CH_2Cl_2) 2965.4, 2875.7, 1811.8, 1788.7, 1742.0 cm^{-1}; ^1H NMR ($CDCl_3$, 400 MHz) δ 7.91-7.88 (m, 2 H), 7.81-7.79 (m, 2 H), 4.54 (d, 2 H, J = 6.4 Hz), 4.47 (s, 2 H), 4.43 (d, 2 H, J = 6.0 Hz), 1.41 (s, 3 H); ^{13}C NMR ($CDCl_3$, 100 MHz) 161.5, 152.7, 135.1, 128.8, 124.3, 79.1, 75.4, 39.5, 20.8; HRMS (HESI) *m/z* calcd for $C_{14}H_{14}NO_6$ $[M+H]^+$ 292.0816, found 292.0819.

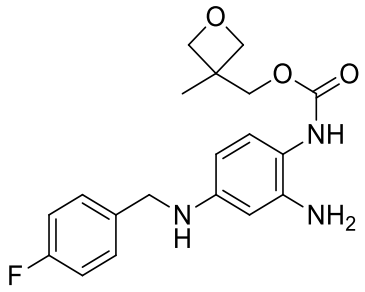

***N*-(2-Amino-4-{[(4-fluorophenyl)methyl]amino}phenyl)[(3-methyloxetan-3-yl)methoxy] carboxamide (NR579_45)**. A solution of crude (3,4-diaminophenyl)[(4-fluorophenyl)methyl]amine (0.077 g) and Et_3N (0.090 mL, 0.64 mmol) in CH_2Cl_2 (1.30 mL) at rt was treated dropwise via syringe over 15 min with a solution of (3-methyloxetan-3-yl)methyl(1,3-dioxobenzo[*c*]azolidin-2-yloxy)formate (0.101 g, 0.347 mmol) in CH_2Cl_2 (1.30 mL). The reaction mixture was allowed to stir for 18 h, concentrated under reduced pressure, dissolved in EtOAc (20 mL), and washed with sat. aq. $NaHCO_3$ (3 x 10 mL). The combined aqueous washes were extracted with EtOAc (2 x 20 mL) and the combined organic layers were dried ($MgSO_4$), filtered, and the solvent evaporated under reduced pressure to give crude product (0.110 g) as an olive green oil that was purified by chromatography on SiO_2 (40-50% EtOAc in hexanes) to give NR579_45 (0.033 g, 0.092 mmol, 29% over 2 steps) as a dark brown oil: IR (CH_2Cl_2) 3346.5, 2960.4, 2877.0, 1701.7, 1619.5, 1524.5, 1508.1 cm^{-1}; ^1H NMR ($CDCl_3$, 400 MHz) δ 7.30 (dd, 2 H, *J* = 8.2, 5.4 Hz), 7.02 (app. t, 2 H, *J* = 8.6 Hz), 6.93 (d, 1 H, *J* = 7.6 Hz), 6.21 (br s, 1 H), 6.06 (d, 1 H, *J* = 8.4 Hz), 6.00 (s, 1 H), 4.58 (app. br s, 2 H), 4.39 (app. br s, 2 H), 4.25 (s, 2 H), 4.20 (s, 2 H), 3.80 (br s, 3 H), 1.35 (s, 3 H); ^{13}C NMR ($CDCl_3$, 100 MHz) δ 161.2 (d, *J* = 243.0 Hz), 155.5, 147.9, 143.1, 135.2 (d, *J* = 3.0 Hz), 129.0 (d, *J* = 8.0 Hz), 127.9, 115.6 (d, *J* = 21.0 Hz), 113.9, 104.6, 100.8, 79.6, 69.4, 47.7, 39.5, 21.3; HRMS (HESI) *m/z* calcd for $C_{19}H_{23}N_3O_3F$ $[M+H]^+$ 360.1723, found 360.1712.

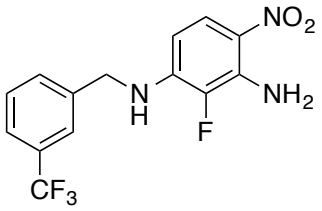

2-Fluoro-4-nitro-*N*^{1}-(3-(trifluoromethyl)benzyl)benzene-1,3-diamine. To a stirred solution of 2,3-difluoro-6-nitroaniline (0.200 g, 1.11 mmol, 1.00 equiv) in dry DMSO (4.6 mL) were added 3-(trifluoromethyl)benzylamine (0.195 mL, 1.34 mmol, 1.2 equiv) followed by Et_3N (0.135 g, 1.34 mmol, 1.2 equiv) and I_2 (cat. 2 mg). The reaction mixture was heated to 120 °C for 24 h, cooled to room temperature, diluted with water (25 mL) and extracted with EtOAc (3 x 15 mL). The combined organic layers were washed with brine, dried (Na_2SO_4), filtered and concentrated under reduced pressure. The residue was purified by chromatography on SiO_2 (EtOAc/hexanes, 1:10 to 1:4 to 1:3) to afford 2-fluoro-4-nitro-*N*^{1}-(3-(trifluoromethyl)benzyl)benzene-1,3-diamine as a yellow solid (0.280 g, 76%): Mp 156.0-157.2 °C; IR (ATR) 3495.2, 3383.4, 1627.4, 1480.1, 1411.1, 1275.1, 1250.8, 1120.3, 1070.0, 797.8 cm^{-1}; ^{1}H NMR (400 MHz, $CDCl_3$) δ 7.86 (dd, *J* = 9.6, 1.6 Hz, 1 H), 7.59-7.57 (m, 2 H), 7.54-7.47 (m, 2 H), 6.15-6.00 (m, 3 H), 4.93 (br, 1 H), 4.54 (d, *J* = 6.0 Hz, 2 H); ^{13}C NMR (100 MHz, $CDCl_3$) δ 140.9 (d, *J* = 9.5 Hz), 138.9, 138.0 (d, *J* = 228.6 Hz), 135.2 (d, *J* = 12.9 Hz), 131.5 (q, *J* = 32.5 Hz), 130.5, 129.6, 125.6 (d, *J* = 3.5 Hz), 124.9 (q, *J* = 3.7 Hz), 124.1 (q, *J* = 272.4 Hz), 124.0 (q, *J* = 3.7 Hz), 123.7 (d, *J* = 2.9 Hz), 100.7 (d, *J* = 2.9 Hz), 46.8; ^{19}F NMR (471 MHz , $CDCl_3$) δ -62.7 (s, 3 F), -160.6 (s, 1 F); HRMS (HESI) *m/z* calcd for $C_{14}H_{12}N_3O_2F_4$ $[M+H]^+$ 330.0860, found 330.0858.

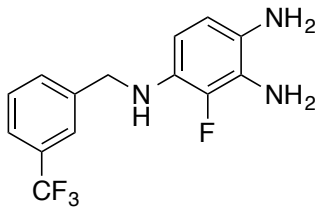

3-Fluoro-N^4-(3-(trifluoromethyl)benzyl)benzene-1,2,4-triamine. To a stirred solution of 2-fluoro-4-nitro-N^1-(3-(trifluoromethyl)benzyl)benzene-1,3-diamine (0.280 g, 0.85 mmol) in MeOH (2 mL) was added zinc powder (0.278 g, 4.25 mmol) followed by the dropwise addition of saturated ammonium chloride (0.80 mL). The reaction mixture was stirred vigorously at room temperature overnight, diluted with EtOAc (2 mL) and water (1 mL), and filtered through Celite. The Celite was washed with EtOAc and the solution was extracted with EtOAc (3 x 5 mL). The combined organic layers were dried (Na_2SO_4) and concentrated to afford crude product as a dark red solid (0.190 g, 75%) that was used in the next step without further purification: ^{1}H NMR (400 MHz, $CDCl_3$) δ 7.63 (s, 1 H), 7.56 (d, 1 H, J = 7.6 Hz), 7.52 (d, 1 H, J = 7.6 Hz), 7.44 (t, 1 H, J = 7.6 Hz), 6.37 (dd, 1 H, J = 8.4, 2.0 Hz), 5.99 (t, 1 H, J = 8.8 Hz), 4.36 (s, 2 H), 3.98 (br s, 1 H), 3.52 (br s, 2 H), 3.10 (br s, 2 H). ^{19}F NMR (471 MHz, $CDCl_3$) δ -62.5 (s, 3 F), -155.8 (s, 1 F).

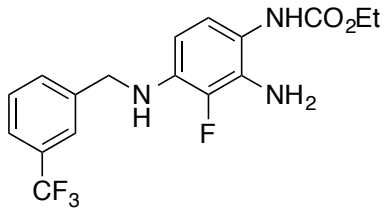

Ethyl (2-amino-3-fluoro-4-((3-(trifluoromethyl)benzyl)amino)phenyl)carbamate (RL648_73). An oven-dried 5-mL round bottomed flask equipped with a magnetic stir bar under argon was charged at 0 °C with 3-fluoro-N^4-(3-(trifluoromethyl)benzyl)benzene-1,2,4-triamine (0.06 g, 0.20 mmol), CH_2Cl_2 (1 mL) and DIPEA (0.043 mL, 0.25 mmol). Ethyl chloroformate (0.02 mL, 0.20 mmol) was added dropwise via syringe at 0 °C. The resulting mixture was stirred for 1 h at 0 °C and for 3 h at room temperature, and quenched by addition of water. The aqueous layer was extracted with CH_2Cl_2 (3 x 2 mL). The combined organic extracts were dried (Na_2SO_4) and concentrated under reduced pressure, and the residue was purified by chromatography on

SiO_2 (EtOAc/hexanes, 4:1 to 3:1) to afford RL648_73 as a dark red solid (0.045 g, 60%). Recrystallization from CH_2Cl_2/hexanes gave colorless crystals: Mp 129.3-129.7 °C; IR (ATR) 3405.8, 3290.2, 1675.9, 1452.2, 1329.1, 1246.2, 1159.5, 1112.9, 1071.9, 915.3, 700.9 cm^{-1}; ^1H NMR (400 MHz, $CDCl_3$) δ 7.61 (s, 1 H), 7.54 (app t, 2 H, *J* = 7.2 Hz), 7.45 (t, 1 H, *J* = 7.6 Hz), 6.74 (dd, 1 H, *J* = 8.4, 1.2 Hz), 6.11 (br s, 1 H), 6.02 (t, 1 H, *J* = 8.8 Hz), 4.41 (d, 2 H, *J* = 5.2 Hz), 4.30 (br s, 1 H), 4.20 (q, 2 H, *J* = 7.2 Hz), 3.86 (br s, 2 H), 1.28 (t, 3 H, *J* = 7.2 Hz); ^{13}C NMR (100 MHz, acetone-d_6) δ 156.0, 143.1, 141.8 (d, *J* = 227.9 Hz), 135.5 (d, *J* = 9.7 Hz), 132.4, 131.8, 130.9 (q, *J* = 31.8 Hz), 130.1, 125.5 (q, *J* = 271.5 Hz), 124.5 (q, *J* = 3.9 Hz), 124.3 (q, *J* = 3.9 Hz), 122.3, 116.5, 101.3, 61.2, 47.4, 15.0; ^{19}F NMR (376 MHz, $CDCl_3$) δ -62.6 (s, 3 F), -155.5 (s, 1 F); HRMS (HESI) *m/z* calcd for $C_{17}H_{18}N_3O_2F_4$ $[M+H]^+$ 372.1330, found 372.1328.

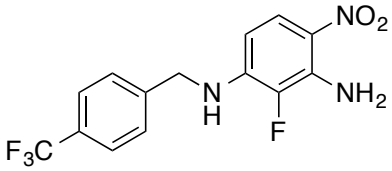

2-Fluoro-4-nitro-*N*^{1}-(4-(trifluoromethyl)benzyl)benzene-1,3-diamine. A solution of 2,3-difluoro-6-nitroaniline (0.100 g, 0.557 mmol, 1.00 equiv) in dry DMSO (4.6 mL) was treated with 4-(trifluoromethyl)benzylamine (0.081 mL, 0.557 mmol, 1.00 equiv) followed by Et_3N (0.09 mL, 0.669 mmol, 1.20 equiv) and I_2 (cat. 1 mg). The reaction mixture was heated to 120 °C for 24 h, cooled to room temperature, diluted with water (25 mL) and extracted with EtOAc (3 x 15 mL). The combined organic layers were washed with brine, dried (Na_2SO_4), filtered and concentrated under reduced pressure. The residue was purified by chromatography on SiO_2 (EtOAc/hexanes,1:10 to 1:5 to 1:3) to afford the 2-fluoro-4-nitro-*N*^{1}-(4-(trifluoromethyl)benzyl)benzene-1,3-diamine (0.120 g, 65 %) as a yellow solid: Mp 165.4-166.7

°C; IR (ATR) 3487.3, 3377.3, 1629.0, 1548.9, 1479.9, 1410.9, 1328.9, 1274.9, 1235.7, 1200.3, 1178.0, 1153.7, 1090.4, 1066.1, 1015.8, 786.5, 754.9 cm^{-1}; ^1H NMR (500 MHz, $CDCl_3$) δ 7.86 (dd, 1H, *J* = 9.5, 1.0 Hz), 7.63 (d, 2 H, *J* = 8.0 Hz), 7.44 (d, 2 H, *J* = 8.0 Hz), 6.00-6.12 (m, 3H), 4.94 (br s, 1 H), 4.55 (d, *J* = 6.0 Hz, 2 H); ^{13}C NMR (100 MHz, acetone-d_6) δ 144.2 (d, *J* = 1.0 Hz), 141.5 (d, *J* = 9.0 Hz), 137.6 (d, *J* = 227.0 Hz), 135.8 (d, *J* = 13.0 Hz), 128.8 (q, *J* = 32.0 Hz), 127.6, 125.4 (q, *J* = 4.0 Hz), 124.5 (d, *J* = 4.0 Hz), 124.5 (q, *J* = 269.0 Hz), 122.9 (d, *J* = 2.0 Hz), 100.7 (d, *J* = 4.0 Hz), 45.5; ^{19}F NMR (376 MHz, $CDCl_3$) δ -62.9 (s, 3 F), -160.7 (s, 1 F); HRMS (HESI) *m/z* calcd for $C_{14}H_{12}N_3O_2F_4$ $[M+H]^+$ 330.0860, found 330.0858.

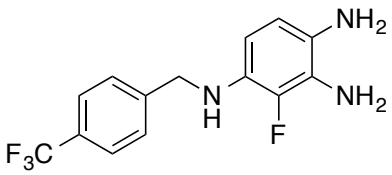

3-Fluoro-*N*^{4}-(4-(trifluoromethyl)benzyl)benzene-1,2,4-triamine. To a solution of 2-fluoro-4-nitro-*N*^{1}-(4-(trifluoromethyl)benzyl)benzene-1,3-diamine (0.066 g, 0.2 mmol) in MeOH (0.5 mL) was added zinc powder (0.066 g, 1.00 mmol) followed by the dropwise addition of a solution of saturated ammonium chloride (0.19 mL). The reaction mixture was stirred vigorously at room temperature for 5 h and filtered through Celite. The Celite was washed with EtOAc and the aqueous solution was extracted with EtOAc (3 x 2 mL). The combined organic layers were dried (Na_2SO_4) and concentrated to afford 3-fluoro-*N*^{4}-(4-(trifluoromethyl)benzyl)benzene-1,2,4-triamine (0.060 g, 100%) as a dark red solid that was used in the next step without further purification: ^1H NMR (400 MHz, $CDCl_3$) δ 7.58 (d, 2 H, *J* = 8.0 Hz), 7.47 (d, 2 H, *J* = 8.0 Hz), 6.35 (dd, 1 H, *J* = 8.4, 1.6 Hz), 5.99 (t, 1 H, *J* = 8.4 Hz), 4.37 (s, 2 H), 4.02 (br s, 1 H), 3.52 (br s, 2 H), 3.13 (br s, 2 H); HRMS (HESI) *m/z* calcd for $C_{14}H_{14}N_3F_4$ $[M+H]^+$ 300.1118, found 300.1113.

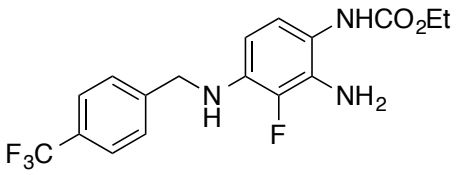

Ethyl (2-amino-3-fluoro-4-((4-(trifluoromethyl)benzyl)amino)phenyl)carbamate (RL648_81). An oven-dried 5-mL round bottomed flask equipped with a magnetic stir bar under argon was charged at 0 °C with 3-fluoro-N^4-(4-(trifluoromethyl)benzyl)benzene-1,2,4-triamine (0.06 g, 0.20 mmol), CH_2Cl_2 (1 mL) and DIPEA (0.043 mL, 0.25 mmol). Ethyl chloroformate (0.02 mL, 0.20 mmol) was added dropwise via syringe at 0 °C. The reaction mixture was stirred for 1 h at 0 °C and then for 3 h at room temperature, quenched with water, and extracted with CH_2Cl_2 (3 x 2 mL). The combined organic extracts were dried (Na_2SO_4) and concentrated under reduced pressure. The residue was purified by chromatography on SiO_2 (EtOAc/hexanes, 4:1 to 3:1) to afford a dark red solid. Recrystallization from CH_2Cl_2/hexanes gave RL648_81 (0.035 g, 47%) as colorless crystals: Mp 171.4-172.2 °C; IR (ATR) 3399.7, 3338.2, 3299.0, 1675.6, 1643.9, 1617.8, 1528.4, 1489.2, 1478.0, 1442.6, 1323.3, 1248.8, 1157.5, 1112.7, 1103.4, 825.7, 781.0, 775.4, 767.9, 672.9 cm^{-1}; ^1H NMR (400 MHz, $CDCl_3$) δ 7.59 (d, 2 H, J = 8.0 Hz), 7.46 (d, 2 H, J = 8.0 Hz), 6.73 (d, 1 H, J = 8.4 Hz), 6.13 (br s, 1 H), 5.99 (t, 1 H, J = 8.8 Hz), 4.42 (s, 2 H), 4.33 (br s, 1 H), 4.19 (q, 2 H, J = 7.2 Hz), 3.86 (br s, 2 H), 1.29 (t, 3 H, J = 7.2 Hz); ^{13}C NMR (100 MHz, acetone-d_6) δ 156.0, 146.4, 141.7 (d, J=227.7 Hz), 135.4, 132.5, 129.3 (q, J = 32.0 Hz), 128.5, 126.1 (q, J = 3.9 Hz), 125.5 (q, J = 271.0 Hz), 122.3, 116.4, 101.3, 61.2, 47.4, 15.0; ^{19}F NMR (471 MHz, $CDCl_3$) δ -62.5 (s, 3 F), -156.1 (s ,1 F); HRMS (HESI) *m/z* calcd for $C_{17}H_{18}N_3O_2F_4$ $[M+H]^+$ 372.1330, found 372.1327.

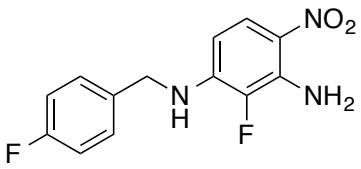

2-Fluoro-*N*^{1}-(4-fluorobenzyl)-4-nitrobenzene-1,3-diamine. A solution of 2,3-difluoro-6-nitroaniline (1.00 g, 5.57 mmol, 1.00 equiv) in dry DMSO (6 mL) was treated with 4-fluorobenzylamine (0.79 mL, 6.68 mmol, 1.20 equiv) followed by Et_3N (0.93 mL, 6.68 mmol, 1.2 equiv) and I_2 (cat. 5 mg). The reaction mixture was heated to 120 °C for 24 h, cooled to room temperature, quenched with water (30 mL) and extracted with EtOAc (3 x 30 mL). The combined organic layers were washed with brine, dried (Na_2SO_4), filtered and concentrated under reduced pressure. The residue was treated with a small amount of Et_2O (5 mL), sonicated, and filtered. The filter cake was washed with Et_2O (3 x 3 mL) to afford product (1.20 g) as a yellow solid. The filtrate was concentrated in vacuo and the residue was purified by chromatography on SiO_2 (EtOAc/hexanes/Et_3N, 1:4:0.1 to 1:3:0.1) to afford additional product (0.2 g) which was combined with the earlier fraction to provide 2-fluoro-*N*^{1}-(4-fluorobenzyl)-4-nitrobenzene-1,3-diamine (1.40 g, 90%) as a yellow solid: Mp 195.0-195.7 °C; IR (ATR) 3504.6, 3387.1, 3329.3, 3070.2, 2950.9, 1625.5, 1601.3, 1578.9, 1549.1, 1506.2, 1483.8, 1267.6, 1239.6, 1174.4, 1086.8, 991.7, 848.2, 837.0, 820.2, 805.3, 751.2 cm^{-1}; ^{1}H NMR (400 MHz, $CDCl_3$) δ 7.90 (dd, 1 H, *J* = 9.6, 2.0 Hz), 7.33 (dd, 2 H, *J* = 8.4, 5.2 Hz), 7.12-7.06 (m, 2 H), 6.12 (dd, 1 H, *J* = 9.6, 8.0 Hz), 6.07 (br s, 2 H), 4.86 (br s, 1 H), 4.47 (s, 2 H); ^{13}C NMR (125 MHz, acetone-d_6) δ 163.0 (d, *J* = 243.2 Hz), 142.6 (d, *J* = 9.3 Hz), 138.5 (d, *J* = 228.2 Hz), 136.7 (d, *J* = 13.4 Hz), 136.2 (d, *J* = 3.4 Hz), 129.9 (d, *J* = 8.2 Hz), 125.4, 123.9 (d, *J* = 2.6 Hz), 116.1 (d, *J* = 21.6 Hz), 101.8 (d, *J* = 3.5 Hz), 46.2; ^{19}F NMR (376 MHz, $CDCl_3$) δ -114.3 (s, 1 F), -161.1 (s, 1 F); HRMS (HESI) *m/z* calcd for $C_{13}H_{12}N_3O_2F_2$ $[M+H]^+$ 280.0892, found 280.0890.

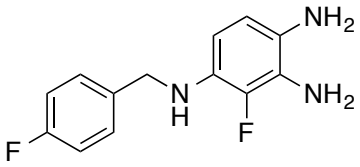

3-Fluoro-*N*^{4}-(4-fluorobenzyl)benzene-1,2,4-triamine. A stirred solution of 2-fluoro-*N*^{1}-(4-fluorobenzyl)-4-nitrobenzene-1,3-diamine (0.200 g, 0.716 mmol) in MeOH (2 mL) was treated with zinc powder (0.230 g, 3.58 mmol) followed by the dropwise addition of a solution of saturated ammonium chloride (0.68 mL). The reaction mixture was stirred vigorously at room temperature overnight, and filtered through Celite. The Celite was washed with EtOAc and the filtrate was extracted with EtOAc (3 x 3 mL). The combined organic layers were dried (Na_2SO_4) and concentrated under reduced pressure to afford 3-fluoro-*N*^{4}-(4-fluorobenzyl)benzene-1,2,4-triamine (0.120 g, 67%) as a dark red solid that was used in the next step without further purification: ^{1}H NMR (500 MHz, $CDCl_3$) δ 7.32 (dd, 2 H, *J* = 8.5, 5.5 Hz), 7.04-6.98 (m, 2H), 6.38 (d, 1 H, *J* = 8.5 Hz), 6.03 (t, 1 H, *J* = 8.5 Hz), 4.26 (s, 2 H), 3.21 (br, 5 H); ^{19}F NMR (471 MHz, $CDCl_3$) δ -115.7 (s, 1 F), -155.8 (s, 1 F); HRMS (HESI) *m/z* calcd for $C_{13}H_{14}N_3F_2$ $[M+H]^+$ 250.1150, found 250.1148.

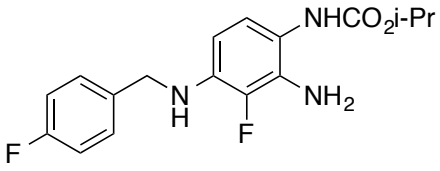

Isopropyl (2-amino-3-fluoro-4-((4-fluorobenzyl)amino)phenyl)carbamate (RL648_86). An oven-dried 5-mL round bottomed flask equipped with a magnetic stir bar under argon was charged at 0 °C with 3-fluoro-*N*^{4}-(4-fluorobenzyl)benzene-1,2,4-triamine (0.120 g, 0.48 mmol), CH_2Cl_2 (2.5 mL) and DIPEA (0.10 mL, 0.60 mmol). Isopropyl chloroformate (1 M in toluene, 0.48 mL) was added dropwise via syringe at 0 °C. The reaction mixture was stirred for 1 h at 0

°C, for 3 h at room temperature, and quenched by addition of water. The aqueous layer was extracted with CH_2Cl_2 (3 x 4 mL), and the combined organic extracts were dried (Na_2SO_4) and concentrated under reduced pressure. The residue was purified by chromatography on SiO_2 (EtOAc/hexanes, 4:1 to 3:1) to give a light red solid, which was washed with a small amount of Et_2O to afford RL648_86 (0.035 g, 21%) as a colorless solid: Mp 177.5-178.2 °C; IR (ATR) 3407.6, 3338.7, 3295.8, 1675.9, 1646.0, 1618.1, 1532.3, 1487.6, 1442.8, 1323.5, 1284.4, 1263.9, 1249.0, 1155.8, 1112.9, 1101.7, 1066.3, 823.9, 781.1 cm^{-1}; ^1H NMR (500 MHz, $CDCl_3$) δ 7.21 (dd, 2 H, *J* = 8.5, 5.5 Hz), 7.02 (app t, 2 H, *J* = 8.5 Hz), 6.74 (d, 1 H, *J* = 8.5 Hz), 6.11 (br s, 1 H), 6.06 (t, 1 H, *J* = 8.5 Hz), 4.98 (sept, 1 H, *J* = 6.0 Hz), 4.31 (d, 2 H, *J* = 3.0 Hz), 4.19 (br s, 1 H), 3.86 (br s, 2 H), 1.28 (d, 6 H, *J* = 6.0 Hz); ^{13}C NMR (125 MHz, $CDCl_3$) δ 162.2 (d, *J* = 245.2 Hz), 155.1, 141.4 (d, *J* = 233.8 Hz), 135.1 (d, *J* = 10.4 Hz), 135.0 (d, *J* = 3.1 Hz), 130.8 (d, *J* = 11.4 Hz), 129.0 (d, *J* = 8.1 Hz), 121.6, 115.6 (d, *J* = 21.5 Hz), 115.5, 102.0, 69.2, 47.4, 22.2; ^{19}F NMR (471 MHz, $CDCl_3$) δ -115.5 (s, 1 F), -156.2 (s,1 F); HRMS (HESI) m/z calcd for $C_{17}H_{20}N_3O_2F_2$ $[M+H]^+$ 336.1518, found 336.1518.

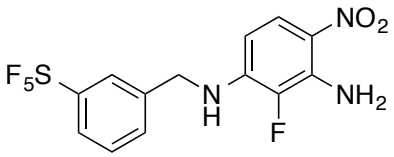

2-Fluoro-4-nitro-*N*^{1}-(3-(pentafluoro-λ^6-sulfanyl)benzyl)benzene-1,3-diamine. A suspension of 2,3-difluoro-6-nitroaniline (0.500 g, 2.78 mmol, 1.00 equiv) in dry DMSO (5 mL) was treated with 3-(pentafluorosulfanyl)benzylamine (0. 714 g, 3.06 mmol, 1.1 equiv) followed by Et_3N (0.43 mL, 3.06 mmol, 1.1 equiv) and I_2 (cat. 5 mg). The reaction mixture was heated to 120 °C for 24 h, cooled to room temperature, diluted with water (30 mL) and extracted with EtOAc (3 x 30 mL). The combined organic layers were washed with brine, dried (Na_2SO_4), filtered, and

concentrated under reduced pressure. To resulting residue was treated with a small amount of Et_2O (2 mL), sonicated, and filtered, and the filter cake was again washed with Et_2O (3 x 3 mL) to afford a yellow solid (0.51 g). The filtrate was concentrated in vacuo and the residue was purified by chromatography on SiO_2 (acetone/hexanes, 1:10 to 1:4 to 1:3) to afford additional product (0.17 g). The fractions were combined to yield 2-fluoro-4-nitro-*N*^{1}-(3-(pentafluoro-λ^6-sulfanyl)benzyl)benzene-1,3-diamine (0.68 g, 63%) as a yellow solid: Mp 169.5-170.0 °C; IR (neat) 3494.7, 3384.8, 1630.9, 1548.9, 1481.8, 1412.8, 1286.1, 1273.0, 1239.5, 1205.9, 1176.1, 1140.7, 1105.3, 1086.6, 890.9, 859.2, 820.1, 795.9, 775.4, 751.1, 687.8 cm^{-1}; ^{1}H NMR (400 MHz, $CDCl_3$) δ 7.85 (dd, 1 H, *J* = 9.6, 1.6 Hz), 7.72-7.68 (m, 2 H), 7.50-7.46 (m, 2 H), 6.07 (br s, 2 H), 6.02 (dd, 1 H, *J* = 9.6, 8.0 Hz), 4.50 (br s, 1 H), 4.54 (d, 2 H, *J* =1.5 Hz); ^{13}C NMR (100 MHz, acetone-d_6) δ 153.9 (t, *J* = 16.1 Hz), 141.3 (d, *J* = 9.4 Hz), 141.3, 137.6 (d, *J* = 228.7 Hz), 135.8 (d, *J* = 13.3 Hz), 135.7, 130.8, 129.5, 124.6 (t, *J* = 4.7 Hz), 124.4 (t, *J* = 4.7 Hz), 122.9 (d, *J* = 2.8 Hz), 100.7 (d, *J* = 3.0 Hz), 45.4; ^{19}F NMR (376 MHz, $CDCl_3$) δ 84.0 (quint, *J* = 150.4 Hz, 1 F), 62.7 (d, *J* = 150.4 Hz, 4 F), -160.4 (s, 1 F); HRMS (HESI) *m/z* calcd for $C_{13}H_{12}N_3O_2F_2S$ $[M+H]^+$ 388.0549, found 388.0549.

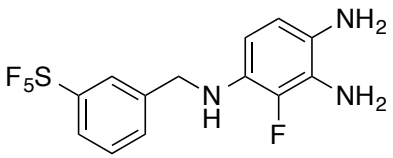

3-Fluoro-*N*^{4}-(3-(pentafluoro-λ^6-sulfanyl)benzyl)benzene-1,2,4-triamine. A stirred solution of 2-fluoro-4-nitro-*N*^{1}-(3-(pentafluoro-λ^6-sulfanyl)benzyl)benzene-1,3-diamine (0.500 g, 1.29 mmol) in MeOH (4 mL) was treated with zinc powder (0.422 g, 6.45 mmol) followed by dropwise addition of a solution of saturated ammonium chloride (1.22 mL). The reaction mixture was stirred vigorously at room temperature overnight, and filtered through Celite. The Celite was

washed with EtOAc and the filtrate was extracted with EtOAc (3 x 5 mL). The combined organic layers were dried (Na_2SO_4), and concentrated under reduced pressure to afford 3-fluoro-N^4-(3-(pentafluoro-λ^6-sulfanyl)benzyl)benzene-1,2,4-triamine (0.390 g, 85%) as a red solid that was used in the next step without further purification: ^{1}H NMR (400 MHz, $CDCl_3$) δ 7.74 (s, 1 H), 7.64 (d, J = 8.4 Hz, 1 H), 7.51 (d, J =7.6 Hz, 1 H), 7.41 (t, J = 8.0 Hz, 1 H), 6.39 (d, J = 7.6 Hz, 1 H), 5.98 (t, J = 8.4 Hz, 1 H), 4.35 (s, 2 H), 3.32 (br, 5 H).

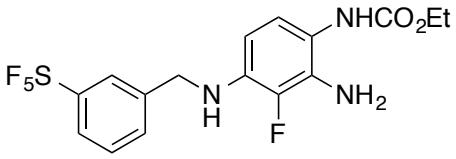

Ethyl (2-amino-3-fluoro-4-((3-(pentafluoro-λ^6-sulfanyl)benzyl)amino)phenyl)carbamate (RL673_02). An oven-dried 5-mL round bottomed flask equipped with a magnetic stir bar was charged under argon at 0 °C with 3-fluoro-N^4-(3-(pentafluoro-λ^6-sulfanyl)benzyl)benzene-1,2,4-triamine (0.20 g, 0.56 mmol), CH_2Cl_2 (3 mL) and DIPEA (0.12 mL, 0.7 mmol). Ethyl chloroformate (0.055 mL, 0.56 mmol) was added dropwise via syringe at 0 °C. The reaction mixture was stirred for 1 h at 0 °C, then 3 h at room temperature, quenched with water and extracted with CH_2Cl_2 (3 x 5 mL). The combined organic extracts were dried (Na_2SO_4), concentrated under reduced pressure, and purified by chromatography on SiO_2 (EtOAc/hexanes, 5:1 to 4:1 to 3:1) to afford the product as a yellow solid. Recrystallization from CH_2Cl_2/hexanes afford RL673_02 (0.123 g, 44%) as a colorless solid: Mp 141.3-142.1 °C; IR (ATR) 3420.2, 3375.41, 2985.9, 1688.7, 1636.5, 1524.6, 1483.6, 1287.9, 1254.4, 1241.3, 829.4, 816.4, 786.5, 688.7 cm^{-1}; ^{1}H NMR (400 MHz, $CDCl_3$) δ 7.73 (s, 1 H), 7.65 (d, 1 H, J = 8.0 Hz), 7.50 (d, 1 H, J = 7.6 Hz), 7.42 (t, 1 H, J = 8.0 Hz), 6.74 (d, 1 H, J = 7.6 Hz), 6.24 (br s, 1 H), 6.00 (t, 1 H, J = 8.8 Hz), 4.40 (s, 2 H), 4.19 (q, 2 H, J = 7.2 Hz), 3.98 (br s, 3 H), 1.28 (t, 3 H, J = 7.2 Hz); ^{13}C

NMR (100 MHz, $CDCl_3$) δ 155.5, 154.4 (quint, *J* = 16.9 Hz), 141.3 (d, *J* = 233.6 Hz), 140.7, 134.7 (d, *J* = 9.8 Hz), 130.9, 130.3, 129.2, 125.0 (t, *J* = 4.6 Hz), 124.8 (t, *J* = 4.6 Hz), 121.7, 115.6, 101.9, 61.7, 47.6, 14.6; ^{19}F NMR (565 MHz, $CDCl_3$) δ 84.5 (quint, *J* = 146.9 Hz, 1 F), 62.8 (d, *J* = 146.9 Hz, 4 F), -155.8 (s, 1 F); HRMS (HESI) *m/z* calcd for $C_{16}H_{18}N_3O_2F_6S$ $[M+H]^+$ 430.1018, found 430.1015.

Detailed values for main figures

Figure 3C. Retigabine: control (-29.5 ± 0.9; n=11), 100 nM (-30.43 ± 1.2; n=4), 1 μM (-39.35 ± 1.2; n=4) and 10 μM (-53.47 ± 0.9; n=4) and **SF0034:** control (-32.65 ± 0.9; n=21), 100 nM (-39.67 ± 0.9; n=4), 1 μM (-56.62 ± 0.5; n=5) and 10 μM (-73.21 ± 2.8; n=5).

Figure 3D. Retigabine: EC_{50} 3.3± 0.8 μM, $\Delta V_{1/2\ max}$ = 41 mV, slope = 0.93, n= 4-11; **SF0034:** EC_{50} 0.60 ± 0.06 μM, $\Delta V_{1/2\ max}$ = 50 mV, slope = 0.92, n= 5-21.

Figure 4A$_3$. NR561_40: Control (-32.82 ± 1.1; n=8), 100 nM (-38.71 ± 0.6; n=4), 1 μM (-60.45 ± 1.5; n=4) and 10 μM (-75.21 ± 1.7; n=4).

Figure 4B$_3$. NR561_50: Control (-27.75 ± 1.5; n=9), 100 nM (-34.91 ± 1.9; n=5), 1 μM (-48.56 ± 2.3; n=5) and 10 μM (-69.71 ± 1.7; n=4).

Figure 4C$_3$. NR579_04: Control (-29.35 ± 2.4; n=9), 100 nM (-31.25 ± 2.3; n=4), 1 μM (-31.77 ± 2.1; n=4) and 10 μM (-35.65 ± 2.1; n=4).

Figure 4D$_3$. NR561_62: Control (-27.99 ± 1.2; n=9), 100 nM (-33.52 ± 1.6; n=5), 1 μM (-43.15 ± 2.3; n=5) and 10 μM (-66.84 ± 2.4; n=4)].

Figure 4A$_4$. NR561_40: EC_{50} 0.91 ± 0.08 μM, $\Delta V_{1/2\ max}$ = 51 mV, slope = 0.83, n= 4-8.

Figure 4B$_4$. NR561_50: EC_{50} 0.74 ± 0.07 μM, $\Delta V_{1/2\ max}$ = 40 mV, slope = 1.1, n= 4-9.

Figure 4C$_4$. NR579_04: EC_{50} NA, $\Delta V_{1/2\ max}$ = NA, slope = NA, n= 4-9.

Figure 4D$_4$. NR561_62: EC_{50} 1.48 ± 0.18 μM, $\Delta V_{1/2\ max}$ = 35 mV, slope = 1.2, n= 4-9.

Figure 5. Retigabine: EC_{50} 3.3 ± 0.8 μM; max $\Delta V_{1/2}$ 33.88 ± 1.46 (n= 4-11), **SF0034:** EC_{50} 0.60 ± 0.06 μM; max $\Delta V_{1/2}$ 50.04 ± 1.56 (n= 5-21), **NR561_40:** EC_{50} 0.91 ± 0.08 μM; max $\Delta V_{1/2}$ 50.90 ± 3.1 (n= 4-8), **NR561_50:** EC_{50} 0.74 ± 0.07 μM; max $\Delta V_{1/2}$ 39.6 ± 1.7 (n= 4-9), **NR561_29:** EC_{50} 0.76 ± 0.17 μM; max $\Delta V_{1/2}$ 27.81 ± 1.72 (n= 4-10), **NR561_45:** EC_{50} 1.34 ± 0.17 μM; max $\Delta V_{1/2}$ 34.1 ± 3.05 (n= 4-9), **NR579_38:** EC_{50} 2.55 ± 0.46 μM; max $\Delta V_{1/2}$ 13.74 ± 3.9 (n= 4-5), **NR579_46:** EC_{50} 3.53 ± 0.84 μM; max $\Delta V_{1/2}$ 46.67 ± 2.67 (n= 4-8), **NR561_87:** EC_{50} 4.03 ± 1.21 μM; max $\Delta V_{1/2}$ 32.78 ± 5.0 (n= 4-7), **NR579_04:** EC_{50} NA ; max $\Delta V_{1/2}$ NA (n= 4-9), **NR561_62:** EC_{50} 1.48 ± 0.18 μM; max $\Delta V_{1/2}$ 34.74 ± 0.74 (n= 4-9), **NR579_45:** EC_{50} 4.49 ± 1.05 μM; max $\Delta V_{1/2}$ 26.91 ± 0.99 (n= 4-5) and **NR579_36:** EC_{50} NA ; max $\Delta V_{1/2}$ NA (n= 4-5).

Figure 6A$_3$. NR561_50: Control (-39.07 ± 1.23; n=5), 100 nM (-38.65 ± 0.85; n=5) and 1 μM (-42.35 ± 1.2; n=4).

Figure 6B$_3$ NR561_50: Control (-48.8 ± 2.96; n=4), 100 nM (-53.52 ± 3.5; n=4) and 1 μM (-59.16 ± 5.0; n=4).

Figure 6C$_3$. NR561_40: Control (-39.38 ± 3.1; n=6), 100 nM (-42.22 ± 2.0; n=6) and 1 μM (-52.04 ± 1.5; n=6).

Figure 6D$_3$. NR561_40: Control (-45.80 ± 2.0; n=4), 100 nM (-66.8 ± 3.1; n=4) and 1 μM (-79.15 ± 2.5; n=4).

Figure 6E$_3$. NR561_29: Control (-45.99 ± 1.4; n=4), 100 nM (-48.50 ± 1.52; n=4) and 1 μM (-64.5 ± 1.2; n=4).

Figure 6F$_3$. NR561_29: Control (-53.37 ± 1.8; n=4), 100 nM (-60.5 ± 2.5; n=4) and 1 μM (-65.2 ± 0.92; n=4).

Figure 8A$_3$. Control (-32.67 ± 1.3; n=5), 100 nM (-50.31 ± 1.44; n=5), 1 μM (-73.9 ± 2.3; n=5) and 10 μM (-90.31 ± 1.29; n=5).

Figure 8A$_4$. RL648_81: EC_{50} 0.19 ± 0.02 μM, $\Delta V_{1/2\ max}$ = 52 mV, slope = 0.74, n= 5; **SF0034:** EC_{50} 0.60 ± 0.06 μM, $\Delta V_{1/2\ max}$ = 50 mV, slope = 0.92, n= 5-21.

Figure 8B$_3$. RL648_81: Control (-50.43 ± 2.69; n=7), 100 nM (-54.43 ± 2.7; n=7), 1 μM (-55.4 ± 2.5; n=4) and 10 μM (-58.1 ± 2.6; n=4)

Figure 8C$_3$. RL648_81: Control (-53.95 ± 4.5; n=5), 100nM (-56.92 ± 3.8; n=5), 1μM (-64.4 ± 3.5; n=5) and 10 μM (-63.4 ± 1.8; n=4).

Figure 8D. SF0034: EC_{50} 0.60 ± 0.06 μM; max $\Delta V_{1/2}$ 50.04 ± 1.56 (n= 5-21), **RL648_81:** EC_{50} 0.19 ± 0.02 μM; max $\Delta V_{1/2}$ 51.12 ± 3.5 (n= 5), **RL648_73:** EC_{50} 0.30 ± 0.05 μM; max $\Delta V_{1/2}$ 47.0 ± 3.9 (n= 4-6), **RL648_86:** EC_{50} 0.34 ± 0.07 μM; max $\Delta V_{1/2}$ 49.9 ± 2.5 (n= 4-5), **NR573_02:** EC_{50} 0.88 ± 0.28 μM; max $\Delta V_{1/2}$ 42.5 ± 4.5 (n= 4-11).

Figure 8E. RL648_73: control (-44.52 ± 2.0; n=4), 100 nM (-43.53 ± 1.1; n=4), 1μM (-48.8 ± 3.0; n=4) and 10 μM (-49.8 ± 1.7; n=3), **RL648_86:** control (-44.51 ± 4.0; n=5), 100 nM (-45.93 ± 4.1; n=4), 1μM (-52.4 ± 3.9; n=4) and 10 μM (-49.7 ± 2.4; n=4) and **RL673_02:** control (-

42.5 ± 2.9; n=4), 100 nM (-41.7 ± 3.0; n=4) and 1μM (-42.8 ± 2.4; n=4) and 10 μM (-55.7 ± 2.5; n=4).

Figure 8F. RL648_73: control (-53.92 ± 4.1; n=4), 100nM (-59.5 ± 2.5; n=4), 1μM (-61.4 ± 2.6; n=4) and 10 μM (-60.4 ± 2.3; n=4), **RL648_86:** control (-54.84 ± 1.5; n=4), 100nM (-55.14 ± 1.4; n=4), 1μM (-58.4 ± 2.5; n=4) and 10 μM (-60.2 ± 2.9; n=3) and **RL673_02:** control (-64.35 ± 3.8; n=4), 100nM (-67.5 ± 5.5; n=4), 1μM (-74.4 ± 4.5; n=4) and 10 μM (-75.2 ± 1.8; n=4)

Figure 9A$_3$. RL648_81: Control (-40.5 ± 2; n=5), 100 nM (-47.7 ± 1.3; n=4), 1 μM (-61.57 ± 1.4; n=4) and 10 μM (-64.9 ± 1.3; n=4).

Figure 9B$_3$. RL648_81: Control (-43.5 ± 0.8; n=4), 100 nM (-43.1 ± 2.5; n=4), 1 μM (-42.75 ± 2.7; n=4) and 10 μM (-41.1 ± 2; n=4).